

Copyright
by
Michele Anne Zacks
2007

**The Dissertation Committee for Michele Anne Zacks certifies that this is the
approved version of the following dissertation:**

Biological studies of GPI-anchoring in *T. cruzi*

Committee:

Dr. Nisha Garg, Supervisor

Dr. David Walker

Dr. Ashok Chopra

Dr. Robert Davey

Dr. Paul Boor

Dr. Anant Menon

Dean, Graduate School

BIOLOGICAL STUDIES OF GPI-ANCHORING IN *T. CRUZI*

by

Michele Anne Zacks, B.A., M.S.

Dissertation

Presented to the Faculty of the Graduate School of

The University of Texas Medical Branch

in Partial Fulfillment

of the Requirements

for the Degree of

Doctor of Philosophy

The University of Texas Medical Branch

August, 2007

Dedication

To my brother Jon Michael Zacks and to people with challenges of all kinds who try to achieve their best- sometimes failing and other times, exceeding expectations.

Acknowledgements

People

To my family: My father, Howard, above all deserves the honorable mention for logging in a record number of Sprint cell phone minutes listening to my stories about graduate school and laboratory research. His own experiences as a graduate student give timelessness and humor to the process. My mother, Claudia, by example and necessity as a law student, shaped me into an independent and self-driven individual with a distinct level of stubbornness and ambition. These qualities have been beneficial to the Ph.D. process. My three brothers Jon, Matthew and Stephen, each exceptional in different ways, have consistently reminded me, by example, of the importance of striving to make a contribution. Geri, my step-mother, was my faithful cheerleader.

To the students and postdocs at UTMB and elsewhere: Many of them have been a constant inspiration with their work and personalities and they have provided me with reality checks, open ears, and beers. My classmate Ivy Greene was there *with* me- and there *for* me- throughout this long process. Long live Salsa's *Green Iguana* margarita! Rene Rjnbrand, although he never wanted to be thanked, must be thanked! I so much appreciate him for tolerating interruptions to discuss my project and any kind of technical questions, for providing me with immense practical advice and for his willingness to comment on my writing and thinking. All of this was of no benefit to him and yet he did so. To him, I most definitely owe my development as a molecular biologist by introducing me to the strange cloning language and Dutch protocols. And I owe him for any cloning success I have had. Even better, he made the work fun. Shane Wilkinson, my *T. cruzi* colleague- simply an excellent scientist and one of the best molecular parasitologists in this field- cheerfully and speedily replied from England to all my technical queries.

To my dissertation committee, the pieces in the puzzle: I appreciate Dr. Garg for accepting me as a student when she first arrived at UTMB and for allowing me to work on my preferred choice among all the possible projects we discussed. I admire -and hope I can continue to emulate - her incisive writing style and sharp critical analysis of the scientific literature. I thank Dr. Davey for his always-open door for discussions of my project, for his creative suggestions for experiments, and for generously providing me with any reagents, plasmids or other important tools to get the job done; Dr. Menon, for interesting conversation about science over beers at the Poop Deck; Dr. Chopra, for his incisive checklists and thoughtfulness on how to approach experimental questions; Dr. Walker, for always reminding us students of the "big picture"; Dr. Doughty, for moral support or a kick in the butt, as necessary; Dr. Boor, for his willingness to sit on my committee at the end point.

To so many of my "teachers" at UTMB and elsewhere: *Boston:* Dr. N. Ramesh pushed me to go to graduate school to pursue my interest in infectious diseases. His brilliance and excitement for conversation about all kinds of science is unforgettable.

My former bosses, Raif S. Geha and Donald A. Harn have each given me unique and valuable insight on approaching the challenges of scientific research. **Galveston:** Dr. Stanley Lemon, Dr. Hervé Lerat, and Dr. Lynn Soong provided me with high-quality rotation experiences. Dr. Mary Moslen and Dr. Mary Kanz formally taught me critical thinking and how to give effective presentations. Their efforts were of long standing importance in my professional development. Dr. Alan Barrett was always willing to serving as my “mock audience”, allowing me to butcher my talks without embarrassment.

To the Experimental Pathology program/GSBS: I owe tremendous gratitude to Dr. Norbert Herzog, Dr. Stephen Higgs, Dr. Dorian Coppenhaver and Harriet Ross (our “Jewish grandmother” and, until recently, our Experimental Pathology Program Coordinator) for keeping me on track throughout the years. They provided me with tremendously important personal and professional behind-the-scenes support at every step of the process and especially at the closing stages. Without all their extensive time and advice, this dissertation would not have been completed.

To my friends: My dear intellectual friend, Tony Merino, inspired me with his excellence in ceramic art critique, his lyrical paintings on clay and his odd mixture of genius and humanity. We sustained our friendship for over three years almost solely through email. I am honored to be included in his ring of fire. He is truly a “gemstone in the rough” with. His support and acceptance was enormous and sustained me through the most difficult stretches. Rebecca Teague, a former medical student and neighbor, included me in many dinner parties and took care of me when I was sick. Thanks to all the phone conversations, emails, letters and visits from my distant friends: Bert Philip, Deborah Ahern, Ramona Gonski, Roni Powalski, Alison Rabkin, and Marco Vignuzzi-Fabri. To coffee and drinking breaks, house cleaning and/or country & western dancing with Heather Blais, Martina Chambliss, Kim Nethery, Jami Ryan and Terri and Aaron Lucius. They all made me smile, even when I didn’t feel like smiling!

And finally, biggest THANKS to **Tracy Jay Goble**, for his beautiful heart, for his desire to understand how things work and his excitement about science. His positive attitude, his generous nature and his love for family - especially his kids -, friends and even random strangers, is my biggest inspiration. He met me at the late stage of my Ph.D. program, accepted me into his life and has endured with his powerful sense of “ohm”. He is my best friend. He puts up with me and almost always sees the good in me!

Funding sources

The following have provided support for this study and for presentation of this work at scientific meetings: National Institutes of Health (Grant #AI053098), Sealy Recruitment Fund, American Heart Association, American Health Assistance Foundations, UTMB Department of Pathology, James W. McLaughlin Predoctoral Fellowship in Infection and Immunity (UTMB), and UTMB Graduate School of Biomedical Sciences, for stipend support and travel scholarship. Dr. Slobodan Paessler generously provided me with essential bench space, reagents, and stipend support to complete my experiments and the writing of my dissertation.

Copyrighted material

Figure 2 reprinted with permission from McConville MJ et al, 2002. *Secretory pathway of trypanosomatid parasites*. Microbiol Molec Biol Rev. 66:122-154.

Adapted by permission from Macmillan Publishers Ltd: [EMBO J], (Ohishi, K., N. Inoue, and T. Kinoshita, 2001. *PIG-S and PIG-T, essential for GPI anchor attachment to proteins, form a complex with GAA1 and GPI8*. Embo J, 20:4088-98), copyright (2001).

“The life cycle of *T. cruzi*” reprinted with permission from U.S. Centers for Disease Control (CDC) Division of Parasitic Diseases Image Library, *DPDx: CDC’s web site for parasitology identification*. Available from: <http://www.dpd.cdc.gov/dpdx>

Figures 1, 2 and 3 reprinted with permission from Zacks MA, 2007. *Impairment of cell division of Trypanosoma cruzi epimastigotes*. Mem Inst Oswaldo Cruz 102: 111-5.

BIOLOGICAL STUDIES OF GPI-ANCHORING IN *T. CRUZI*

Publication No. _____

Michele Anne Zacks, Ph.D.

The University of Texas Medical Branch, 2007

Supervisor: Nisha Jain Garg

Trypanosoma cruzi, a protozoan parasite transmitted to humans via triatomine insects, causes chronic chagasic cardiomyopathy (CCM) in ~30% of infected individuals. This dissertation sought to characterize *T. cruzi*'s pathogenic mechanisms by cellular, biochemical, and molecular genetics approaches. In several protozoans, including *T. cruzi*, dominant cell surface proteins are attached to the parasite membrane by glycosylphosphatidylinositol (GPI) anchors and play roles in host cell attachment and invasion, and in parasite differentiation and replication. In other organisms, a transamidase, GPI8, is involved in this anchoring process. This study investigated the effects of protein-GPI depletion on *T. cruzi* growth and development by over-expressing TcGPI8 mutated in putative active site residues, which were determined based on significant homology to other GPI8s and plant endopeptidases containing conserved Cys and His residues in their active sites. In *T. cruzi* expressing TcGPI8 mutant alleles (C198A or H156A), no alteration in GPI-anchoring efficiency or impairment of *in vitro* infectivity, differentiation or replication was observed. These results indicate that TcGPI8's active site may not be comprised of H198A and C156A and, therefore, differs from that of yeast, human and *Leishmania* GPI8. Alternatively, targeted disruption of *TcGPI8* in *T. cruzi* was employed to provide protein-GPI deficient mutants. Unintended disruption of the *GAPDH* gene resulted from this approach and marked growth and developmental defects were observed in these parasites at the epimastigote stage.

Table of Contents

LIST OF TABLES	XIII
LIST OF FIGURES	XIV
LIST OF ILLUSTRATIONS	XVI
LIST OF ABBREVIATIONS	XVII
CHAPTER 1:	1
<i>TRYPANOSOMA CRUZI</i> AND CHAGAS DISEASE	1
The life cycle of <i>T. cruzi</i>	1
Chagas disease	2
Transmission of <i>T. cruzi</i>	3
Treatment	5
Mechanism of host cell invasion.....	5
<i>In vitro</i> and <i>in vivo</i> experimental models.....	9
CHAPTER 2:	10
GLYCOCONJUGATES AND THE GPI-ANCHORING MECHANISM	10
Glycoconjugates.....	10
Overview.....	10
Glycoconjugates in parasitic protozoans	10
Structure of glycoconjugates.....	10
Function of glycoconjugates	13
Significance of GPI-anchored proteins in parasite development and disease	19
The GPI-anchoring mechanism	23
Overview.....	23

The transamidation (TAM) mechanism.....	26
Biochemical evidence of TAM.....	28
Reporter assays	28
PLAP Assay	28
<i>T. brucei</i> VSG117 assay	31
Crosslinking studies	32
Identification of the genes involved in transamidation.....	33
Yeast and mammalian GPI8: reverse genetics approach.....	33
Trypanosome GPI8: forward genetics approach.....	35
<i>Summary</i>	36
Characteristics of the GPI8 protein.....	37
Homology of GPI8 to endopeptidases	38
Endopeptidase mechanism.....	39
Active site studies of GPI8	40
Yeast GPI8 (yGPI8).....	41
Human GPI8 (hGPI8)	42
<i>Leishmania mexicana</i> GPI8 (LmGPI8)	43
Other proteins involved in the TAM mechanism	44
Yeast	45
yGAA1	45
GPI16 and GPI17	46
CDC91	47
Mammalian cells.....	48
GAA1	48
PIG-S and PIG-T.....	49
PIG-U	50
Trypanosomes.....	52
GPI16	52
TTA1 and TTA2	52

TbGAA1	53
Summary	53
CHAPTER 3:	57
Introduction	55
Objective of Study	55
Specific Aim	55
Hypothesis.....	56
Experimental Approach	56
Over-expression of mutated GPI8	56
Targeted disruption of <i>TcGPI8</i>	57
Materials & methods.....	58
Isolation, cloning and characterization of <i>TcGPI8</i>	58
Genetic transformation of <i>T. cruzi</i>	58
Cloning.....	58
Constructs for over-expression of TcGPI8 in <i>T. cruzi</i>	59
Constructs for targeted disruption of <i>TcGPI8</i>	61
Cell culture.....	61
Transformation methods	62
Genetic screening of transformants	65
Chromosomal DNA extraction	65
PCR analysis	65
Southern blot analysis	66
Arbitrarily primed, nested PCR	67
Protein analysis in transformants	67
Generation and affinity purification of TcGPI8 antisera	67
Protein extraction	68
Western blot analysis	69
FACS analysis of GPI-anchored proteins	70
<i>T. cruzi</i> development.....	71
Fibroblast infection	71

Confocal microscopy	71
Results.....	72
Characterization of GPI8 in <i>T. cruzi</i>	72
Cloning of <i>TcGPI8</i> and gene sequence analysis.....	72
Detection of TcGPI8 in <i>T. cruzi</i>	74
Over-expression of TcGPI8 putative active site mutants	77
Selection of <i>T. cruzi</i> transfectants	77
Screening of transformants by PCR analysis.....	77
Surface expression of GPI-anchored proteins in pTEX transformants.....	78
Life cycle development in pTEX transformants.....	79
Targeted disruption of <i>TcGPI8</i>	80
Generation of transformants	80
Effects of <i>neo^r-TcGPI8</i> transformation on <i>T. cruzi</i> development.....	81
Evaluation of life cycle development in <i>neo^r-TcGPI8</i> transformants.....	81
Transformation with <i>ble^r-TcGPI8</i> construct	82
Evaluation of integration of <i>neo^r</i> via PCR and Southern blot analysis.....	83
Evaluation of targeted disruption of <i>TcGPI8</i> via PCR analysis	83
Identification of the site of integration of <i>GAPDHIR-neo^r</i> cassette in <i>T. cruzi</i> genome.....	85
CHAPTER 4:	90
Conclusions.....	86
Over-expression of TcGPI8 mutants	86
Integration of <i>GAPDHIR-neo^r</i> adjacent to the <i>GAPDH</i> gene.....	90
BIBLIOGRAPHY	129
VITA	150

List of Tables

Table 1:	Primers	91
Table 2:	<i>TcGPI8</i> cloning constructs.....	92
Table 3:	<i>T. cruzi</i> expression vectors.....	92
Table 4:	Mammalian expression vectors.....	93
Table 5:	Bacterial expression vectors	93
Table 6:	Cloning vectors and constructs for targeted disruption of <i>TcGPI8</i> ..	94

List of Figures

Figure 1:	The <i>T. cruzi</i> expression vector, pTEX.....	95
Figure 2:	Experimental approach to over-expression of TcGPI8 in <i>T. cruzi</i>	96
Figure 3:	Experimental approach to targeted disruption of <i>TcGPI8</i> in <i>T. cruzi</i>	97
Figure 4:	Cloning of <i>TcGPI8</i> in expression vectors.....	98
Figure 5:	Site-directed mutagenesis of <i>TcGPI8</i>	99
Figure 6:	Cloning strategy for <i>neomycin-resistance</i> (<i>neo^r</i>)-based <i>TcGPI8</i> disruption construct.....	100
Figure 7:	Cloning strategy for <i>phleomycin resistance</i> (<i>ble^r</i>)-based <i>TcGPI8</i> disruption construct.....	101
Figure 8:	Experimental design for expression of TcGPI8 _{FH} in mammalian cells	102
Figure 9:	Expression of TcGPI8 _{FH} in bacteria.....	103
Figure 10:	Experimental design for screening of <i>T. cruzi</i> pTEX transformants by PCR analysis	104
Figure 11:	Experimental design for evaluation of <i>TcGPI8</i> disruption with <i>neo^r-TcGPI8</i> construct	105
Figure 12:	Experimental design for identification of the site of integration of the <i>GAPDHIR-neo^r</i> cassette into the <i>T. cruzi</i> genome.	106
Figure 13:	CLUSTAL W (1.82) multiple sequence alignment of GPI8 in <i>T. cruzi</i> , <i>T. brucei</i> , <i>L. mexicana</i> , <i>S. cerevisiae</i> (yeast), <i>H. sapiens</i> (human), <i>T. gondii</i> , and <i>P. falciparum</i> , and legumain in <i>C. ensiformis</i>	107

Figure 14:	RT-PCR analysis of <i>GPI8</i> mRNA in <i>T. cruzi</i>	110
Figure 15:	Southern blot analysis of <i>T. cruzi GPI8 (TcGPI8)</i>	111
Figure 16:	Antibody optimization and specificity screening by detection of over-expression of epitope-tagged TcGPI8 in mammalian and bacterial cells.	112
Figure 17:	Characterization of pTEX constructs and <i>T. cruzi</i> /pTEX transfectants	114
Figure 18:	Detection of expression of epitope-tagged TcGPI8 in <i>T. cruzi</i> transfectants	118
Figure 19:	Surface expression of GPI-anchored proteins in <i>T. cruzi</i> pTEX transfectants.	119
Figure 20:	Growth of <i>T. cruzi</i> transfectants as epimastigotes	120
Figure 21:	Confocal analysis of <i>neo^r-TcGPI8</i> transformants.....	121
Figure 22:	Confocal analysis of <i>neo^r-TcGPI8</i> transformants following electroporation with <i>ble^r-TcGPI8</i>	122
Figure 23:	Evaluation of <i>neo^r</i> integration into genome of <i>neo^r-TcGPI8 T. cruzi</i> transfectants	123
Figure 24:	Evaluation of targeted disruption of <i>TcGPI8</i> in <i>neo^r-TcGPI8</i> transformants.....	125
Figure 25:	Identification of the site of integration of <i>GAPDHIR-neo^r</i> cassette in the <i>T. cruzi</i> genome	126

List of Illustrations

Illustration 1:	The life cycle of <i>T. cruzi</i>	2
Illustration 2:	The mechanism of host cell invasion by <i>T. cruzi</i>	8
Illustration 3:	Schematic representation of a GPI-anchored protein with conserved glycan core.....	11
Illustration 4:	Membrane orientation of glycoconjugates.....	12
Illustration 5:	Biosynthesis of glycosylphosphatidylinositol (GPI)-linked glycoconjugates.....	21
Illustration 6:	Requirements for GPI transfer to protein and the GPI-anchoring mechanism	26
Illustration 7:	The postulated catalytic mechanism for GPI-anchor attachment by GPI8	27
Illustration 8:	The mini-PLAP GPI-reporter assay.....	30
Illustration 9:	General experimental approaches for the identification of the transamidase, GPI8, in yeast, mammalian cells and trypanosomes	34
Illustration 10:	Characteristics of GPI8s in the organisms studied to date.....	38
Illustration 11:	The ClustalW alignment of GPI8s.....	41
Illustration 12:	The TAM complex.....	54

List of Abbreviations

Δ	null mutant, e.g., Lm Δ <i>GPI8</i>
2-D	two-dimensional
A	alanine
A ₆₀₀	absorbance at wavelength of 600
α	anti (antibody)
<i>A. thaliana</i> (<i>At</i>).....	<i>Arabidopsis thaliana</i>
AA	amino acid
AD	arbitrary degenerate
<i>amp^r</i>	β -lactamase (ampicillin resistance) gene
ANOVA	analysis of variance
B	both primers
BFT	bloodstream form trypanosome (<i>T. brucei</i>)
BHK(21)	baby hamster kidney cell line
<i>ble^r</i>	bleomycin (phleomycin) resistance gene (<i>Streptoalloteichus hindustans</i> phleomycin-ble binding protein)
BN-PAGE	blue native polyacrylamide-gel electrophoresis
C2C12	murine skeletal muscle (cell line)
<i>C. ensiformis</i>	<i>Canavalia ensiformis</i>
CCM	chronic chagasic cardiomyopathy
CHO	Chinese hamster ovary
CL	<i>T. cruzi</i> CL-Brener strain
CMV	cytomegalovirus
Cys (C)	cysteine
DAF	decay-accelerating factor (CD55)
dATP	2'-deoxyadenosine 5'-triphosphate
dCTP	2'-deoxycytidine 5'-triphosphate
dGTP	5' deoxyguanylate triphosphate
DMEM	Dulbecco's Modified Eagle's Medium
dpi	days post-infection
dsRNAi	double stranded RNA interference
dTTP	2'-deoxythymidine 5'-triphosphate
eGFP	enhanced green fluorescent protein
Enz	enzyme
ER	endoplasmic reticulum

EST	expressed sequence tag
EtN	ethanolamine
EtNP	ethanolamine phosphate
EtNP-T	ethanolamine phosphotransferase
F	forward (primer)
FBS	fetal bovine serum
Flu.....	influenza virus hemagglutinin epitope tag
Flu ₃ His ₆ (FH)	epitope tag composed of three copies of Flu and six His residues
FS	flanking sequence
FSC	forward scatter properties
GAPDH	glyceraldehyde phosphate dehydrogenase
gDNA	genomic (chromosomal) DNA
GIPL	glycoinositol phospholipid (“free” GPI)
GlcN	glucosamine
GlcNAc	N-acetylglucosamine
GPI	glycosylphosphatidylinositol
<i>GPI8-132</i>	TcGPI8 peptide (amino acid #132-145) antibody
GPI-AP	GPI-anchored protein
GPI-AP ⁻	GPI-anchored protein deficient
GPI-PLC	GPI-phospholipase C
<i>H. sapiens</i> (h)	<i>Homo sapiens</i> (human)
HAA	hydrophobic amino acid
HAM	hydroxylamine
HDZ	hydrazine
hGPI8	human GPI8
His (H)	histidine
HPLC	high performance liquid chromatography
HRF	homologous restriction factor (CD59)
HRP	horseradish peroxidase
I	IPTG-induced
iCa ⁺²	intracellular Ca ⁺²
IP ₃	inositol triphosphate
IPTG	isopropyl β-D-1-thiogalactopyranoside
IR	intergenic region
kb.....	kilobase
kDa	kilodalton

<i>L. mexicana</i> (<i>Lm</i>)	<i>Leishmania mexicana</i>
lgp	lysosomal glycoproteins
LIT	liver infusion tryptose
LmGPI8	<i>Leishmania mexicana</i> GPI8
LPG	lipophosphoglycan
LPPG	lipopeptido-phosphoglycan
M	molecular weight marker
mAb	monoclonal antibody
MASP	mucin-associated surface protein
µg	microgram
MNNG	N-methyl-N'-nitro-N-nitrosoguanidine
MT	mannosyltransferase
<i>neo^r</i>	neomycin resistance gene (neomycin phosphotransferase, pMC1neo, Stratagene)
ng.....	nanogram
NHS	N-hydroxysuccinimide
NO	nitric oxide
ORF	open reading frames
<i>P. falciparum</i> (<i>Pf</i>)	<i>Plasmodium falciparum</i>
PARP	procyclic acidic repetitive protein (procyclin)
PBS	phosphate buffered saline
PCR	polymerase chain reaction
PG	phosphoglycan
pI	isoelectric point
PI	phosphatidylinositol
PLAP	placental alkaline phosphatase
PLC	phospholipase C
PM	plasma membrane
PPG	proteophosphoglycan
PV	parasitophorous vacuole
R	reverse (primer)
S	serine
<i>S. cerevisiae</i> (<i>y</i>)	<i>Saccharomyces cerevisiae</i> (yeast)
SB	Southern blot
SDM	site-directed mutagenesis
SDS-PAGE	sodium dodecyl sulfate-polyacrylamide gel electrophoresis
SH.....	sulphydryl

SSC	side scatter properties
Sylvio	<i>T. cruzi</i> SylvioX10/4 strain
<i>T. brucei</i> (<i>Tb</i>)	<i>Trypanosoma brucei</i>
<i>T. cruzi</i> (<i>Tc</i>)	<i>Trypanosoma cruzi</i>
<i>T. gondii</i> (<i>Tg</i>)	<i>Toxoplasma gondii</i>
TAIL-PCR	thermal asymmetric interlaced PCR
TAM	transamidase
TcGPI8	<i>T. cruzi</i> GPI8
Tf	transfectant
TM	trademark
ts	temperature sensitive
TS	trans-sialidase
TTA	trypanosomatid transamidase (TTA1, TTA2)
U	uninduced (not IPTG-induced)
UDP	uridine-diphosphate
VSG	variant surface glycoprotein
ω	omega, sequence at the C terminus that signals GPI anchor addition
WB	Western blot
WT	wild type
X-Gal	5-bromo-4-chloro-3-indolyl-beta-D-galactopyranoside
yGPI8	yeast GPI8

Chapter 1:

Trypanosoma cruzi and Chagas disease

THE LIFE CYCLE OF *T. CRUZI*

Trypanosoma cruzi (*T. cruzi*) is a parasitic protozoan of the ancient branch of eukaryotes (Kingdom Eukaryota, Order Kinetoplastida)¹ and is endemic in South and Central America, and Mexico. It has a complex life cycle, alternating between an insect and vertebrate host. It reproduces asexually in the midgut of the insect vector, differentiating from the replicative epimastigote to the metacyclic trypomastigote form. After taking a blood meal, the insect sheds metacyclic trypomastigotes in its feces. The mammalian host in contact with feces becomes infected by scratching of the skin or by rubbing of mucosal surfaces. Metacyclic trypomastigotes invade host cells and differentiate into amastigotes. Amastigotes replicate inside the cell and subsequently convert into infective trypomastigotes that are released in the blood stream by host cell lysis. Released trypomastigotes can then infect other host cells or are ingested by the vector to complete its life cycle (Illustration 1)².

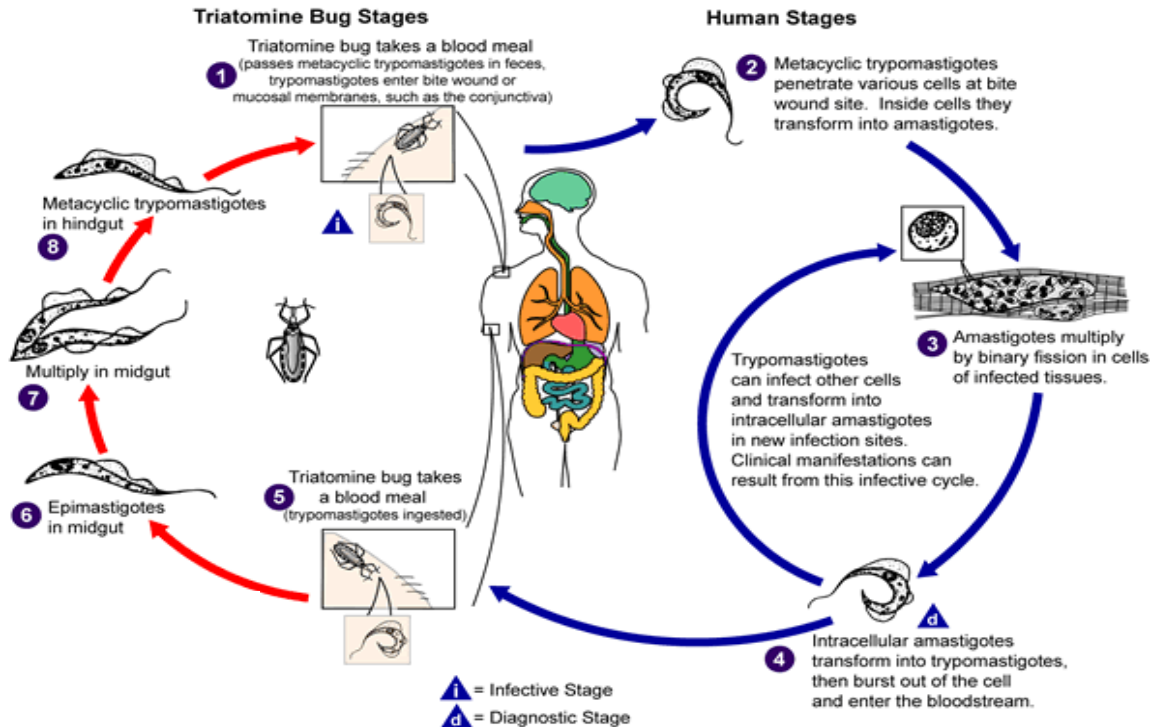


Illustration 1: The life cycle of *T. cruzi*. Reprinted with permission from U.S. Centers for Disease Control (CDC) Division of Parasitic Diseases Image Library, *DPDx: CDC's web site for parasitology identification*; <http://www.dpd.cdc.gov/dpdx>.

CHAGAS DISEASE

T. cruzi is the etiological agent of Chagas disease in humans³. Currently, the World Health Organization (WHO) estimates that 11-18 million individuals are infected worldwide⁴. In the acute phase of infection, individuals may experience local inflammation diagnosable as either a "chagoma" at the skin infection site or as "Romaña's

sign," a swelling of the eyelids⁵. At this early stage, parasites can be detected in the bloodstream. The acute phase is followed by asymptomatic infection. Eventually, after a period of 10-30 years, ~15-30% of infected individuals develop chronic chagasic cardiomyopathy (CCM), leading to an estimated 13,000-50,000 deaths annually. A smaller percentage of infected individuals (<5%) develop the digestive form of chronic disease, manifested as megacolon and megaesophagus⁴. The host factors that predispose the infected individuals to develop Chagas disease after 10-25 years in the "indeterminate" phase are unknown. The importance of parasite persistence and autoimmune-mediated damage has been investigated extensively; however, their relative contributions to the progression of chronic disease remain controversial⁶. More recently, host susceptibility to parasite-induced oxidative stress and mitochondrial damage, to which the heart may be particularly susceptible, has been explored as alternative hypothesis to explain the selective cardiomyopathy in chronically-infected individuals⁷.

TRANSMISSION OF *T. CRUZI*

Transmission of *T. cruzi* occurs predominantly via insect vectors of the subfamily Triatominae, family Reduviidae, referred to as "kissing bugs." Residing in the peridomestic habitat of mud-thatch houses in rural areas⁸, *Triatoma infestans*, the most common species currently responsible for transmission, is widely distributed throughout South America⁹. In addition, region-specific domestic species, e.g. *Rhodnius prolixus* in Venezuela, Colombia and Central America¹⁰, *Panstrongylus herreri* in Peru¹¹, *Rhodnius species* in Ecuador¹², and *Triatoma barberi* in Mexico⁹ contribute to transmission. Improvements in housing conditions and vector control measures instituted by the Southern Cone Initiative in 1991, a collaborative effort between Argentina, Brazil,

Bolivia, Chile, Paraguay and Uruguay, which has focused mainly on residential insecticide spraying, has contributed to a decline in transmission in endemic countries¹³. However, concern remains that reinfestation of these houses by secondary sylvatic vectors, e.g., *Triatoma sordida*, in Brazil and other South American countries¹⁴, and the amplification of other local peridomestic or sylvatic species will compromise the long-term efficacy of vector control measures^{11-13,15-16}.

The potential exists for the emergence of Chagas disease as a disease of public health importance in the United States (U.S.). Triatomine vectors are present in the U.S., e.g. *Triatoma sanguisuga* in the eastern United States, *Triatoma gerstaeckeri* in Texas and New Mexico, and *Triatoma rubida* and *Triatoma protracta* in Arizona and California¹⁷, and infection of domestic dogs and wild animals in the U.S. has been demonstrated¹⁷⁻²². Thus, autochthonous transmission has been suggested²³⁻²⁴, and to date, five cases of human infections transmitted by native triatomine vectors have been reported in the southern U.S.²⁵⁻²⁷.

Blood transfusion²⁸⁻³¹ and organ transplantation³² represent further routes of *T. cruzi* transmission. Although several countries in Latin America screen all blood donations for *T. cruzi*, infection rates of 0.1% to 24.4% of blood recipients occur in other countries with incomplete screening^{13, 33-37}. Due to significant increases in immigration to the U.S. and Canada from endemic countries³⁸ and in perinatal transmission³¹, it is estimated that 50,000-100,000 people residing in the U.S. may be infected with *T. cruzi*³⁹. Thus, overall, 1 in 25,000 U.S. blood donors may be infected; however, seropositivity rates reported include 1 in 7500 in Los Angeles, and 1 in 9000 in Miami⁴⁰. Due to the potential risk to transfusion recipients^{28,41-42}, in 2002, the U.S. Federal Drug Administration (USFDA) solicited manufacturers to submit applications for licensing of a test to screen blood products⁴³. Until February of 2007⁴⁴, following the USFDA's

approval of the first antibody test (ORTHO[®] *T. cruzi* ELISA Test System, Ortho-Clinical Diagnostics, Inc., Raritan, NJ), screening of the U.S. blood supply was not performed⁴⁵. These conditions have contributed to the transmission of *T. cruzi* by blood-borne, congenital, and to a lesser extent, vector-borne routes^{28, 46}.

TREATMENT

The anti-parasitic drugs benznidazole and nifurtimox have been used to treat patients early in infection⁵. However, their limited effectiveness for treatment in the chronic phase has prompted efforts to identify additional drug targets⁴⁷. No vaccine is currently available, in spite of intensive efforts to identify and evaluate vaccine targets⁴⁸. Therefore, studies designed to improve our understanding of the pathological mechanism of Chagas disease at the cellular and tissue level are warranted.

MECHANISM OF HOST CELL INVASION

T. cruzi is capable of infecting a wide range of phagocytic and non-phagocytic mammalian cells *in vitro*⁴⁹ and *in vivo*⁵. *T. cruzi* enters phagocytic cells via engulfment, whereas entry into non-phagocytic cells occurs by a distinct process, which is “active” or energy-driven⁵⁰⁻⁵¹. In non-phagocytic cells, trypomastigotes attach to the host cell and enter it by forming a parasitophorous vacuole (PV). Parasites escape the PV and replicate as amastigotes in the cell cytoplasm. Subsequently, amastigotes differentiate into trypomastigotes. Host cell lysis releases trypomastigotes into the bloodstream, allowing them to either be ingested by the insect vector or to infect new cells and tissues (Illustration 2) ².

The mechanism of active cell invasion by *T. cruzi* has been well studied and is believed to occur predominantly as described below (Illustration 2, reviewed in ⁵²⁻⁵³), although recent observations indicate that an alternative pathway exists⁵⁴⁻⁵⁵. The principal mechanism is described, as follows. First, trypomastigotes attach to the host cell by specific ligand-receptor interactions⁵⁶⁻⁶⁰. In particular, the transfer of sialic acid residues from the host cell to the parasite surface facilitates this attachment⁵⁶⁻⁶⁰. Parasite attachment initiates phospholipase C activation and the release of inositol triphosphate in the host cell⁶¹. An intracellular signaling cascade results in the triggering of a transient increase of intracellular Ca^{+2} (iCa^{+2}) in the host cell cytoplasm⁶²⁻⁶⁵. These signaling events (reviewed in ⁶⁶) are dependent upon cAMP⁶⁷, transforming growth factor β -receptor engagement on the host cell⁶⁸, and expression by *T. cruzi* of both oligopeptidase B⁶⁹⁻⁷⁰ and a 120-kDa alkaline peptidase⁷¹.

The consequent entry of *T. cruzi* into the cell proceeds by an unusual mechanism. iCa^{+2} release induces the recruitment of host cell lysosomes to the plasma membrane (PM)⁷²⁻⁷³ with the aid of microtubules^{61,74}. Lysosomes fuse with the PM, and subsequently, *T. cruzi* internalizes in a membrane-bound structure, the parasitophorous vacuole⁷². This process is linked to the host exocytic mechanism used to repair and recycle plasma membrane components⁷⁵⁻⁷⁷.

The concerted action of two *T. cruzi* proteins, trans-sialidase and the hemolysin, TcTox, are believed critical to the escape of the parasite from the parasitophorous vacuole into the cytoplasm⁷⁸⁻⁸¹. Lysosomal fusion with the parasitophorous vacuole results in acidification of the vacuole from ~pH 7 to 5.5⁸⁰. During this time, upregulation of *T. cruzi* trans-sialidase occurs. Trans-sialidase functions to transfer sialic acid residues from host proteins to the parasite surface molecules, and is believed to protect *T. cruzi* from destruction by lysosomal enzymes. While in the parasitophorous vacuole, *T. cruzi*

also secretes TcTox, a protein named for its hemolytic activity at this acidic pH. It is postulated that TcTox initiates pore formation, facilitating the disruption of the parasitophorous vacuole^{79,81-82}, and thereby enables the escape of trypomastigotes into the cytoplasm where they differentiate into amastigotes^{80-81,83-85}. Amastigotes are also infective⁸⁶⁻⁸⁸ and appear to invade and escape from the PV by a related, but not identical, mechanism as that used by trypomastigotes⁸⁵. In the cytoplasm, a 20-hour period of quiescence is followed by several cycles of replication and culminates in the conversion of amastigotes into trypomastigotes⁵³. Host cell lysis releases infective parasites that can infect neighboring cells or enter the bloodstream.

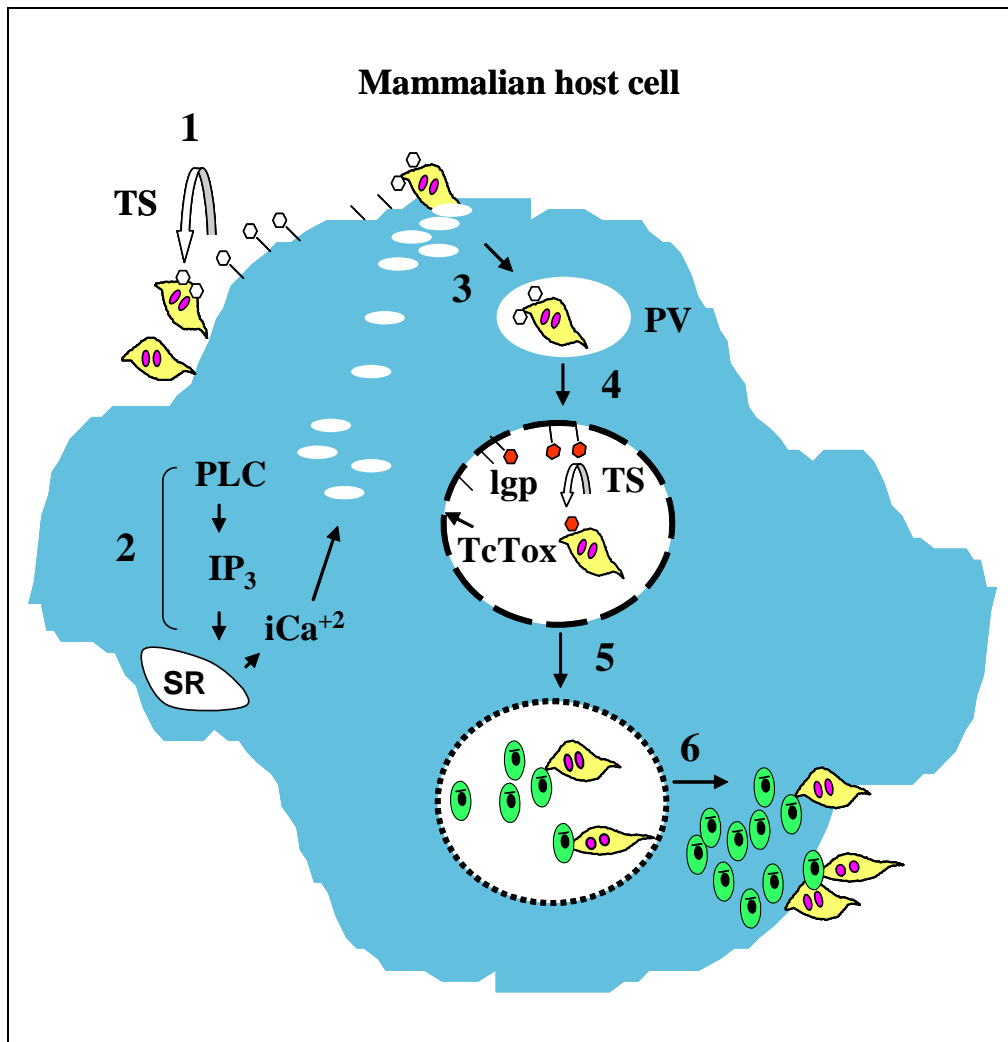


Illustration 2: The mechanism of host cell invasion by *T. cruzi*. 1) Trypomastigotes attach to surface of host cell, facilitated by sialic acid transfer from host to parasite surface by trans-sialidase (TS). 2) Phospholipase C (PLC) activation and release of inositol triphosphate (IP_3) leads to an intracellular calcium (iCa^{+2}) increase in host cytoplasm (and in parasite). 3) Host lysosomes are recruited to the cell membrane and metacyclic trypomastigotes are internalized, forming the parasitophorous vacuole (PV). 4) TS transfer of sialic acid from lysosomal glycoproteins (lgp) may dually render the parasitophorous vacuole membrane susceptible and the *T. cruzi* membrane resistant to lysis via TcTox produced by *T. cruzi*. 5) Trypomastigotes transform into amastigotes, which replicate and are released into the cytoplasm. 6) Cell lysis occurs, resulting in release of trypomastigotes and amastigotes into the extracellular space.

IN VITRO AND IN VIVO EXPERIMENTAL MODELS

In vitro and *in vivo* models of *T. cruzi* infection and pathogenesis make it possible to study host-parasite factors that are important in infection and disease development. All life cycle stages of *T. cruzi* can be cultivated *in vitro*. Epimastigote forms replicate axenically in growth medium that mimics the insect gut environment (liver infusion tryptose); epimastigote forms can be grown to stationary phase to generate metacyclic trypomastigotes. These then infect fibroblasts, macrophages and other mammalian cells in which parasites replicate as amastigotes. Thus, investigation of the effects of the genetic manipulation of the parasite on all stages of parasite development can be achieved.

In addition, the study of pathogenesis of acute and chronic disease has been possible, as a variety of mouse strains exhibit differential susceptibility to *T. cruzi* infection⁸⁹. In particular, infection of the C3H/HeN mouse with the SylvioX10/4 strain of *T. cruzi* mimics human disease⁹⁰⁻⁹¹. Development of disease is characterized by an "immediate early" phase of infection (3-5 dpi), followed by an increase in blood and tissue parasite loads during the acute phase (25-40 dpi). During this period, inflammatory foci with extracellular parasites commonly termed "amastigote nests" can be detected via immunohistochemical staining of tissue sections. With immune control of parasites, the chronic phase of disease development (130-180 dpi) begins. During this phase, detection of parasites in blood by microscopic evaluation and in tissue by immunohistochemical staining is minimal. However, it is possible to detect *T. cruzi* kinetoplast DNA in blood and tissue using PCR. Persistent diffuse inflammation and fibrosis in heart tissue are the hallmarks of chronic disease.

Chapter 2:

Glycoconjugates and the GPI-anchoring mechanism

GLYCOCONJUGATES

Overview

Glycoconjugates are utilized by eukaryotic organisms ranging from yeast to humans for the cell surface expression of a wide variety of proteins and lipids. The glycoconjugates are expressed as enzymes or receptors, serving a diversity of functions, including cell signaling and cell survival⁹²⁻⁹⁵. In parasitic protozoans, glycoconjugates play roles in infectivity, survival, virulence and immune evasion. The structures and functions of parasite glycoconjugates that have been best characterized for their roles in the survival and virulence of parasitic protozoans are described below.

Glycoconjugates in parasitic protozoans

Structure of glycoconjugates

Glycosylphosphatidylinositols (GPIs) represent unique structures for the anchorage of proteins and lipids to cellular membranes. The hydrophobic GPI is inserted into the membrane, orienting the protein, lipid or phosphosaccharide component on the extracellular face of the membrane⁹⁶. The GPI structure has been determined using

purified glycoconjugates by a combination of radiolabeling techniques, chemical and/or enzymatic treatments, followed by high performance liquid chromatography (HPLC) or other chromatographic techniques⁹⁷. These studies have shown the GPI anchor to consist of a basic core glycan structure that has proven to be highly conserved among all eukaryotic organisms (Illustration 3)⁹⁴.

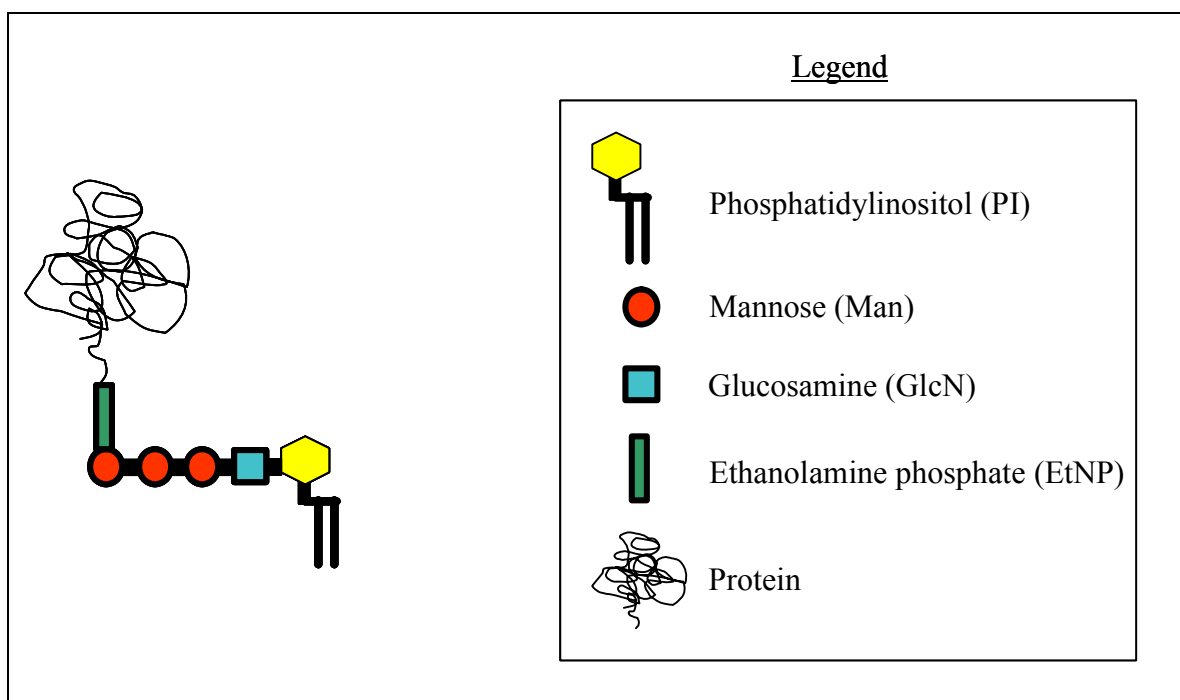


Illustration 3: Schematic representation of a GPI-anchored protein with conserved glycan core. Ethanolamine-phosphate-Man α 1-2 Man α 1-6Man α 1-4GlcN α 1-6PI represents the structure of GPI-anchors which is common to eukaryotic organisms ranging from *S. cerevisiae* to mammals⁹⁸.

The differences are represented in the extensive variability in the carbohydrate side-chain modifications and lipids among the divergent eukaryotic organisms as well as between species, strains and/or developmental stages of lower eukaryotes⁹⁹. In addition, parasitic protozoans express other unique phosphosaccharides such as lipophosphoglycan (LPG) and proteophosphoglycans (PPG) which have been structurally characterized¹⁰⁰.

GPI-anchored macromolecules are classified into the following groups: GPI-anchored proteins (GPI-APs), glycoinositol phospholipids (GIPLs or "free" GPIs) and GPI-anchored phosphosaccharides⁹⁴. GPI-anchored proteins contain a conserved core glycan structure attached to a protein by covalent linkage with an ethanolamine phosphate residue of the GPI. Structural models suggest that GIPLs are uniformly distributed along the parasite membrane with GPI-projecting above them^{94,96,100}. These structures are depicted schematically below (Illustration 4).

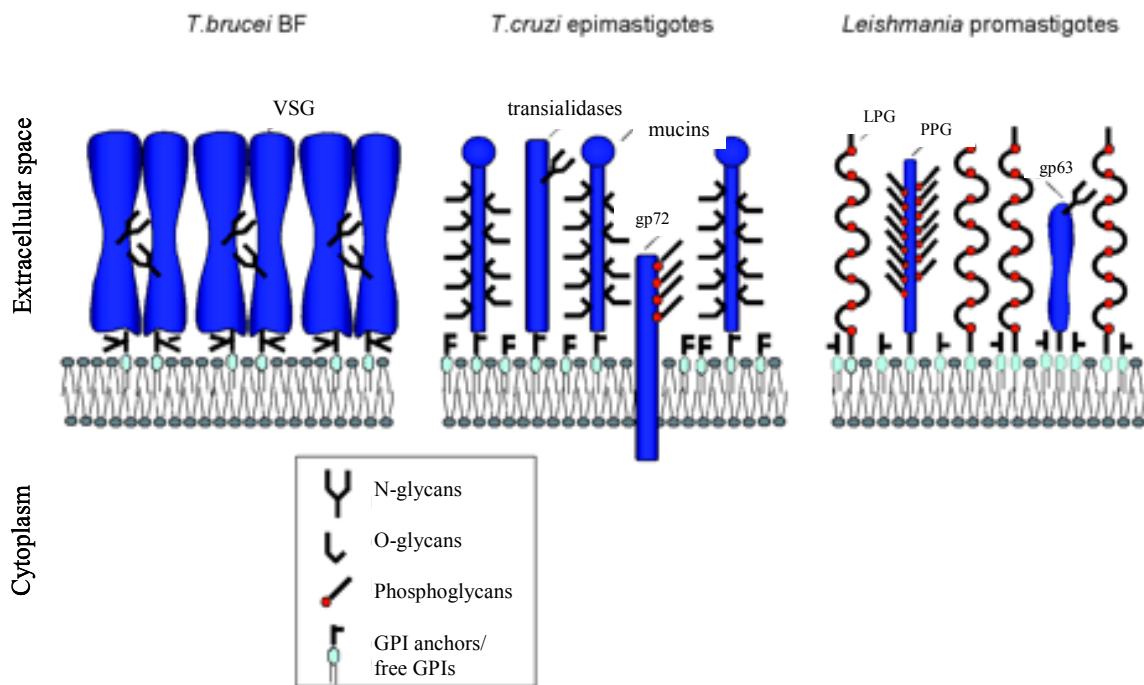


Illustration 4: Membrane orientation of glycoconjugates. GPI-anchored proteins, e.g., VSG, gp63, trans-sialidases and mucins, contain a glycosylphosphatidylinositol (GPI) anchor covalently linked to a polypeptide. Free GPIs or glycoinositol phospholipids (GIPLs) are not attached to proteins. Phosphosaccharides, e.g., LPG and PPG, contain repeating phosphoglycan units linked to an oligosaccharide “cap”. Abbreviations: BF, bloodstream form. Reprinted with permission from McConville MJ et al, *Secretory pathway of trypanosomatid parasites*. Microbiol Molec Biol Rev, 2002. 66(1): p.124.

FUNCTION OF GLYCOCONJUGATES

Among the trypanosomatid parasites, *Leishmania*, *Trypanosoma brucei* and *Trypanosoma cruzi* are major causes of animal and human disease. Each organism expresses unique glycoconjugates that are developmentally regulated and contain stage-specific modifications that ultimately reflect their functional importance in the respective life cycles. Glycoconjugates play critical roles in parasite attachment to host cells, as well as in invasion, differentiation and replication. Possible advantages conferred by this distinct anchor structure include: provision of a protective barrier or structural stability to the cell via tight packing of molecules, the ability to release proteins as soluble mediators, and finally, lateral clustering of molecules to create functional subdomains of the plasma membrane or to maintain cell polarity⁹⁶. Recent studies suggest that GPI-initiated stimulation of the innate immune response may contribute to parasite survival by limiting the uncontrolled replication that would lead to host death or severe pathogenesis, which would ultimately prevent infection and dissemination in the host¹⁰¹.

Leishmania

Leishmania are transmitted to humans by the bite of infected sandflies. The insect stage promastigotes differentiate into infective metacyclic promastigotes that are taken up by macrophages. In macrophages, *Leishmania* replicates as amastigotes within the phagolysosome¹⁰². The glycoconjugates LPG¹⁰³⁻¹⁰⁴, GIPLs¹⁰⁰ and protein-GPIs¹⁰⁵ are found to be expressed at distinct stages and have important functions in sandfly-parasite and macrophage-parasite interactions^{103, 106}.

LPG is a glycoconjugate, unique to *Leishmania*, which is anchored to the membrane via a phosphatidylinositol-linked glycan core. The core has a series of repeating oligosaccharide units bound to a “cap” structure (Illustration 4)¹⁰⁵.

Modifications in the sugars attached to these conserved repeat structures were demonstrated to account for differences in vector competence for *Leishmania*, e.g., *L. major* or *L. donovani* preference for *Plebotomus papatasi* versus *Plebotomus argentipes* vectors, respectively¹⁰⁷. LPG is highly upregulated in promastigotes¹⁰⁸ and facilitates the parasite's attachment to lectins in the sandfly midgut¹⁰⁹. During the process of metacyclogenesis, LPG is modified to larger sugar chain length, enabling it to detach from the midgut. This is necessary to allow metacyclic promastigotes to migrate to the anterior of the sandfly for transmission¹⁰⁸⁻¹⁰⁹. LPG may also contribute to survival in the phagolysosome. First, LPG appears to protect the parasite by inactivating hydrolytic enzymes¹¹⁰. Secondly, it may prevent the complement-mediated lysis¹¹¹ by rendering the metacyclic promastigote inaccessible to the membrane attack complexes¹¹².

Another important virulence factor in *Leishmania* is the protein-GPI, gp63 (Illustration 4)¹¹³⁻¹¹⁵. As the major surface protease of the promastigote¹¹⁶, it protects the parasite from complement-mediated lysis and facilitates its entry into macrophages via complement receptors, e.g., CR3,¹¹⁷ or via attachment to fibronectin¹¹⁸⁻¹²⁰.

In the amastigote stage, GIPLs and proteophosphoglycans (PPGs) (Illustration 4) are the predominant glycoconjugates¹⁰⁵. PPG activates complement and is postulated to prevent complement-mediated lysis of amastigotes, as it is released and binds complement away from the parasite surface¹²¹. GIPLs and LPG both appear to be capable of blocking the microbicidal respiratory burst of the macrophage by inactivating the intracellular signaling molecule, protein kinase C and inhibiting nitric oxide (NO) production¹²²⁻¹²⁴. Recently, GIPLs on promastigotes and amastigotes were shown to be involved in invasion by recognition of β -D-galactofuranose on the host surface¹²⁵. Thus, glycoconjugates in *Leishmania* play key roles in infectivity and survival.

T. brucei

African trypanosomes, *T. brucei* (*T.b.*) *species*, are transmitted by tsetse flies and exist as extracellular organisms, alternating between the procyclic stage in the insect vector and the bloodstream form in blood, lymph and interstitial fluids of the vertebrate host. *T.b. rhodesiense* and *T.b. gambiense* cause African sleeping sickness in humans whereas *T. b. brucei* infects cattle⁵ and has been used as a model organism to study African trypanosomes.

Variant surface glycoprotein (VSG) is the predominant glycoconjugate found on the bloodstream form of *T. brucei* (Illustration 4). VSG is a family of hundreds of genes that encode 55-to-60 kDa GPI-anchored proteins¹²⁶. Interestingly, these VSG molecules have low primary sequence homology, yet adopt similar tertiary conformations, based on crystallographic analysis of the N-terminal domain and other structural predictions¹²⁷. VSG molecules are abundant on the parasite surface, providing a dense surface coat that protects the bloodstream form from complement-mediated lysis. VSG also allows *T. brucei* to evade specific antibody responses via antigenic variation¹²⁸. The rapid switch to expression of a new VSG variant¹²⁶ allows escape and growth of a new variant, which explains the waves of fever observed in the disease, when this new clonal population multiplies¹⁰⁰. Structural models suggest that the VSG molecules project above a layer created by α -galactose side chains of the GPI core¹²⁹, providing a protective coat of VSG along with a dense lipid barrier that nonetheless enables diffusion and receptor-mediated uptake of nutrients. The fatty acid of VSG is remodeled to myristic acid obtained from the extracellular environment, a process that is essential to its survival¹³⁰⁻¹³².

Procyclic acidic repetitive protein (PARP, procyclin) is the predominant GPI-AP expressed in the procyclic form of *T. brucei*¹³³. Two distinct types of repeat units in PARP have been identified^{134, 135}, and both may protect *T. brucei* from proteolytic

enzymes in the tsetse midgut¹³⁶. In addition, PARP is believed to enable *T. brucei* to attach to the tsetse midgut, binding lectins in the epithelial layer¹³⁷. GPI-anchored proteins are also likely to be involved in providing nutrients by receptor-mediated mechanisms, e.g., uptake of iron via the GPI-anchored transferrin-receptor¹³⁸. Therefore, as in *Leishmania*, glycoconjugates are important determinants of survival throughout the life cycle of *T. brucei*.

T. cruzi

Whereas in *Leishmania species* and *Trypanosoma brucei*, a relatively small number of dominant glycoconjugates are found, in *T. cruzi*, a large number of GPI-anchored proteins and glycoconjugates have been identified as virulence determinants. Trans-sialidases and mucins (Illustration 4) are two major families of GPI-anchored proteins that are critical to the development of *T. cruzi* in the mammalian host.

Trans-sialidases

The trans-sialidase (TS) gene superfamily comprises ~140 genes (reviewed in ¹³⁹) that encode proteins containing the SDGTW amino acid consensus motif of bacterial neuraminidases¹⁴⁰. Although not all TS variants are enzymatically active¹³⁹, TSA-1 is an enzymatically active protein which is highly expressed in trypomastigote forms¹⁴¹. TSA-1 is believed to transfer sialic acid residues from host cell proteins and attaches sialic acid to parasite mucin-like proteins^{56,68,141-145}. Transsialidation appears to be necessary for *T. cruzi* attachment to host cell ligands during invasion¹⁴⁶⁻¹⁴⁹.

Furthermore, TSA-1 plays a unique role in parasite escape from the parasitophorous vacuole. TSA-1 transfers sialic acid residues from lysosomal glycoproteins on the internal membrane of the parasitophorous vacuole to trypomastigote

mucins. This mechanism is believed to protect *T. cruzi* from destruction during the acidification of the parasitophorous vacuole that occurs following fusion with lysosomes⁷⁸. The removal of sialic acid from lysosomal glycoproteins may render the parasitophorous vacuole membrane susceptible to effects of acidic pH, TcTox pore-forming activity, and consequent loss of membrane integrity^{53,78,150}. Thus, trans-sialidase activity appears to contribute to the escape of *T. cruzi* into the cytoplasm^{85,151}.

Tc85, another member of the TS superfamily (reviewed in ¹⁵²), binds to laminin and cytokeratin *in vitro*. This interaction, if it occurs *in vivo*, would presumably facilitate movement of *T. cruzi* through the extracellular matrix, allowing it to traverse the tissues to invade other organs^{153,154}. The amastigote-specific TSs, *ASP-1* and *ASP-2*, have also been identified¹⁵⁵⁻¹⁵⁶, although their precise role is presently unknown. In summary, TSs are a heterogeneous group of developmentally regulated GPI-anchored proteins of which some members are known to be critical to the life of *T. cruzi* in the host cell.

Mucins

The genetic diversity of the trans-sialidases is exceeded by *T. cruzi* mucins¹⁵⁷, another superfamily of GPI-anchored proteins, with >500 genes identified¹⁵⁸⁻¹⁶¹. Mucins are expressed in all stages of *T. cruzi*, with a family of 35-50 kDa proteins identified in epimastigote and metacyclic trypomastigote forms whereas larger (80-200 kDa) proteins are expressed in trypomastigote forms. Mucins are the acceptors for sialic acid attachment by trans-sialidases. They are named for their similarity to mammalian mucins, which are highly O-glycosylated molecules that function in cell-cell interactions^{139, 162}. The complexity of the structure of *T. cruzi* mucins is highlighted by demonstration of changes in lipid structure during transition from epimastigote to metacyclic trypomastigotes¹⁶³. In addition, recently, a new mucin family with >1300 copies (mucin-

associated surface proteins, MASP) was described with publication of the complete *T. cruzi* genome sequence¹⁶⁴. It is postulated that the large number of mucin variants may enable *T. cruzi* to evade the immune response. *T. cruzi* mucins such as Ssp-3⁵⁶ and gp35/50¹⁴⁵, expressed in the trypomastigote and metacyclic trypomastigote stages, respectively, have been ascribed analogous function in parasite ligand-host receptor binding⁵⁶. Together, the interaction between TSs and mucins is critical to the life cycle of *T. cruzi*.

Other glycoconjugates

Other GPI-anchored proteins have been investigated for their contribution to attachment and internalization. Gp82⁵⁷, along with the mucin gp35/50⁵⁸, is involved in the intracellular Ca⁺² signaling cascade that enables the parasite to gain entry into the host cell⁶⁵. Gp82-deficient isolates of *T. cruzi* revealed that gp82 expression was correlated with invasion capacity⁶⁰. Alternatively, loss of expression of the metacyclic trypomastigote specific protein, gp90, is associated with increased infectivity¹⁶⁵, which ultimately may be related to decreased Ca⁺² signaling⁶⁵. Of particular interest are recent mouse studies suggesting that gp82 and/or the related gp30 facilitate *T. cruzi* infection of the gut mucosa via the oral route⁶⁰. Finally, a homologue of the *Leishmania* major surface protease, gp63, has been recently identified in *T. cruzi* and may serve equivalent functions¹⁶⁶.

GIPLs and the GPI-anchored phosphoglycan (PG), lipopeptido-phosphoglycan (LPPG), have also been identified in *T. cruzi*. GIPLs are responsible for stimulation of the immune response in macrophages^{167,168}. LPPG has been characterized structurally¹⁶⁶, but its specific function in *T. cruzi* is currently unknown.

SIGNIFICANCE OF GPI-ANCHORED PROTEINS IN PARASITE DEVELOPMENT AND DISEASE

Several investigators have utilized genetic approaches to evaluate the overall importance of glycoconjugates in parasitic trypanosomes⁹⁵. In early studies, phenotypic GPI mutants of *T. cruzi* and *Leishmania* were generated by episomal over-expression of *T. brucei* GPI-phospholipase C (GPI-PLC)¹⁶⁹⁻¹⁷¹. In both *T. cruzi* and *Leishmania*, the expression of GPI-PLC resulted in a depletion of GPI-anchored proteins as well as GIPLs. The GPI-PLC-expressing *T. cruzi* and *Leishmania* grew well in axenic cultures as epimastigotes and promastigotes, respectively. However, these mutants exhibited an inability to replicate as intracellular amastigotes and a failure to maintain active infection in animal models of Chagas disease and leishmaniasis, respectively. The loss of virulence in GPI-PLC expressing *T. cruzi* and *Leishmania* suggested the importance of GPIs for completion of their life cycle. This GPI-PLC approach resulted in a general depletion of GPIs and therefore, did not distinguish between the relative significance of protein-GPIs and other GPI-glycoconjugates in trypanosome development and virulence. Thus, focus has been placed on identification and functional characterization of the genes involved in GPI biosynthesis and the construction of genetic mutants defective in different steps in the GPI pathway(s) (Illustration 5)⁹⁵. This has provided an alternative approach for evaluating the importance of glycoconjugates in the complex life cycles of trypanosomes.

In *L. mexicana* and *L. major*, disruption of GPI biosynthetic genes by homologous recombination has allowed characterization of the importance of GIPLs, GPI-phosphosaccharides, and protein-GPIs to development and virulence. These studies have shown that GIPLs/GPI-phosphosaccharides are important to virulence in the mammalian host, while protein-GPIs are essential to survival in the insect¹⁷²⁻¹⁷⁷, although LPG appears to be more important to virulence in *L. major* than in *L. mexicana* [reviewed in

¹⁷⁸]. In *T. brucei*, protein-GPIs were found to be essential to survival of bloodstream forms and were required for procyclics to establish infection in tsetse flies¹⁷⁹⁻¹⁸⁰, although not essential for growth of promastigotes¹⁸¹. To date, no genetic mutants of the *T. cruzi* GPI-phosphosaccharide and/or GIPL biosynthetic pathways have been developed. In comparison to the effects of glycoconjugate deficiency in these trypanosomatids, mammalian cell mutants defective in GPI biosynthesis or protein-GPI anchoring machinery are viable¹⁸²⁻¹⁸⁷. The results of the genetic studies outlined above have important implications, as enzymes involved in GPI biosynthesis and/or protein-GPI anchoring might serve as potential targets for chemotherapeutic interventions of parasitic diseases.

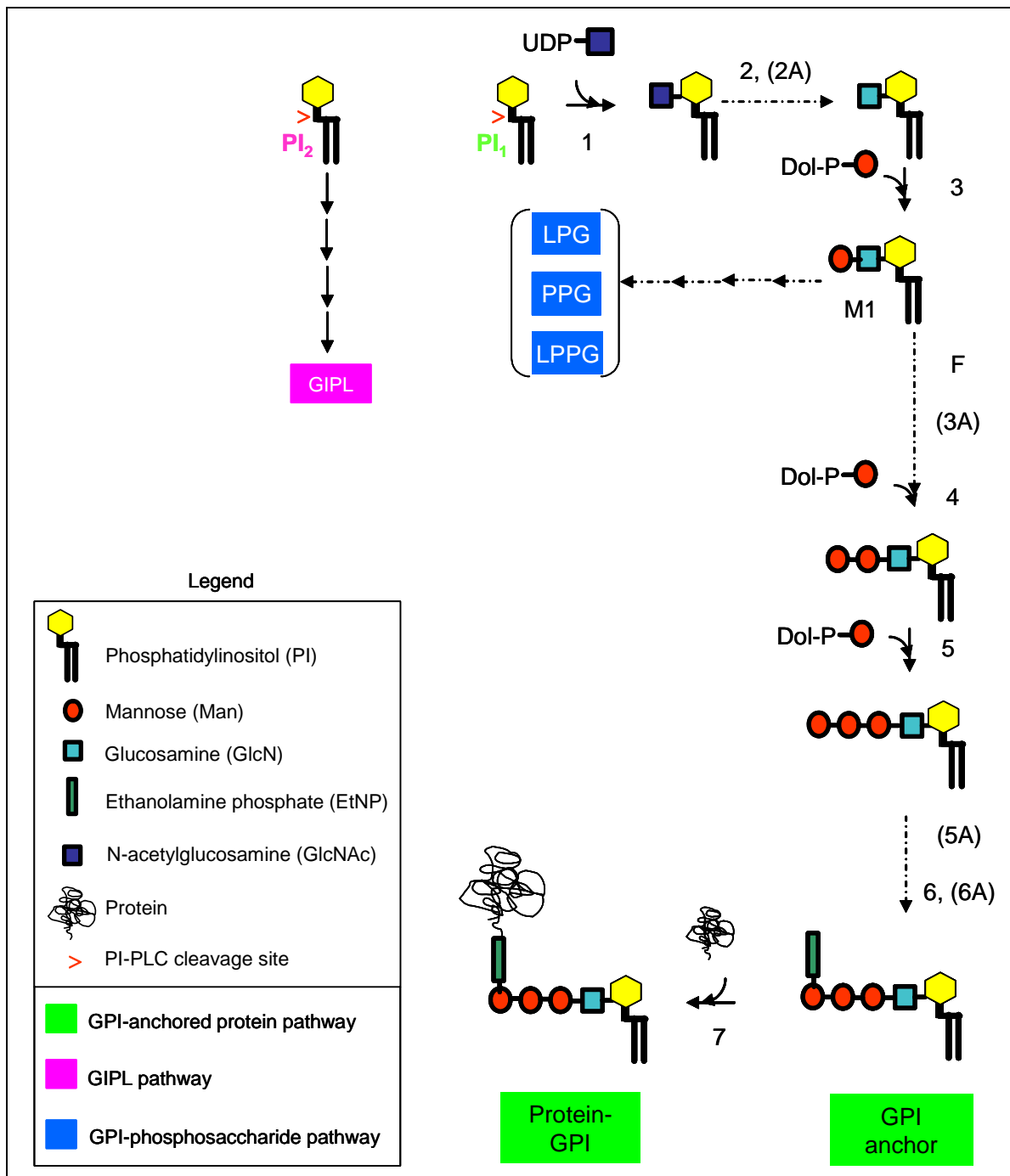


Illustration 5: Biosynthesis of glycosylphosphatidylinositol (GPI)-linked glycoconjugates. 1) GlcNAc transferase complex: Uridine-diphosphate-N-acetylglucosamine (UDP-GlcNAc) donates GlcNAc to phosphatidylinositol (PI)¹⁸⁸⁻¹⁹⁰, 2) GlcNAc-PI-de-N-acetylase: removal

of N-acetyl group from GlcNAc¹⁹¹⁻¹⁹², 2A) inositol-acyltransferase: addition of acyl group to GlcN-PI at position 2^{y,m, 193-197}, 3) GPI- α 1-4mannosyltransferase (MT), GPI-MT-I: transfer of mannose from dolichol-phosphate (Dol-P)-mannose to position 4 of GlcN¹⁹⁸, F) Flippase: translocation of the GPI-anchor precursor, GlcN-PI, within the endoplasmic reticulum membrane from the cytoplasmic to the luminal face¹⁹⁹, 3A) Ethanolamine phosphotransferase (EtNP-T), EtNP-T-I: addition of EtNP to the first mannose^{y,m,200-202}, 4) GPI- α 1-6mannosyltransferase GPI-MT-II: transfer of mannose from Dol-P-mannose to position 6 of the first mannose²⁰³⁻²⁰⁴, 5) GPI- α 1-2mannosyltransferase, GPI-MT-III: transfer of mannose from Dol-P-mannose to position 2 of the second mannose²⁰⁵⁻²⁰⁶, 5A) GPI- α 1-2mannosyltransferase, GPI-MT-IV: transfer of mannose from Dol-P-mannose to position 2 of the third mannose^{y,207}, 6) EtNP-T-III: transfer of EtNP from PI-EtN to the third mannose at position 6²⁰⁷⁻²⁰⁹, 6A) EtNP-T-II: transfer of EtNP to the second mannose at position 6^{y,210}, 7) Transamidase complex: removal of the GPI-anchoring signal sequence of the precursor protein and formation of an amide linkage between the amino group of EtNP in the GPI and the carboxyl group of the protein^{173, 185, 211-212}. Steps that are unique to the respective organism are indicated as follows: ^y, yeast; ^m, mammalian cells (reviewed in ²¹³). GIPLs and the GPI-phosphosaccharides, e.g., lipophosphoglycan (LPG), proteophosphoglycan (PPG), or lipophosphopeptidoglycan (LPPG) are formed from distinct precursors from the protein-GPI pathway, designated respectively as PI₂ and M1 (Man α 1-4GlcN-PI)²¹⁴. Zacks MA et al. *Recent developments in the molecular, biochemical and functional characterization of GPI8 and the GPI-anchoring mechanism [review]*. Mol Membr Biol, 2006. 23(3): p. 211.

THE GPI-ANCHORING MECHANISM

Overview

Cell surface expression of protein-GPIs involves both GPI biosynthesis and protein-GPI assembly⁹⁵. In overview, this process requires the targeting of a precursor protein to the endoplasmic reticulum via an N-terminal signal sequence, the recognition of a C-terminal GPI-anchoring signal sequence, the anchoring of the protein to a GPI and subsequently, the trafficking of the protein-GPI to the cell membrane for insertion into the phospholipid bilayer (Illustration 6)⁹⁵. The early steps in the assembly of GPI-anchors occur on the cytoplasmic face of the endoplasmic reticulum^{199,215,216}. The subsequent anchoring of the GPI to proteins is believed to occur on the luminal face of the ER where precursor proteins are translocated²¹⁶⁻²¹⁷. A flippase enzyme has been postulated to accomplish the change in orientation of the GPI-anchors from the outer to the inner membrane²¹⁸. The final step in GPI-anchoring involves the attachment of the preformed GPI to a precursor protein. Following GPI-attachment, GPI-anchored proteins are transported to the cell surface via Golgi vesicles²¹⁹.

Newly synthesized proteins that are destined to be GPI-anchored have two signal peptides. First, an N-terminal signal sequence directs the translocation of the protein across the ER membrane²²⁰⁻²²². Second, a C-terminal GPI-anchor addition signal sequence of the precursor protein is recognized, cleaved and replaced by the GPI-anchor in a postulated transamidase (TAM) reaction²²³. Analysis of the primary sequences of proteins that are demonstrated to receive GPI-anchors as well as signal sequence mutagenesis studies have been used to determine the characteristic features of the GPI anchor addition signal sequence. Sequence analysis of a variety of GPI-anchored proteins

has been used to create computer algorithms, e.g., DGPI²²⁴, and more recently, GPI-SOM²²⁵, to predict the presence of this C-terminal signal sequence in protein sequences²²⁶⁻²³³. Mutagenesis studies of these sequences indicate variabilities in the acceptable GPI-anchoring signals between organisms, particularly humans and trypanosomes. These analyses suggest that there are differences in the catalytic site of the postulated transamidase²³⁴⁻²³⁵.

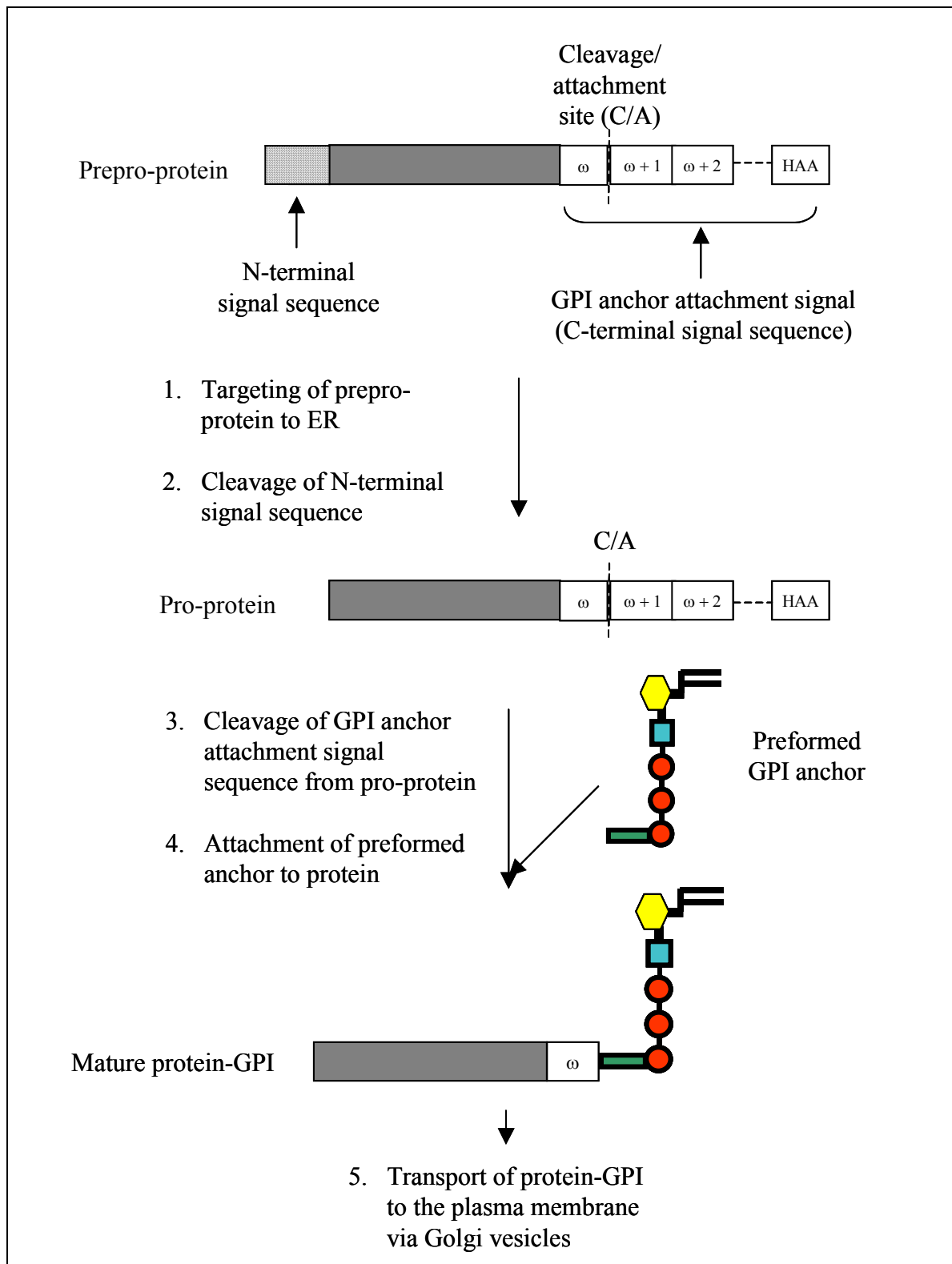


Illustration 6: Requirements for GPI transfer to protein and the GPI-anchoring mechanism. Precursor proteins (Prepro-protein) destined to receive a GPI-anchor contain two signal sequences, an N-terminal signal sequence and a C-terminal signal sequence, which respectively direct the translocation of the protein to the endoplasmic reticulum (ER) and the anchoring of the GPI to the protein. The C-terminal signal sequence is composed of three amino acids, (referred to as ω (omega), $\omega+1$, $\omega+2$), a short hydrophilic spacer element (designated ---), and a series of hydrophobic amino acids (HAA). Cleavage occurs between the ω and $\omega+1$ site and is followed by GPI attachment⁹⁸. Zacks MA, Garg N. *Recent developments in the molecular, biochemical and functional characterization of GPI8 and the GPI-anchoring mechanism [review]*. Mol Membr Biol, 2006. 23(3): p. 212.

THE TRANSAMIDATION (TAM) MECHANISM

GPI8 is believed to function as an enzyme which performs: 1) the proteolytic cleavage of the C-terminal signal sequence of precursor proteins, an endoproteolytic reaction and 2) the formation of a covalent bond between the carboxyl group of the protein and the amino group of the ethanolamine phosphate in the GPI, an amidation reaction (Illustration 7). Biochemical evidence indicates that these two enzymatic activities – endoproteolysis and amidation – are accomplished by a single enzyme and, therefore, have been termed a *transamidation* reaction²³⁶⁻²³⁷.

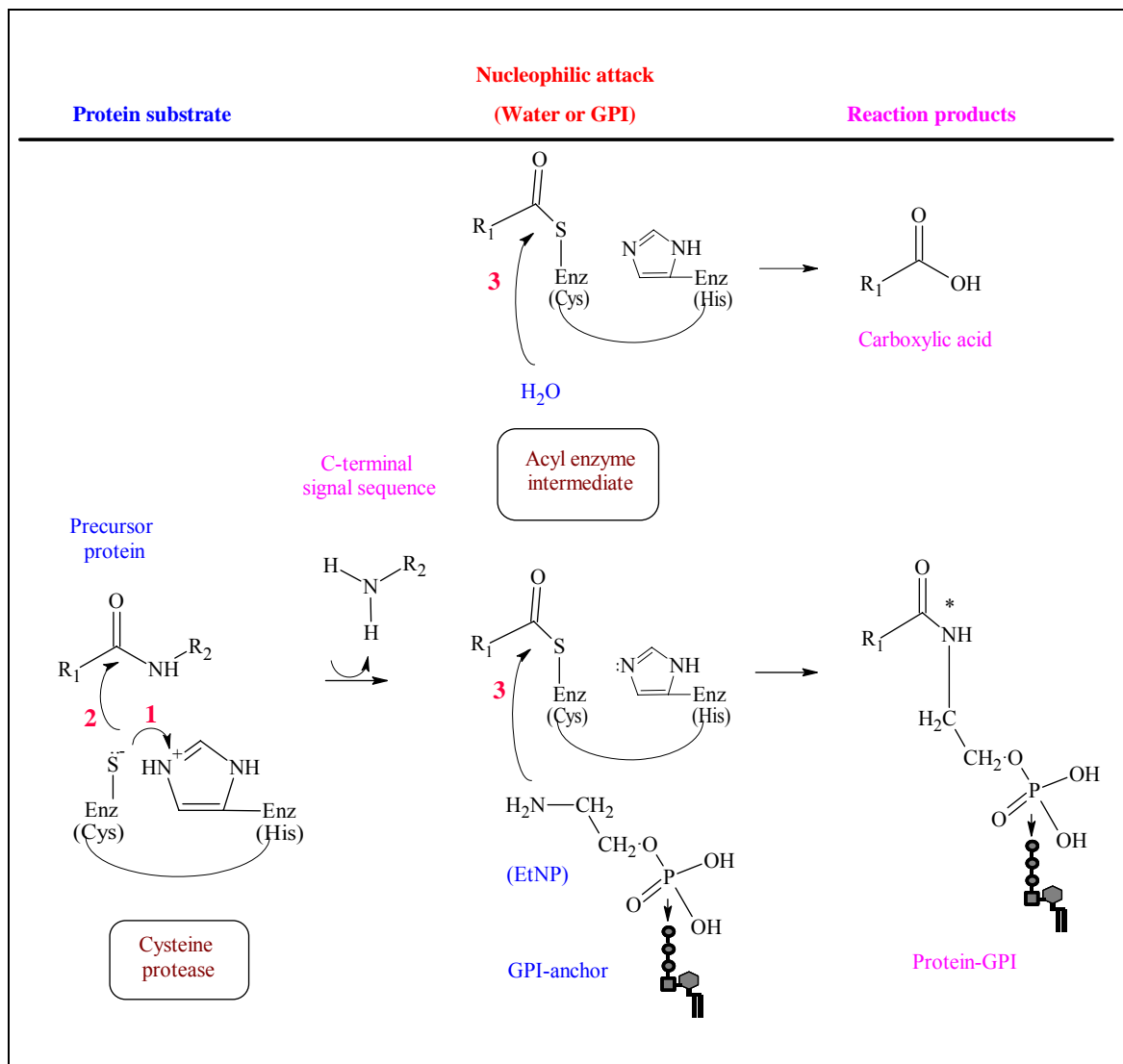


Illustration 7: The postulated catalytic mechanism for GPI-anchor attachment by GPI8. Cleavage of the C-terminal signal sequence of the precursor protein is believed to occur in an endoproteolytic reaction in which the peptide bond is cleaved between the ω and $\omega+1$ site within the protein chain, followed by GPI attachment to the protein in an amidation reaction. Cysteine proteases (enzyme, Enz) perform peptide bond hydrolysis via general acid: base catalysis, as follows: 1) The sulfhydryl (SH) group of the cysteine (Cys) residue is deprotonated by the histidine (His) residue, which acts as a “general base” or proton acceptor; 2) Nucleophilic attack of the Cys’s sulfur on the carbonyl carbon results in the cleavage of the peptide and the formation of an acyl-enzyme intermediate. 3) The transfer of acyl to water (H_2O), which serves as a nucleophile, releases

the Enz and results in the formation of carboxylic acid on the cleaved peptide. When GPI serves as the nucleophile, an amide bond (*) is formed between the nitrogen in the ethanolamine phosphate (EtNP) of the GPI and the carbonyl group of the protein, completing the attachment of a GPI to the protein. Alkyl groups of the protein are represented as R; R₁ corresponds to the portion of the precursor protein that is GPI-anchored; R₂ corresponds to the peptide or, in the case of protein-GPI anchoring, the C-terminal signal sequence that is released. (Diagram created in ChemSketch 5.0, Advanced Chemistry Development Inc.). Zacks MA, Garg N. *Recent developments in the molecular, biochemical and functional characterization of GPI8 and the GPI-anchoring mechanism [review]*. Mol Membr Biol, 2006. 23(3): p. 215.

BIOCHEMICAL EVIDENCE OF TAM

Several approaches have been used to support that a TAM mechanism accomplishes the anchoring of the GPI to a precursor protein^{95,223}. *In vitro* assays have been used to demonstrate the successive cleavage of the C-term SS and the attachment of a GPI-anchor in mammalian and yeast systems, as well as in *T. brucei*²³⁸⁻²⁴⁰. Specifically, GPI-reporter protein assays, protein crosslinking studies, and *in vitro* biochemical assays have been used to demonstrate key aspects of the TAM biochemical mechanism.

Reporter assays

Reporter assays have been utilized to monitor the steps involved in GPI-anchoring using precursor proteins, either endogenous protein substrates^{238-239,241-242} or reporter proteins such as placental alkaline phosphatase (PLAP)^{229, 241} or VSG117²⁴³.

PLAP Assay

In vitro PLAP translation assay (Illustration 8) was developed to demonstrate the post- (or co-) translational processing of the engineered protein precursor, pre-pro-PLAP,

by rough microsomal membranes isolated from different organisms including yeast²⁴² and mammalian cells²⁴⁴. Rough microsomes provide the enzymatic activity for cleavage of the N-terminal signal sequence, the C-terminal GPI-anchoring signal sequence, followed by GPI-anchor attachment. Initially, a full-length PLAP construct was used as the GPI-reporter protein. Later, the reporter assay was refined to utilize a more convenient truncated version or "mini-PLAP"^{229, 241}. Hydrazine (HDZ) or hydroxylamine (HAM) was further added as a co-reactant in the PLAP assay. HDZ and HAM serve as nucleophiles in the anchoring reaction, competing with the GPI-anchor to form a mini-PLAP product²⁴⁵, presumed to be a hydrazide or a hydroxamate, respectively. This observation has provided support for TAM-mediated anchoring, as hydrazine or hydroxylamine would participate in this reaction by formation of a hypothesized carbonyl intermediate. Since mature mini-PLAP has not been detected in assays of rough microsomes which are GPI-anchoring deficient, the TAM is believed to perform proteolytic cleavage of the anchoring signal sequence as well as the linkage of the GPI-anchor to the protein²³⁶.

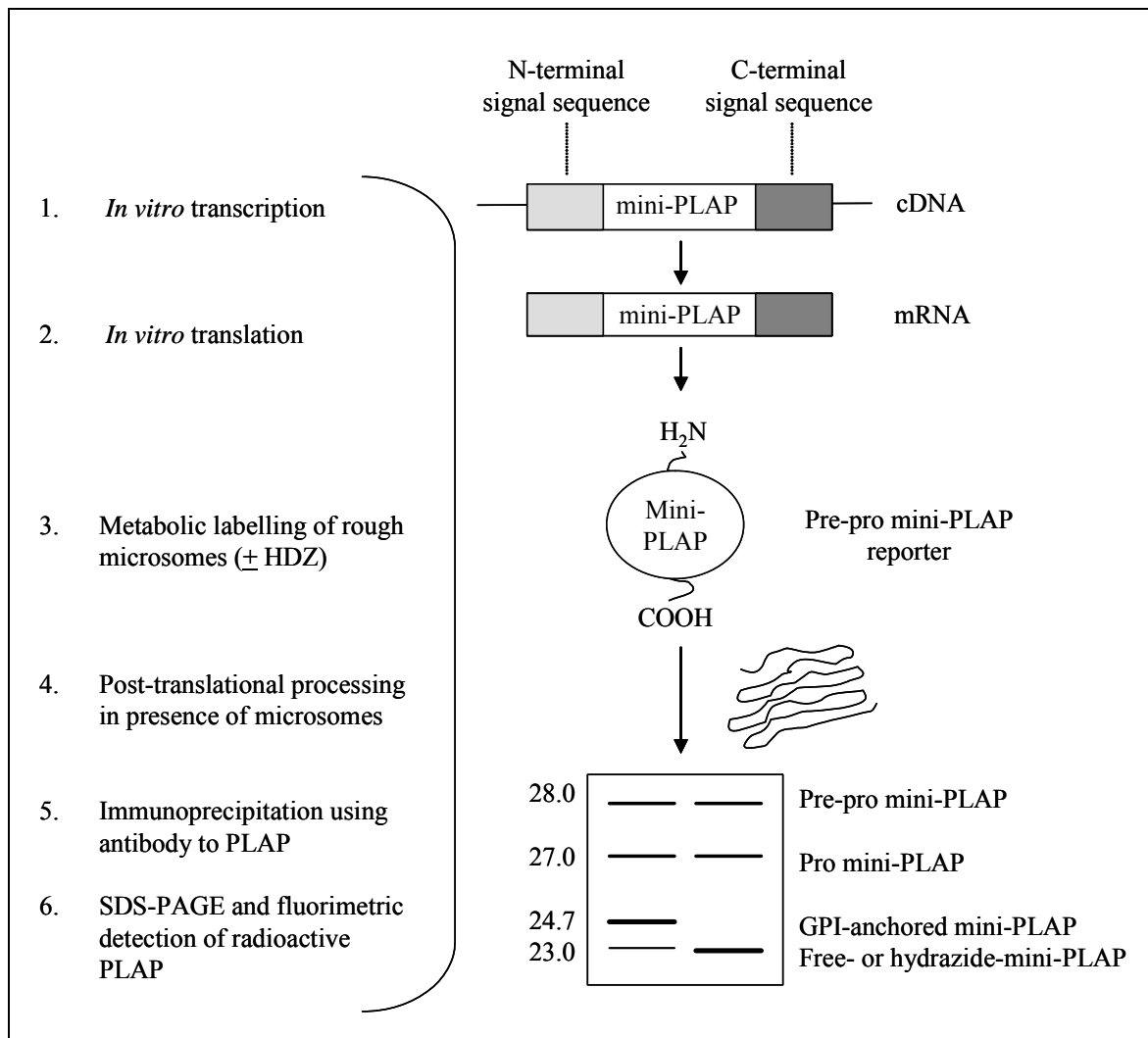


Illustration 8: The mini-PLAP GPI-reporter assay. Pre-pro-miniPLAP cDNA is transcribed *in vitro* and then translated *in vitro* using rabbit reticulocyte lysates. The translation reactions are incubated with metabolically radiolabeled rough microsomal membranes isolated from the cells of interest. Reactions are performed in the presence or absence of hydrazine (HDZ). The reaction products are then assessed by immunoprecipitation with anti-PLAP antibody and are readily identified by SDS-PAGE migration of the indicated radiolabeled proteins^{229,241}.

***T. brucei* VSG117 assay**

A trypanosome cell free system was developed to monitor the processing of VSG117 as a VSG-hydrazide form in GPI-anchoring competent *T. brucei*. This assay utilized rough microsomes of *T. brucei* procyclic forms that were engineered to express a reporter precursor protein, the non-endogenous VSG variant, VSG117. The fate of this GPI-reporter protein could be monitored by metabolic labeling, followed by immunoprecipitation with anti-VSG117 antibody. Immunoprecipitation reactions were resolved by SDS-PAGE and the migration visualized by fluorometric analysis, analogous to the mini-PLAP assay. This assay showed that VSG117 was released in 20-40 minutes following addition of HDZ and that release was optimal at 37°C, suggestive of enzyme-mediated activity. Monitoring of this reaction with HDZ following complete inhibition of GPI-anchor biosynthesis by mannosamine demonstrated that HDZ was incorporated into VSG, acting directly as a nucleophilic amine to form a hydrazide, in further support of the hypothesized TAM mechanism²³⁹.

This assay was further used to evaluate the role of GPI8 in the GPI-anchoring mechanism of trypanosomes. When *T. brucei* was depleted of soluble endoplasmic reticulum contents by incubation under high pH conditions, the extracted rough microsomes were unable to form VSG-hydrazide. Reconstitution of rough microsomes with recombinant *Leishmania mexicana* GPI8 (LmGPI8) restored the production of VSG-hydrazide. These results suggest that LmGPI8 is a soluble protein that functions as a homologue of the *T. brucei* GPI8 to perform GPI-anchoring. Further, this activity is sensitive to treatment of either recombinant LmGPI8 or of *T. brucei* microsomal membranes with iodoacetamide, indicative of the importance of disulfide bond formation or of catalysis by sulfhydryl residue(s) in the anchoring mechanism. Thus, the VSG117

assay provided further evidence of the role of GPI8 in TAM-mediated GPI-anchoring in trypanosomes²⁴³.

Crosslinking studies

The association of mammalian GPI8 with pro-protein substrates has been demonstrated *in vitro*²⁴⁶⁻²⁴⁷. One approach was to crosslink human GPI8 (hGPI8) to the prepro-mini-PLAP reporter protein into which an artificial photoreactive probe was incorporated. *In vitro* transcription/translation of the mini-PLAP was performed in the presence of rough microsomes from human cells, demonstrating the translocation and processing of prepro-mini-PLAP to mature (GPI-anchored) mini-PLAP into rough microsomes²⁴⁶.

To demonstrate that human GPI8 (hGPI8), presumed to be present in rough microsomes, was associated with this artificial substrate, similar crosslinking experiments were subsequently performed with rough microsomes from human cells that over-express recombinant (FLAG-tagged) hGPI8. Anti-FLAG antibody effectively co-precipitated the photoreactive mini-PLAP crosslinked to hGPI8, demonstrating its close proximity to this artificial substrate in the GPI-anchoring reaction²⁴⁶. A similar conclusion that hGPI8 associated with mini-PLAP was obtained using semi-permeabilized cells treated with the crosslinking agent, bismaleimido-hexane. While PLAP was crosslinked to hGPI8 in K562 cells, no association was detected in hGPI8-deficient K562 mutants, providing evidence that GPI8 is a necessary component in GPI-anchoring²⁴⁷.

IN VITRO BIOCHEMICAL ASSAY

An assay was developed to reconstitute peptidase or GPI-anchoring activity of GPI8 *in vitro*^{212, 243}. Monitoring the cleavage of a fluorogenic peptide substrate, designed to mimic a signal sequence for GPI-anchoring, by whole *T. brucei* lysates, provided indirect evidence for TAM-like activity. This methodology was subsequently used in a reaction with recombinant TbGPI8, providing direct evidence for the role of GPI8 in proteolytic cleavage²¹².

IDENTIFICATION OF THE GENES INVOLVED IN TRANSAMIDATION

Both reverse (phenotype to gene) and forward (gene to phenotype) genetic approaches have been utilized in different eukaryotic organisms to identify *GPI8*, the gene that encodes the TAM responsible for GPI-anchoring (Illustration 9)^{95, 213}.

Yeast and mammalian GPI8: reverse genetics approach

The first indication that GPI8 plays a role in transamidation was provided by studies of the yeast, *Saccharomyces cerevisiae*. Several temperature-sensitive mutant yeast strains, defective in their ability to express GPI-APs on their surface, were generated via chemical mutagenesis²⁴⁸. By transforming the temperature-sensitive strain with a yeast chromosomal DNA library, the complementing gene, named yeast *GPI8* (*yGPI8*), was isolated and sequenced²¹¹. *yGPI8* was disrupted in the parental wild type strain. This proved to be lethal²¹¹, as would be hypothesized from studies indicating that GPI-APs are essential in yeast^{201, 249-252}. A human homologue of *yGPI8* was cloned using

the yGPI8 sequence information and expressed in the temperature-sensitive yeast strain under control of a yeast promoter; hGPI8 was able to rescue the growth of these temperature-sensitive mutants²¹¹.

By similar approach to that in yeast, the human *GPI8* (*hGPI8*) gene was identified and characterized (Illustration 9). Unlike in yeast, mammalian cells appear to be less

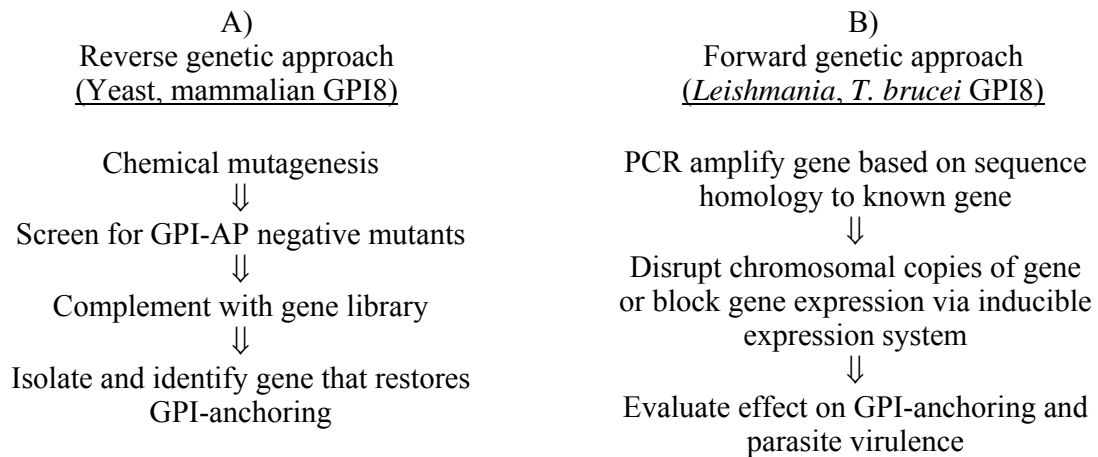


Illustration 9: General experimental approaches for the identification of the transamidase, GPI8, in yeast, mammalian cells and trypanosomes. A reverse genetics approach was utilized in yeast and mammalian cells, whereby mutants were created using chemical mutagenesis and phenotypic screening of these mutants indicated a protein defect or deficiency. Subsequently, by transformation of the mutant cells with a library of genes, the gene was isolated by its ability to restore or "complement" the phenotype conferred by the protein deficiency. In the trypanosomes *L. mexicana* and *T. brucei*, the *GPI8* gene was identified using a forward genetics approach. Based upon homology to the other known *GPI8*s, the genes were cloned and sequenced. The general experimental strategy utilized PCR amplification of the gene from the chromosomal copy based upon homology to other known *GPI8*s, PCR product cloning, followed by sequencing of the gene. Gene disruption ("knockout") or inducible repression of expression ("knock-down") was then performed to demonstrate the effect on GPI-anchoring.

dependent *in vitro* upon GPI-APs. Thus, viable cell lines defective in surface expression of GPI-APs could be generated^{183,186-187}. Chemical (N-methyl-N'-nitro-N-

nitrosoguanidine) mutagenesis of the human lymphoblast K562 cell line, followed by fluorescence activated cell sorting of a DAF-negative cell population and fusion with previously characterized mutants, allowed the isolation of a new genetic mutant, designated class K, which lacked surface expression of GPI-anchored proteins, exhibited markedly increased amounts of mature GPIs, but was deficient in a step preliminary to or associated with protein transfer of assembled GPIs^{183, 211}. In the parental K562 line, the *hGPI8* gene was PCR-cloned based upon homology to the *yGPI8*, and hGPI8 was shown to be defective in the class K mutant line. Expression of hGPI8 by transfection of the class K line resulted in the restoration of GPI-anchoring¹⁸⁵. Together, these results indicated that *yGPI8* is likely to be responsible for attaching the GPI-anchor to proteins in yeast and that hGPI8 is a functional homologue.

Trypanosome GPI8: forward genetics approach

In both *Leishmania mexicana* (*Lm*) and *T. brucei* (*Tb*), the *GPI8* genes were identified by the forward genetics approach (Illustration 9). *LmGPI8* null mutants were produced by targeted disruption of both alleles of *LmGPI8* in *L. mexicana* promastigotes. This resulted in loss of surface expression of the major GPI-anchored protein, gp63¹⁷³, which was secreted in unanchored form²⁵³. Expression of non-protein linked glycoconjugates, LPG and GIPLs, was unaffected. This indicated that *LmGPI8* is involved exclusively in GPI-anchoring to proteins and not the synthesis of GPIs. Furthermore, episomal expression of *LmGPI8* in null mutants (*LmΔGPI8*) restored expression of gp63¹⁷³. These data establish that *LmGPI8* is responsible for GPI-anchoring, as for the yeast and mammalian homologues.

In *T. brucei* procyclic insect form, *TbGPI8* null (*TbΔGPI8*) mutants were generated via targeted disruption of *TbGPI8* using a homologous recombination

approach. This resulted in the loss of GPI-anchored procyclin expression. In addition, Tb Δ GPI8 accumulated GPI-anchor precursors. When TbGPI8 expression was restored to Tb Δ GPI8 by integration of a copy of *TbGPI8* in the tubulin locus, procyclins were detected at wild type levels¹⁸⁰. In bloodstream forms, the double stranded RNA interference (dsRNAi) approach was used for functional studies. In this system, *TbGPI8* mRNA depletion occurs upon tetracycline induction of T7 promoter-driven transcription of complementary *TbGPI8* RNA. These RNAs hybridize to form double-stranded RNA. Thereby, expression of the corresponding RNA-encoded protein, e.g., TbGPI8, is reduced. In *T. brucei*, the loss of TbGPI8 expression resulted in the accumulation of the unanchored form of VSG¹⁸⁰. Thus, TbGPI8 functions analogously to yeast, human and *L. mexicana* GPI8s in the anchoring of GPIs to proteins.

Summary

Search of public genomic databases reveals that *GPI8* homologues exist in apicomplexan parasites (*Plasmodium falciparum*, *Toxoplasma gondii*), in plants (*Arabidopsis thaliana*), and other eukaryotes (*Caenorhabditis elegans*, *Drosophila melanogaster*)²⁵⁴. These genes have not as yet been functionally characterized. Further investigations of their activity will likely increase our understanding of the transamidase mechanism, substrate specificity, and the overall function and essentiality of GPI-anchored proteins in other organisms. Several predicted features of GPI8s in these organisms combined with experimentally demonstrated characteristics suggest that trypanosome (*Leishmania*, *T. brucei* and *T. cruzi*) GPI8s are distinct from human and yeast GPI8²⁵⁵ and that species-specific inhibitors can be developed for anti-protozoal therapeutics, as has been demonstrated for other GPI-biosynthetic enzymes^{195-196,256-257}.

CHARACTERISTICS OF THE GPI8 PROTEIN

The yGPI8 was predicted to encode a 47 kDa protein with three potential N-glycosylation sites. The topology of a *type I* protein (containing a lumenally oriented N-terminal domain) localized to the endoplasmic reticulum (ER) was predicted by the presence of a transmembrane segment and of a hydrophobic N-terminal SS. These features were confirmed experimentally²¹¹. LmGPI8 was predicted to encode a 38 kDa protein, as compared to 47 kDa yeast and human GPI8, with 31% identical sequence to yGPI8 and hGPI8. An N-terminal SS was present; however, LmGPI8 lacks the predicted C-terminal transmembrane helical domain found in yGPI8 and hGPI8¹⁷³. TbGPI8 was predicted to encode a 37 kDa protein with one potential N-glycosylation site. As for LmGPI8, there is no predicted C-terminal helical transmembrane domain. The comparative features of GPI8s in different organisms are summarized in Illustration 10⁹⁵. These protein predictions suggest that GPI8s may comprise two general groups: 1) *type I* transmembrane proteins, e.g., yeast and human GPI8, and 2) soluble proteins, e.g., *T. brucei* and *L. mexicana* GPI8²⁵⁸.

Organism	Accession no.	No. of amino acids	Predicted (detected) protein size in kDa	No. of predicted (confirmed) N-glycosylation sites	Trans-membrane domain
<i>S. cerevisiae</i>	P49018	395	47 (50)	3 (3)	Yes
<i>H. sapiens</i>	Q92643	411	47 (45)	0	Yes
<i>L. mexicana</i>	AJ242865	349	38 (42)	3 (nd)	No
<i>T. brucei</i>	AJ308106	319	37 (nd)	1 (nd)	No
<i>T. cruzi</i>	na ¹	325	37 (nd)	1 (nd)	No

Illustration 10: Characteristics of GPI8s in the organisms studied to date. The predicted and/or experimentally confirmed features of the GPI8 protein in *S. cerevisiae*²¹¹, *H. sapiens*¹⁸⁵, *L. mexicana*²⁵³, *T. brucei*²¹² and *T. cruzi* are listed. ¹*TcGPI8* sequence is identified as "GPI-anchor transamidase subunit 8, putative", location in genome: 8643:107468-108445²⁵⁹. Abbreviations: nd, not demonstrated; na, not available.

HOMOLOGY OF GPI8 TO ENDOPEPTIDASES

The hypothesis that GPI8 functions in the catalysis of transamidation arose from the amino acid homology, predicted motifs and secondary structural features that suggested GPI8s function as proteases⁹⁵. Specifically, GPI8s are classified among the CD clan of cysteine proteases, and are further subdivided into the C13 family, based upon their mechanism of peptide bond hydrolysis²⁶⁰⁻²⁶¹. This family includes peptidases found in legumes^{83,262-264}, in mammals²⁶⁵⁻²⁶⁶ and in nematodes, e.g., *Schistosoma mansoni*²⁶⁷⁻²⁶⁸.

The asparaginyl endopeptidases, originally identified in leguminous plants and so named *legumains*, have been shown to participate in the proteolytic processing of concanavalin A and of other pro-proteins present in their seeds^{83,262,269,270-271}. These

peptidases exhibit specificity for cleavage of small peptides and proteins at asparagine residues²⁷². More recently, mammalian homologues of legumain have been identified in lysosomes²⁶⁵⁻²⁶⁶ and may function in the proteolytic processing of bacterial antigens and pro-enzymes²⁷³. A group of homologues in *Schistosoma species* – cathepsin B, D, and L and hemoglobinase – cooperate in the degradation of hemoglobin²⁶⁸. Finally, clostripain, gingipain and numerous other examples have been described in pathogenic bacteria such as *Porphyromonas gingivalis* and *Clostridium histolyticum*²⁷⁴⁻²⁷⁶. The presence of conserved residues in the predicted active site of these peptidases dictates their catalytic activity. Likewise, the role of GPI8 in GPI-anchoring in yeast²⁷⁷, mammalian cells²⁷⁸ and *Leishmania*²⁵³ is suggested by the significant amino acid homology of GPI8s with other C13 peptidases.

ENDOPEPTIDASE MECHANISM

Cleavage of a protein within the peptide chain, *endopeptidation*, has been demonstrated to occur via general acid-base catalysis (Illustration 7). The conserved residues defining the catalytic diad of the active site of C13 proteases function in concert to cleave the peptide bond. First, the histidine (His) residue acts as a "general base" (proton acceptor), deprotonating the sulfhydryl group of cysteine. Secondly, the sulfur of the cysteine (Cys) residue mounts a nucleophilic attack on the carbonyl carbon of the peptide²⁶¹. This results in the hydrolysis of the peptide bond. In the postulated GPI-anchoring mechanism, the GPI-anchor then acts as the nucleophile, forming an amide bond between the nitrogen in the ethanolamine phosphate and the carbonyl group of the peptide. Although differences exist in the substrate specificity, in part dictated by the amino acid residue(s) in the protein that is (are) susceptible to cleavage by the peptidase,

the critical importance of Cys in the catalytic mechanism is suggested by the sensitivity of GPI-anchoring in trypanosome cell-free systems to sulfhydryl alkylating reagents^{212,239,243}.

ACTIVE SITE STUDIES OF GPI8

At present, no 3D structure has been constructed for any member of the C13 family²²⁴ to facilitate a molecular model for understanding the catalytic and other domains of GPI8. Alternatively, functional studies of purified enzymes as well as site-directed mutagenesis of conserved residues in the putative active site have been used to characterize their mechanism of activity⁹⁵. For legumain, mutation of putative active site residues representing the proposed catalytic dyad resulted in a loss of protease activity and establishing the histidine and cysteine residues as critical to the active site of legumain²⁷². Among the C13 family proteins identified, two cysteine and two histidine residues are conserved among the majority of the members. This has provided a parallel approach for studying the GPI-anchoring mechanism; active site studies have been published for yGPI8²⁷⁷, hGPI8²⁷⁸, and LmGPI8²⁵³ (Illustration 11).

<i>S. cerevisiae</i>	YR H MANVLSMYRTVKRLGIPDSQIILMLSDDDVACNSRNLFPGSVFNNK-----DHAI	103
<i>H. sapiens</i>	YRHVANTLSVYRSVKRLGIPDSHIVLMLADDMACNPRNPKPATVFSHK-----NMEL	110
<i>L. mexicana</i>	YR H TANALTMYLRLRQHGIDDDHILLFLSDSFACDPRNVYPAEIFSQPPGAHDADGRASM	120
<i>S. cerevisiae</i>	DLYGDSVEVDYRGYEVTVENFIRLLTDRWTEHPKSKRLTDENSNIFIYMTG H GGDDFL	163
<i>H. sapiens</i>	NVYGDDVEVDYRSYEVTVENFLRVLTGRIPPSTPRSKRLSDDRSNILIYMTG H GGNGFL	170
<i>L. mexicana</i>	NLYGCSAQVDYAGSDVDVRRFLSVLQGRYDENTPPTRRLSDNTSNIIIVAG H GAKSYF	180
<i>S. cerevisiae</i>	KFQDAEEIASEDIADAFQQMYEKKRYNEIFFMIDT C QANTMYSKFYSPNILAVGSSEMDE	223
<i>H. sapiens</i>	KFQDSEEITNIELADAFEQMWQKRRYNELLFIIDT C QGASMYERFYSPNIMALASSQVGE	230
<i>L. mexicana</i>	KFYQDTEFLSSSDISETLTMMHQRRYGRVVFLADT C HAIALCEHVEAPNVVCLAASDAES	240

Illustration 11: The ClustalW alignment of GPI8s. For GPI8s identified in *S. cerevisiae* (yeast, accession #P49018), *H. sapiens* (human, accession #Q92643), and *L. mexicana* (accession #AJ242865), the conserved cysteine and histidine residues (highlighted in red) of the indicated GPI8s were mutated and expressed in the respective organism^{253,277-278}.

Yeast GPI8 (yGPI8)

The *yGPI8* gene was cloned into plasmid vectors for expression under control of the native GPI8 promoter, the galactose-inducible *GAL1-10* promoter (chromosomally integrated), or the Cu⁺²-inducible *CUP1* promoter²⁷⁷. The conserved residues in yGPI8 were individually mutated to alanine (A), and these alleles were investigated for their ability to: 1) restore viability and/or GPI-anchoring to conditional temperature-sensitive *yGPI8* mutants or *yGPI8* null mutants (Δ GPI8), or 2) produce dominant-negative phenotypic effects on wild type (parental) yeast strains, e.g., growth impairment, lethality, and/or GPI-anchoring defects²¹¹. The first approach demonstrated that expression of the Cys199A and His157A alleles was not capable of restoring the viability of Δ GPI8 spores or growth of the temperature-sensitive mutants at 37°C whereas the other mutant alleles, Cys85A and His54A, provided functional complementation. The second approach revealed that expression of the Cys199A and His157A alleles resulted in accumulation of GPI-anchor precursors and in growth arrest. In the transformed wild type

yeast, these phenotypic effects were only observed when >10-fold increased expression of mutant yGPI8 alleles was achieved via the *CUP1* or *GAL1-10* promoter.

The phenotypic correlation with the level of GPI8 expression was further confirmed in the Δ *GPI8* strain using the *GAL1-10/yGPI8* construct. In this case, time-dependent depletion of unmutated GPI8 expression was monitored during shift from galactose to glucose-rich medium and correlated with the decline in growth. The effect of GPI8 depletion of GPI-anchoring was evaluated by monitoring of the GPI-anchored protein, GAS1; in the parental strain, GPI-anchoring of GAS1 is demonstrated by a change in apparent SDS-PAGE migration from 105 kDa (unanchored) to 125 kDa (anchored and glycosylated). In contrast, when the Cys199A mutant allele of yGPI8 was expressed in the parental strain, the unanchored 105 kDa form of GAS1 was detected²⁷⁷. Together, these data indicate that Cys199 and His157 represent the catalytic diad of yGPI8, consistent with the proposed enzymatic mechanism.

Human GPI8 (hGPI8)

Since analogous Cys and His residues are conserved in hGPI8, the Cys92, His164, and Cys206 residues were investigated as potential active site residues (Illustration 11). Plasmid vectors containing hGPI8 mutated in these amino acids were constructed for expression in class K hGPI8-defective mutants. The restoration of GPI-anchoring by complementation was assessed in flow cytometric analysis of CD59 expression following transfection. Expression of either the His164A or the Cys206A mutant allele in class K mutants did not functionally complement the hGPI8-deficiency to restore the GPI-anchoring of CD59²⁷⁸ unlike Cys92A.

The mini-PLAP assay (Illustration 8) demonstrated that these mutant alleles were unable to process prepro-mini-PLAP to either the GPI-anchored or the hydrazide-linked

form, unlike in class K mutants that were transfected with unmutated hGPI8. Interestingly, yGPI8 was not able to complement the class K mutants. Further, in class K mutants, expression of a chimeric GPI8, in which ~60 residues of the C-terminal portion of the hGPI8 was replaced with yGPI8 sequence, restored anchoring of CD69²⁷⁸. These data suggest that the conserved residues function in the active site of yGPI8 and hGPI8 but that other properties of the protein may be important in interaction with the TAM complex or the substrate precursor protein, presumably for recognition of the GPI-anchoring signal sequence.

***Leishmania mexicana* GPI8 (LmGPI8)**

In LmGPI8, these potential active site residues are also conserved (Illustration 11). The ability of mutant LmGPI8 alleles to functionally complement *LmGPI8* null mutants (LmΔGPI8) of *L. mexicana* was used to assess the role of these conserved residues in the active site of LmGPI8²⁵³.

As a methodological alternative to FACS analysis of surface expressed GPI-anchored protein in *L. mexicana*, pulse-chase followed by SDS-PAGE/WB analysis was employed. In this approach, metabolic radiolabeling of proteins, e.g incubation of live parasites with ³⁵S-cysteine/methionine, followed by addition of non-radiolabeled medium, enables the monitoring of protein expression with time. WB analysis was employed to evaluate the effects of expression of mutant LmGPI8 alleles on GPI-anchoring of gp63. In addition, *Leishmania* proteins were extracted with Triton-X114 to determine the presence of gp63 in soluble (aqueous) and membrane (detergent) protein fractions comparing LmGPI8 mutant with wild type parasites. Treatment of *Leishmania* with PI-PLC results in the release of surface expressed GPI-anchored proteins into the Triton-X114 aqueous phase; GPI-anchored proteins, e.g., gp63, could then be detected in

the aqueous fraction of PI-PLC treated parasites, suggesting that gp63 is presumably expressed on the surface.

In *LmGPI8* null (*LmΔGPI8*) mutants of *L. mexicana*, PI-PLC treatment failed to release gp63 into the Triton-X114 aqueous phase. Expression and anchoring of gp63 was restored in *LmΔGPI8* transfected with unmutated *LmGPI8* as well as for H63A and C94G mutant alleles. In contrast, gp63 anchoring in *LmΔGPI8* transfected with C216G or H174A was not restored. Pulse-chase/WB analysis showed that gp63 was secreted into the medium in *LmΔGPI8* transfected with C216G and H174A alleles. Detection of gp63 in the detergent fraction (surface expressed gp63) despite PI-PLC treatment indicated that gp63 was unanchored. In addition, wild type *L. mexicana* was transfected with the C216G allele. With increased concentration of selective drug (G418), surface expression of gp63 was diminished in a dose-dependent fashion, further supporting the conclusion that this allele was non-functional. In summary, C216G and H174A produced a dominant-negative effect on GPI-anchoring in wild type *L. mexicana* and were unable to complement GPI8 null mutants²⁵³. Collectively, these results indicated that the *LmGPI8* alleles C216 and H174 were analogous to the active site residues of yGPI8.

OTHER PROTEINS INVOLVED IN THE TAM MECHANISM

While GPI8 is the catalytic component involved in protein-GPI anchoring reaction, it functions in cooperation with other essential proteins as a multi-subunit complex, named the transamidase (TAM) complex. Genetic and biochemical approaches have identified, in addition to GPI8, two protein subunits of this complex, namely GAA1 and GPI16/PIG-T, which are common to all eukaryotic organisms. GPI17/PIG-S and CDC91/PIG-U are detected in yeast and mammalian TAM, but are absent from

trypanosomatids, which, alternatively, possess TTA1 and TTA2. These TAM components are detailed below and their structural features are depicted in Illustration 12⁹⁵.

Yeast

In yeast, four proteins – yGAA1, GPI16, GPI17, and CDC91– have been identified by various experimental approaches as likely components of the TAM complex that accomplish GPI-anchoring in participation with yGPI8^{251,279-281}.

yGAA1

The yeast mutant, *end2*, was used to establish that yGAA1 participates in the attachment of GPI-anchors to precursor proteins. This mutant showed reduced or blocked maturation of the GPI-anchored protein GAS1p at 24°C and 37°C, respectively. In addition, [³H]-inositol incorporation into proteins over a 45 minute pulse time was reduced at both temperatures, indicating that this mutant failed to attach the radioactively-labeled GPI-anchor to proteins, although capable of synthesizing the complete GPI anchor precursor. Complementation of the mutant with a yeast plasmid DNA library led to the identification of a common sequence for 16 of 8000 colonies that were able to grow when shifted to 37°C²⁵¹.

Isolation and sequencing of the complementing gene, named *gaa1* for *GPI-anchor attachment*, predicted a 68 kDa, multipass transmembrane protein with an ER retention sequence and two N-linked glycosylation sequences. Site-directed mutagenesis as well as endoglycosidase treatment indicated N-glycosylation occurred at one site; ER-localization of over-expressed yGAA1 was demonstrated by immunofluorescence staining that co-localized with that of Wbp1p, an ER resident protein. In addition,

yGAA1 was detected in Triton-X100 extracts but not carbonate-extracted protein fractions, indicating that it is a membrane protein²⁵¹.

To evaluate the role of yGAA1 in GPI-anchoring in yeast, two approaches were used. First, the temperature-sensitive *end2* yeast mutant was transfected with a plasmid containing the *ygaal* gene. This resulted in the restored growth at 37°C, as well as incorporation of inositol-containing GPI-anchors into proteins. Secondly, *ygaal* was disrupted in the parental yeast strain. Targeted disruption of *ygaal* was lethal, and growth could be rescued by over-expression of GAA1²⁵¹. While both yGAA1 and yGPI8 are essential for GPI-anchoring, yGAA1 is not homologous to any known proteins in genome databases to suggest its specific function and to guide further study.

GPI16 and GPI17

Another yGPI8 interacting protein, GPI16, was identified by blue native polyacrylamide-gel electrophoresis (BN-PAGE)²⁷⁹, a technique that facilitates the co-immunoprecipitation of membrane-bound and multi-subunit protein complexes. Preservation of native protein complexes is accomplished by extraction in digitonin and visualization on a non-denaturing polyacrylamide gel. The individual subunits are then resolved on a second dimension denaturing gel²⁸². GST-tagged yGPI8 was over-expressed in $\Delta gpi8$ yeast mutants. The multiprotein complex containing yGPI8-GST was extracted from microsomal membranes in digitonin, purified via glutathione-Sepharose affinity chromatography and resolved by BN-PAGE. WB using yGPI8 antiserum confirmed the purification of yGPI8-GST. Mass spectrophotometric analysis of tryptic digests of the protein bands found to associate with yGPI8-GST identified two interacting proteins, GAA1 and YHR188c, based upon published yeast sequence data. YHR188c was renamed GPI16.

To evaluate the role of GPI16 in GPI-anchoring, *Δgpi16* was constructed for evaluation of TAM complex formation and GPI-anchoring, along with the previously described *Δgpi8* mutant. *Δgpi16* mutants accumulated mature forms of GPI-anchors but were unable to process complete GPI-proteins, e.g., mature Gas1p and Cwp1p. In addition, GST-yGPI8 was over-expressed in *Δgpi8* mutants, and co-immunoprecipitation of multiprotein complexes was performed to identify interacting proteins. Under conditions of GST-yGPI8 over-expression, high molecular weight complexes were formed. However, under conditions that resulted in GST-yGPI8 depletion, e.g., shift to glucose rich medium, these complexes were no longer detected, and GPI16 was unstable. Likewise, for *Δgpi16*, upon shift to glucose, there was a decrease in yGPI8 detection²⁷⁹. Deletion of *gpi16* and *gpi17* was lethal²⁸³. *Δgpi16* and *Δgpi17* mutants that express the respective genes under control of *GALI* were constructed. When shifted to growth in glucose to reverse over-expression, these mutants accumulated mature precursors, as is observed in the other anchoring deficient mutants, e.g., *Δgpi8* and *Δgaa1*²⁸⁰. These results suggest that GPI16 and yGPI8 together are required for stable formation of the TAM enzyme complex to provide anchoring activity²⁷⁹⁻²⁸⁰.

CDC91

An additional yeast gene, *cdc91*, which may be involved in the TAM mechanism, was identified²⁸¹ as a structural homologue of PIG-U in mammalian cells, described below, but has not, to date, been functionally characterized in yeast.

Mammalian cells

TAM complex proteins – GAA1, PIG-S, PIG-T and PIG-U – have been identified in mammalian cells^{258,278,280-281,284-285}.

GAA1

The human homologue of yeast *gaal*, *hgaal*, was identified on the basis of homology to yeast proteins. *hgaal* encodes a 621 amino acid protein with multiple transmembrane domains and with amino acids that are 25% identical and 57% homologous to yGAA1. Several approaches have been used to characterize the role of hGAA1 in the TAM mechanism of mammalian cells. First, transfection of K562 cells with pCDNA containing antisense *hgaal* resulted in significant decrease in the surface expression of the GPI-anchored reporter protein, CD8-DAF. Second, disruption of murine *gaal* in mouse F9 embryonic carcinoma cells by homologous recombination approach resulted in the accumulation of mature GPI anchors and the loss of surface expression of GPI-anchored protein, Thy-1²⁷⁸. Third, the importance of GAA1 to the processing of prepro-miniPLAP was determined. Both *mgaal* and *hgaal* are predicted to encode transmembrane proteins²⁸⁴⁻²⁸⁵. Thus, to participate in GPI-anchoring, GAA1 would presumably be present in microsomal membranes. In mini-PLAP assay (Illustration 8), microsomal membranes isolated from Δ *gaal* F9 mutants were capable of cleaving the N-terminal signal peptide to form pro-mini-PLAP. However, the mature GPI-anchored mini-PLAP or the hydrazide-mini-PLAP could not be detected.

Finally, the association between hGPI8 and hGAA1 was evaluated by co-immunoprecipitation experiments. GST-tagged hGPI8 and FLAG-tagged hGaa1 were co-expressed in CHO cells. Co-immunoprecipitation of hGPI8 with hGAA1 using antibodies

to the FLAG-tag suggested that these proteins interact in the TAM complex²⁷⁸ via an essential proline in the seventh transmembrane domain²⁸⁶⁻²⁸⁷. Together with the genetic and biochemical studies, these results indicate that mammalian GAA1 associates with GPI8, which is required for GPI-anchoring. Thus, hGAA1 is believed to function as an essential component of the TAM complex in mammalian cells^{278, 284-285}.

PIG-S and PIG-T

PIG-S and PIG-T, homologues of yeast GPI17 and GPI16, respectively, were identified as the third and fourth proteins that are believed to associate with GPI8 in the TAM complex. FLAG-tagged hGPI8 was expressed in class K hGPI8-deficient mutants. Immunoprecipitation with anti-FLAG antibody followed by SDS-PAGE under denaturing conditions resolved three additional proteins along with hGPI8. N-terminal sequencing identified these as hGAA1, and two additional proteins, which matched to expressed sequence tags (ESTs) and genomic sequences in the human genome sequence and subsequently named *pig-s* and *pig-t*. As for GAA1, however, no information suggesting specific functions of these proteins was obtained by homology search of public sequence databases for further study²⁸⁰.

To investigate their respective roles in GPI-anchoring, *pig-s* and *pig-t* were disrupted in F9 cells by homologous recombination. The GPI-anchored protein, Thy-1, was not expressed on the surface of Δ *pig-s* and Δ *pig-t* mutants. Transfection of the respective PIG-S and PIG-T expression vectors restored Thy-1 expression. Furthermore, in mini-PLAP assays (Illustration 8), microsomes isolated from these mutants were unable to form either the GPI-anchored or hydrazide-protein forms while mutants were not defective in GPI synthesis. Co-immunoprecipitation experiments suggested that PIG-S is a stable subunit of the TAM complex, independent of the level of expression of the

other components. By contrast, PIG-T appeared to be critical for the stable expression and association with Gaa1 and hGPI8²⁸⁰.

Additional evidence for the association between PIG-T and GPI8 was provided by treatment with a compound that traps disulfides, *N*-ethylmaleimide, during protein expression, cell lysis and immunoprecipitation. Under these conditions, the association of PIG-T with hGPI8 was demonstrated by Western blot analysis. In addition, hGPI8 was mutated in conserved cysteine residues and expressed in class K mutants. One cysteine (C) to serine (S) mutant, GPI8^{C92S}, failed to form high molecular weight complexes with the other TAM proteins, suggesting that association of PIG-T with hGPI8 is important to TAM activity²⁵⁸.

PIG-U

A fourth GPI8-interacting protein of the TAM complex, PIG-U, was identified by a reverse genetics approach. GPI-anchored protein deficient (GPI-AP⁻) Chinese hamster ovary (CHO) cells were generated via chemical mutagenesis and selected based upon resistance to cytolysis by the GPI-anchored protein-binding toxin, aerolysin. One GPI-AP⁻ clonal line showed consistent resistance to aerolysin, reduced staining with fluorescent aerolysin and with antibody to decay-accelerating factor (DAF, CD55) and homologous restriction factor (HRF, CD59). In addition, microsomes isolated from this CHO mutant line, though capable of synthesizing mature GPIs, were unable to form GPI-anchored mini-PLAP. Co-transfection of *hgpi8*, *hgaal*, *pig-s* and *pig-t* did not restore GPI-anchoring in this CHO mutant line. These results suggest that this mutant was defective in a new TAM complex gene, which was designated class U²⁸¹.

To identify the defective gene, the class U mutant was transfected with a rat cDNA library and screened for restored aerolysin sensitivity and CD55 expression. FACS

sorting was used to isolate GPI-AP⁺ clones and the plasmid that complemented the defect in GPI-anchoring of mini-PLAP. The *pig-u* gene sequence was thereby obtained and *pig-u* was cloned²⁸¹.

Pig-u was predicted to encode a highly hydrophobic 435 amino acid protein with nine potential transmembrane domains, and containing a 17 amino acid motif present in fatty acid elongases. To further investigate the role of this gene in anchoring, PIG-U was over-expressed in the class U mutant line. This resulted in restored CD59 and CD55 expression. When the 17 amino acid residues corresponding to the elongase motif were mutated to leucines and the recombinant protein was expressed in class U mutants, GPI-anchoring was not restored, indicating that this motif is critical to the function of PIG-U. Subsequent co-immunoprecipitation experiments also indicated that PIG-U associates with the other TAM subunits. However, PIG-U is not required for the formation of the TAM complex, as the high molecular weight complexes of GPI8, GAA1, PIG-T and PIG-S can be purified from class U mutants²⁸¹.

A yeast homologue of *pig-u*, *cdc91*, was also identified in the yeast genome. CDC91 encodes a 394 amino acid protein with 28% identity to PIG-U. Like PIG-U, *cdc91* retains the predicted characteristics of a highly hydrophobic protein with multiple transmembrane domains. Transfection of *cdc91* into *class U* mutants partially restored GPI-anchoring, suggesting that *cdc91* and *pig-u* are functional homologues²⁸¹.

In summary, results of genetic and biochemical studies in yeast and in mammalian cells reflect that GPI8 associates with yGAA1/hGAA1, GPI16/PIG-T, GPI17/PIG-S, and CDC91/PIG-U and that these proteins are components of the TAM complex.

Trypanosomes

GPI16

To identify TAM components in trypanosomes, TbGPI8-FLAG was expressed in *T. brucei*. Immunoprecipitation with anti-FLAG antibody followed by two-dimensional (2-D) electrophoresis to resolve complexes under non-reducing and reducing conditions enabled identification of partial amino acid sequences of the ~70 kDa protein among the proteins that co-immunoprecipitated with TbGPI8. This sequence matched to an ORF in the *T. brucei* genome that was 13% identical and 25% similar to GPI16²⁵⁵. Targeted disruption of *TbGPI16* in *T. brucei* indicated that it is essential for GPI-anchoring²⁸⁸.

TTA1 and TTA2

In *T. brucei*, two additional GPI transamidase subunits were also identified by the described 2-D electrophoresis (40 and 35 kDa proteins) and were named trypanosomatid transamidase 1 (TTA1) and 2 (TTA2), respectively. *tta1* and *tta2* sequences were identified in the *T. brucei* genome, and predicted proteins containing 377 and 410 amino acid proteins, respectively, and 2 and 6 transmembrane domains, respectively. However, their sequence did not correspond to any proteins of known function or contain any suggestive functional motifs. Targeted disruption of *tta1* or *tta2* in *T. brucei* procyclic forms resulted in loss of the surface expression of the GPI-anchored protein, procyclin, while retaining their ability to synthesize GPIs. These subunits were identified in genome sequence database for *Leishmania major* and *T. cruzi*; however, no functional studies have been reported²⁵⁵.

TbGAA1

In *T. brucei*, *Tbgaal1* was PCR-cloned based upon homologous sequence of *yGaa1* and *hGaa1*. *Tbgaal1* was predicted to encode a 461 amino acid protein, as compared to a 621 amino acid for hGAA1. TbGAA1 sequence was 21% identical and 38% similar to hGAA1 and contained several predicted transmembrane domains, as for both human and yeast GAA1. Thus, the role of TbGAA1 in the GPI-anchoring mechanism and its association with TbGPI8 was further investigated. Disruption of *Tbgaal1* resulted in loss of the surface expression of procyclin, and was restored by transfection of *Tbgaal1*. Although TbGAA1 was not detected in the immunoprecipitated complex by anti-GPI8 antibody from wild type *T. brucei*, when epitope-tagged TbGAA1 was over-expressed in *TbΔgaal1* mutants, TbGAA1 was co-immunoprecipitated with TbGPI8 and TTA1, suggesting their association in the TAM complex²⁵⁵.

Thus, in *T. brucei*, the TAM complex appears to be composed of TbGPI8, TbGAA1, TTA1, TTA2 and TbGPI16.

SUMMARY

Jointly, genetic and biochemical studies suggest that GPI8 is responsible for anchoring GPIs to proteins on the luminal face of the endoplasmic reticulum. Genetic and biochemical evidence indicates that GPI8 functions in association with other proteins or enzymes in the TAM complex. However, direct demonstration of the ability of a native purified GPI8 to function as a transamidase awaits further confirmation.

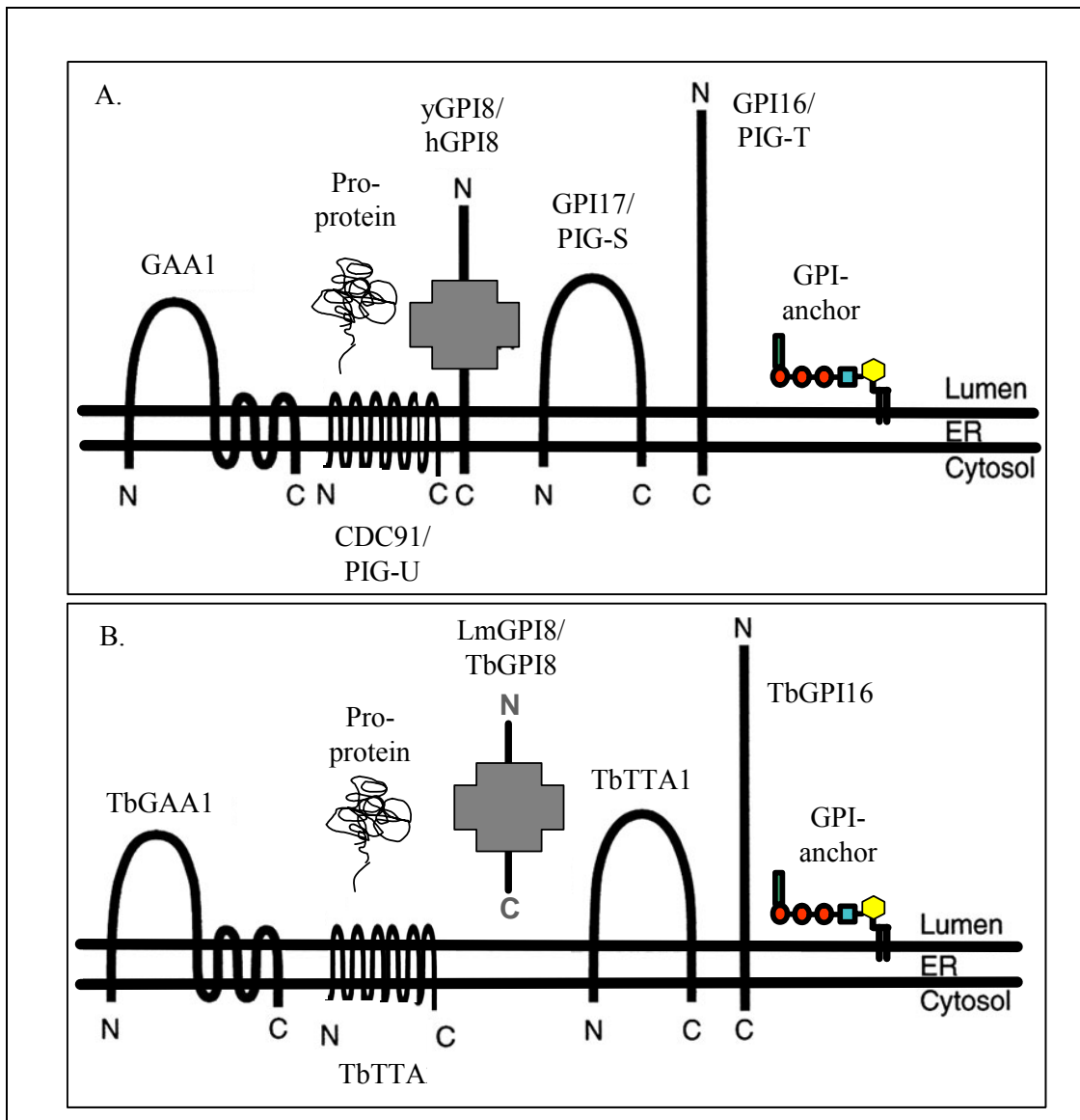


Illustration 12: The TAM complex. A model of GPI8 interaction with other proteins in the TAM complex is presented for A) yeast and human cells, and B) *T. brucei*. Structures are not drawn to scale. The structural and functional properties of the TAM complex, described above, are depicted. Adapted by permission from Macmillan Publishers Ltd: [EMBO J], (Ohishi, K., N. Inoue, and T. Kinoshita, 2001. *PIG-S and PIG-T, essential for GPI anchor attachment to proteins, form a complex with GAA1 and GPI8*. *Embo J*, 20:4088-98), copyright (2001).

Chapter 3:

Characterization of the GPI-anchoring mechanism in *Trypanosoma cruzi* by over-expression of TcGPI8 active site mutants and by targeted disruption of *TcGPI8*

INTRODUCTION

Objective of Study

The overall objective of this investigation was to further characterize the mechanism of pathogenesis of *T. cruzi* utilizing molecular genetics approaches to determine the role of GPI-anchored proteins in the complex life cycle of *T. cruzi*. To determine the function of TcGPI8 in GPI-anchoring activity and its importance to the survival of *T. cruzi*, two alternative experimental methodologies were utilized: 1) over-expression of TcGPI8 mutated in putative active site residues, and 2) targeted disruption of *TcGPI8*²⁸⁹. *In vitro* studies were designed to assess the effect of mutation of the predicted active site of TcGPI8 on the surface expression of GPI-anchored proteins. In addition, we sought to examine whether targeted disruption of the *TcGPI8* gene impairs *T. cruzi* differentiation and replication.

Specific Aim

The specific aim of this investigation was to evaluate the biological effects resulting from reduction or absence of GPI-anchored protein expression in *T. cruzi* via over-expression of mutated TcGPI8 and by targeted disruption of *TcGPI8*.

Hypothesis

The hypothesis of this study was that the *T. cruzi* GPI8 protein (TcGPI8) is the catalytic subunit responsible for the attachment of GPI anchors to proteins and, therefore, that overexpression of putative active site mutant alleles of TcGPI8 or disruption of TcGPI8 would result in the deficiency of surface expressed protein-GPIs and that such deficiency would have detrimental effects on the development and virulence of *T. cruzi*.

Experimental Approach

Over-expression of mutated GPI8

The first experimental approach was to over-express TcGPI8 and putative active site mutants of TcGPI8 via the *T. cruzi* expression vector, pTEX (Figure 1)²⁹⁰ to produce a dominant-negative effect on GPI-anchoring. These studies were designed to establish if the expression of GPI-anchored proteins in *T. cruzi* transfectants over-expressing mutant TcGPI8 alleles is reduced in *T. cruzi* and to evaluate the effects of depletion of surface-expressed GPI-anchored proteins on the development of *T. cruzi* (Figure 2).

For this purpose, *TcGPI8* putative active site mutants (*TcGPI8*^{H198A} and *TcGPI8*^{C156A}) were created by site-directed mutagenesis. To allow for detection of over-expressed protein, the unmutated and mutated forms of *TcGPI8* were cloned in fusion with an epitope-tag. The entire open-reading frame was then subcloned into pTEX. Epimastigote stage parasites were transfected with the recombinant plasmids and selected in G418. TcGPI8 over-expression was demonstrated via Western Blot (WB) analysis. The effect of over-expression of putative TcGPI8 active site mutants on GPI-anchoring was assessed via flow cytometric analysis of transfectants stained with specific antibodies

to GPI-anchored proteins. Finally, *in vitro* development of these transfectants was assessed by infection of fibroblast cell lines.

Targeted disruption of TcGPI8

A homologous recombination-mediated approach to targeted disruption^{70, 291, 292} of the *TcGPI8* gene in *T. cruzi* was undertaken in effort to determine the effect of loss of GPI-anchored protein expression on the *in vitro* development of the parasite (Figure 3). As *T. cruzi* is a diploid organism, it was necessary to target each allele of *TcGPI8* via sequential disruption with different drug resistance cassettes. The constructs for *TcGPI8* disruption were designed such that drug resistance genes, *neo^r* or *ble^r*, which confer resistance to the drug G418 or phleomycin (ble), respectively, were flanked by 400-600 base pairs of the 5' and 3' ends of the *TcGPI8* gene. The *GAPDH-intergenic region* (*GAPDH-IR*) sequence, present upstream of the *neo^r* or *ble^r* genes, provides the necessary splice acceptor site for mRNA processing in *T. cruzi*²⁹³. The replacement of both *TcGPI8* alleles was attempted by sequential electroporation of *T. cruzi* epimastigotes with *neo^r*- and *ble^r*-based constructs. Selection of the transformants was performed in the presence of the respective drug(s). Genomic integration of the *neo^r* cassette was evaluated by PCR amplification using *GAPDH-IR/neo^r* gene-specific primers. In addition, Southern blot analysis of chromosomal DNA isolated from wild type and transfected parasites was performed to evaluate disruption using ³²P-labeled *TcGPI8* and *neo^r* genes as probes. However, PCR analysis indicated that *TcGPI8* was not disrupted. Subsequently, the site of integration of the *GAPDH-IR/neo^r* cassette was determined using an arbitrarily primed, nested PCR approach²⁹⁴⁻²⁹⁵. The phenotypic outcome of this disruption on GPI-anchoring was determined by flow cytometric analysis. Fibroblast infection and confocal imaging was used to assess the outcome of transformation on *in vitro* development²⁸⁹.

MATERIALS & METHODS

Isolation, cloning and characterization of *TcGPI8*

Degenerate primers for use in PCR were designed based on the conserved sequence of the *S. cerevisiae*, human and *Leishmania GPI8* available in the public genomics databases. The full-length cDNA product was subsequently cloned into pTopo(T) (Invitrogen), sequenced, and confirmed by genome database matching.

Genetic transformation of *T. cruzi*

Cloning

Primers used for PCR amplification, site-directed mutagenesis (SDM) or DNA sequencing reactions are listed in Table 1. All PCR reactions used for cloning were performed using *Vent* polymerase (New England Biolabs). For cloning, vectors and inserts were prepared by restriction enzyme digestion, resolved on agarose gels, excised and purified on Qiagen gel extraction column. Ligations were performed at 16°C overnight and transformed in bacteria (strain XL1-Blue, DH5 α , or NovaBlue). Plasmid DNA was prepared by alkaline lysis²⁹⁶, and clones were screened by restriction enzyme digestion. Plasmids to be sequenced were purified via Qiagen miniprep kits, according to the manufacturer's protocol²⁹⁷. Plasmids were submitted to the UTMB Protein Chemistry Laboratory for DNA sequencing.

Constructs for over-expression of TcGPI8 in T. cruzi

The cloning design for construction of pTEX plasmids containing unmutated and mutated TcGPI8 is shown in Figure 4. Plasmids constructed for cloning and expression of TcGPI8 are listed in Table 2 and 3, respectively.

Addition of epitope-tag

TcGPI8 was cloned in fusion with a C-terminal epitope tag consisting of three copies of the hemagglutinin (Flu) gene followed by codons for six histidines (His) (Flu₃His₆), as follows. First, PCR amplification of the *TcGPI8* gene was used to incorporate restriction enzyme sites for subsequent cloning into pRD67 (kindly provided by Dr. Robert Davey, RD), a plasmid that contains the nucleotides encoding Flu₃His₆ followed by a stop codon. The PCR products were cloned into pSTBlue1 (Novagen, San Diego, California). Recombinants were selected based on the presence of β -lactamase (*amp^r*) expression and the absence of β -galactosidase expression indicated by white colony phenotype on agar plates containing ampicillin (50 μ g/ml), X-Gal (70 μ g/ml) and IPTG (80 μ M)²⁹⁸. Subsequently, the entire *TcGPI8_{FH}* open reading frame was sub-cloned into pBSKII for use in site-directed mutagenesis reactions.

Site-directed mutagenesis

The C198A and H156A mutations in *TcGPI8* were produced using Stratagene QuikChange™ Site-Directed Mutagenesis (SDM) (Figure 5), according to the manufacturer's protocol²⁹⁹. Briefly, mutagenic primer pairs (Table 1) were designed to introduce 2-3 nucleotide changes in *TcGPI8*, thereby altering the amino acid coding in the protein. To facilitate screening of clones containing the mutated sequences, *NaeI* or

XhoI restriction enzyme sites were introduced with the H156A or C198A mutations, respectively.

Prior to use in mutagenesis reactions, all primers used in SDM reactions were tested for the optimal annealing temperature in PCR reactions using *taq* DNA polymerase (95°C/30 secs, 35 cycles of 95°C/30 secs, 55°C or 45°C/1 min., and 68°C/10 min) with the template DNA, pBSKII.*TcGPI8_{FH}*. The following primer pairs (Table 1) were used for the mutagenesis of: 1) C198A: *GPI8QC(C/A+XhoI)-F* and *GPI8QC(C/A+XhoI)* and 2) H156A: *GPI8QC(H/A+NaeI)-F* and *GPI8QC(H/A+NaeI)-R*. Mutagenesis reactions were performed at the optimal annealing temperature, using 10-50 ng of plasmid prepared by Qiagen miniprep (95°C/30 sec and 18 cycles of 95°C/30 sec, 45°C or 55°C/1 min., 68°C/10 min). Reaction efficiency was confirmed on agarose gel. Subsequently, reactions were treated with *dpnI* for 1 hour at 37°C to digest methylated template DNA. The SDM reactions were then transformed in bacteria and clones obtained by growth in selective antibiotics as described for pSTBlue1. Preliminary screening of clones for introduced mutations was performed using the respective restriction enzyme: *XhoI* for C198A, *NaeI* for H156A. Subsequently, DNA sequences were confirmed (UTMB Protein Chemistry Laboratory).

Cloning in expression vectors

Mutated and unmutated *TcGPI8_{FH}* open reading frames (ORF) were cloned from pBSKII into pTEX. In addition, the *TcGPI8_{FH}* ORF was cloned into pCDNA3 and pET21b for expression in mammalian cells and bacteria, respectively (Figure 4).

Constructs for targeted disruption of TcGPI8

The cloning strategies used for the *neo^r*- and *ble^r*-based *TcGPI8* disruption constructs are depicted in Figure 6 and Figure 7, respectively. Plasmids used for cloning of the final disruption constructs are listed in Table 6. For transfection of *T. cruzi*, the disruption cassettes were linearized with restriction enzymes, resolved on agarose gel (5 kb *ScaI* fragment for *neo^r*-*TcGPI8*; 4.2 kilobase *ScaI/HindIII* fragment for *ble^r*-*TcGPI8*), and purified on Qiagen columns.

Cell culture

Culture of *T. cruzi* epimastigotes

T. cruzi (SylvioX10/4 strain) was obtained from American Type Culture Collection (Manassas, VA). Wild type and transfected *T. cruzi* epimastigotes were grown axenically at 28°C in liver infusion tryptose (LIT) medium supplemented with 0.01 mg/ml hemin, 10% FBS and antibiotics (penicillin/streptomycin). To maintain consistent growth of epimastigote cultures, periodic conversion of trypomastigotes to epimastigotes was performed⁸⁶. Briefly, trypomastigotes were harvested following fibroblast infection, suspended in liver infusion tryptose (LIT) medium, and maintained at 37°C for 2-3 days. After appearance of amastigote forms, parasites were incubated at 28°C for conversion to the replicative epimastigote form and continuously cultured in LIT medium. To enrich for epimastigote forms, *T. cruzi* transfectants (pTEX) were isolated by density gradient centrifugation (Ficoll-Paque PlusTM; Amersham) and returned to LIT medium. Transfectants were initially selected in 60-100 µg/ml G418. After drug selection was completed, parasites were cultured in G418 concentrations ranging from 200-800 µg/ml for >2 weeks prior to subsequent phenotypic analysis. Growth curves for epimastigotes

were obtained by monitoring the growth of wild type *T. cruzi* and transfectants cultured in G418 (400 µg/ml), as follows. Parasites (5×10^5) were inoculated into 5 ml LIT, and counting on hemacytometer was performed daily for eight consecutive days. Statistical analysis of mean parasite density obtained from triplicate experiments was performed using one-way analysis of variance (ANOVA) for repeated-measures with Bonferroni comparison using GraphPad Prism 4.0 (GraphPad Software, San Diego California USA).

Fibroblast culture

BHK21 cells (baby hamster kidney cell line) were maintained in complete Dulbecco's Modified Eagle's Medium (DMEM, Hyclone) with 10% fetal bovine serum (Gemini Bioproducts). C2C12 cells (murine skeletal muscle cell line, American Type Culture Collection) were maintained at 37°C in 5% CO₂ in complete RPMI 1640 medium (HyClone) with 10% fetal bovine serum.

Transformation methods

DNA constructs used for electroporation of *T. cruzi* are listed in Tables 3 and 6. Constructs used for transfection of mammalian cells and for transformation in bacteria to express protein are listed in Tables 4 and 5, respectively.

Electroporation of *T. cruzi*

For electroporation of *T. cruzi*, plasmid DNA was prepared using standard alkaline lysis method and treated with RNase A. DNA was then purified via phenol-chloroform extraction followed by ethanol precipitation²⁹⁶. For episomal expression, *T. cruzi* epimastigotes were electroporated by standard method for *T. cruzi* with the

following constructs: 1) pTEX, 2) pTEX-*TcGPI8*^{C198A}, and 3) pTEX.*TcGPI8*^{H156A} (Table 3). For targeted disruption, the following constructs were used for electroporation: 1) *neo*^r-based *TcGPI8* disruption construct (4.2 Kb *ScaI/HindIII* fragment), 2) *ble*^r-based *TcGPI8* disruption construct (5 Kb *ScaI* fragment), 3) pTEX, and 4) pTEX_{ble} (Table 6).

For electroporation, parasites were washed twice in cold sterile PBS and suspended at 10⁸ parasites/ml in electroporation buffer (137 mM NaCl, 5 mM KCl, 0.7 mM Na₂HPO₄, 6 mM glucose, 21 mM HEPES, pH 7.5). DNA was added to parasites (4 x 10⁷ parasites in 400 µl per cuvette) and incubated for 10 min on ice. Electroporation was performed three times at 300 volt, 950 µF setting, followed by 10 min recovery on ice. Parasites were then transferred to 5 ml of LIT medium for culture at 28°C; 24-48 hours post-electroporation, 60 µg/ml G418 was added to cultures. To monitor for drug selection, mock electroporated parasites were cultured in the same G418 concentration as for the pTEX transfectants. Following positive selection, indicated by the death of mock-transfected parasites, the G418 concentration was increased to 200 µg/ml. Ble selection was performed at 50-750 µg/ml.

Lipid-mediated transfection of mammalian cells

The experimental design for transfection of BHK21 cells is shown in Figure 8. For transfection into mammalian cells, DNA was prepared by QIAfilter technique according to the manufacturer's protocol²⁹⁷. BHK21 cells were transiently transfected with the following constructs: 1) pCDNA3, 2) pCDNA3.*TcGPI8*_{FH}, 3) pCDNA3.MCAT_{FH}³⁰⁰, 4) pREP10.GFP. Transfection was performed by lipid-mediated method using Lipofectamine2000 (Invitrogen), as follows. Briefly, BHK21 cells were plated at 3 x 10⁵ cells/well in a 24-well plate in 500 µl Dulbecco's Modified Eagle's Medium (DMEM) without antibiotics and allowed to adhere overnight. For transfection,

DNA (800 ng or 1.2 μ g) was suspended in 50 μ l Optimem I and incubated at room temperature for 5 minutes. Two μ l of Lipofectamine2000 was added to 50 μ l of Optimem I, mixed with the DNA/Optimem I suspension, incubated for 20 minutes at room temperature and then added to the BHK21 cells. At 24 and 48 hours post-transfection, *in situ* GFP expression was confirmed via epifluorescent microscopy. Subsequently, transfected BHK21 cells were removed from the wells into PBS by scraping. Cells were harvested by centrifugation (1200xg, 5 min) and washed with PBS.

Transformation of bacteria

For bacterial expression of TcGPI8, DNA prepared by standard alkaline lysis was transformed into *HMS174/DE3* bacteria. The following constructs were used: 1) pREP10.*GFP*, 2) pET21b.*TcGPI8_{FH}*, 3) pET21b.*MCAT_{FH}*³⁰⁰. The experimental design is shown in Figure 9.

For small-scale expression experiments, bacterial cultures (2 ml) were grown to absorbance at wavelength of 600 nm (A_{600}) of 0.5-0.9 in LB medium supplemented with ampicillin (50 μ g/ml). Subsequently, cultures were split into equivalent volumes and one portion was induced with IPTG (1 mM). Induced and uninduced cultures were then incubated on a shaker at 37°C for 3 hours and A_{600} measurements were obtained. Bacteria were pelleted (4000xg, 5 min, 4°C), washed in PBS and suspended in PBS (1:10 dilution of bacteria) on ice. An equal volume of denaturing sample buffer containing 9 molar urea²⁹⁶ was added. Bacteria were further lysed by sonication. Cleared protein supernatant was harvested following centrifugation (16,000xg, 5 min, 4°C) for evaluation of protein expression.

Larger bacterial cultures were induced, harvested and analyzed for protein expression, as described for small-scale test. GFP expression was visualized throughout

the procedures using UV excitation (eGFP excitation λ_{Max} = 488 nm; emission λ_{Max} = 507 nm).

Genetic screening of transformants

Chromosomal DNA extraction

Total genomic DNA (gDNA) was extracted from *T. cruzi* and BHK21 cells according to a published method³⁰¹. Briefly, parasites (≤ 1.5 ml culture) were harvested weekly at 3000xg, 10 min. The pellet was suspended in 150 μ l of TELT lysis buffer (50 mM Tris-HCl pH 8, 62.5 mM EDTA pH 9, 2.5 M LiCl and 4% v/v Triton X-100) and incubated for 5 min. An equal volume of phenol: chloroform: isoamyl alcohol (25:24:1) was added, and the tubes were shaken by hand for 5 min. Following centrifugation at 13,000xg for 5 min, the upper aqueous phase was collected into a new tube. To precipitate the DNA, 300 μ l of absolute ethanol was added and the solution swirled gently and incubated for 5 min. DNA was harvested by centrifugation (13,000xg, 10 min) and washed with 1 ml of absolute ethanol. DNA was dried in a vacuum and dissolved in TE (10 mM Tris-HCl, 1 mM EDTA). For larger parasite cultures (30-100 ml), the volumes of the lysis buffer and other reagents were increased 30- to 100-fold. The yield of DNA was estimated by absorbance at a wavelength of 260 nm (A_{260}). In addition, the quantity and quality of DNA were verified on an agarose gel.

PCR analysis

pTEX or *neo*^r-*TcGPI8* transfectants were screened for the presence of the 1.3 kilobase *GAPDH-IR- neo*^r fragment via PCR amplification using the primer pair

GAPDH-F and *neo^r*-R (Figure 10, Table 1). Parasites were harvested weekly and DNA extracted. PCR was performed using 200 ng of total parasite DNA per reaction. To control for *taq* polymerase efficiency and PCR conditions, PCR reactions were performed in parallel with pTEX (25 ng per reaction). To control for PCR cycling conditions, gDNA quantity and quality, a 780 bp *GAPDH* fragment was also amplified from *T. cruzi* gDNA; 5-10 µl of each 50 µl PCR reaction was resolved on 1% agarose gel. PCR analysis of *neo^r*-*TcGPI8* transfectants was also performed using DNA treated with the restriction enzyme, *dpnI*, which digests plasmid DNA that has been methylated at the N⁶ position of the adenine residues in the sequence GATC, as occurs in the DNA methyltransferase-positive strains of *E. coli* denoted *dam+*. Treatment of DNA with *dpnI* (Stratagene) was performed at 37°C for 24 hr using 5 units of enzyme per 2 µg total DNA in the recommended buffer and, in parallel, the identical quantity of DNA was incubated in buffer without enzyme. Subsequently, PCR was performed as described.

To evaluate whether *TcGPI8* was disrupted in *neo^r*-*TcGPI8* transfectants, primers were designed based on the 5' and 3' *TcGPI8* flanking sequence published in the *T. cruzi* genome database²⁵⁹. PCR reactions were performed using the 5' or the 3' flanking primer in combination with a *TcGPI8*-specific primer (Figure 11, Table 1).

Southern blot analysis

The following DNAs were digested with restriction enzymes and resolved by agarose gel electrophoresis: 1) wild type *T. cruzi*, 2) *T. cruzi* transfectants and 3) plasmid control. DNA was transferred to ZetaProbe GT membrane (BioRad) using semi-dry transfer (BioRad TransBlot). ³²P-labeled probes were generated using random hexamer primer labeling method, as follows: 25-100 ng DNA was denatured by boiling for 10 minutes, and then cooled on ice. The reaction was prepared using 2 µM primer, 2 units

Klenow, Klenow reaction buffer, BSA, 200 μ M each of dCTP, dGTP, dTTP (New England Biolabs), and 3-5 μ l of [α -³²P]-dATP (3000 μ Ci/mmol) in a volume of 50 μ l and incubated overnight at room temperature. To prevent non-specific binding of probe to the membranes, membranes were prehybridized for 30 min-1 hr at 68°C in 5 ml hybridization buffer alone (RapidHyb, Amersham Biosciences). Subsequently, the probe was added, and the hybridization was performed at 68°C for 4-12 hours. Membranes were exposed to phosphor screen and the signal visualized by phosphorimager (Storm860, Molecular Dynamics).

Arbitrarily primed, nested PCR

A set of nested, specific primers were designed based on the *neo^r* gene of pTEX derived from pMC1neo (Stratagene)²⁹⁰, with sufficient product size difference to detect nested PCR products via agarose gel electrophoresis (Figure 12). Thermal asymmetric interlaced (TAIL)-PCR reactions²⁹⁴⁻²⁹⁵ were performed using a *neo^r*-specific primer (forward, F or reverse, R) in combination with one of four arbitrary degenerate (AD) primers (cycling conditions modified from ²⁹⁴). PCR products were purified, cloned and DNA sequence was obtained.

Protein analysis in transformants

Generation and affinity purification of TcGPI8 antisera

Antiserum for detection of TcGPI8 was obtained by immunization of two rabbits with the synthetic peptide, DAYTPPSRRLNTDE, corresponding to residues 132-145 of TcGPI8 (*GPI8-132*; ProSci Corp.). *GPI8-132* antiserum obtained from the second post-immunization bleeding was affinity purified on the *GPI8-132* peptide bound-N-

hydroxysuccinimide (NHS)-activated sepharose HP column according to the manufacturer's protocol (Amersham-Pharmacia).

Briefly, the *GPI8-132* peptide was dissolved in PBS at a concentration of 4 mg/ml; 2 mg of peptide was diluted with coupling solution (1:2). A_{260} of the peptide solution was measured prior to addition to the NHS-column (1:10) for subsequent monitoring of coupling efficiency. Isopropanol was extensively washed out of the column. The peptide solution was loaded on the column and allowed to incubate for 1 hour at room temperature. Washing and deactivation of the column and equilibration of column were performed as described. For antibody binding to the NHS-peptide column, *GPI8-132* antiserum (10 ml) was diluted in PBS (1:2) and loaded on the column. Flow through was collected, the column was extensively washed with PBS, and antiserum was eluted in eight fractions (500 μ l/ fraction).

Antiserum purification was monitored by A_{260} as well as visualization of heavy and light chain antibody bands on SDS-PAGE comparing unpurified sera, flow through and wash fractions to elution fractions #1-6. Based on both methods, fractions 2 and 3 were pooled and dialyzed in PBS (Pierce Slide-A-Lyzer 10K). The specificity of *GPI8-132* antiserum was confirmed using Western blot analysis of triplicate membranes containing recombinant TcGPI8_{FH} expressed in bacteria, which were incubated in parallel with *GPI8-132* antiserum, preimmunization serum from matching rabbit, or antibody to the epitope-tag (anti-Flu) (see below).

Protein extraction

T. cruzi protein lysates were prepared as follows. Parasites were harvested and lysed by repeated freeze-thaw cycles in a dry ice-ethanol bath followed by incubation on ice for 30 minutes in a buffer (10^9 parasites/ml) consisting of 1% Nonidet-P40, 10 mM

Tris-HCl, and 5 mM EDTA with protease inhibitors. BHK21 lysates were prepared by lysis in PBS (1:1 v/v) containing 1% NP40 and protease inhibitors. Protein lysates were stored at -20°C.

Western blot analysis

Protein lysates from *T. cruzi* (2×10^7 parasites equivalents per lane) and BHK21 cells (8×10^4 cell equivalents per lane) were resolved by sodium dodecyl sulfate-polyacrylamide gel electrophoresis (SDS-PAGE; 12%). Western blot analysis was performed as follows. Membranes were blocked in PBS containing 5% non-fat dry milk and 0.05% Tween-20. Next, membranes were incubated with primary or secondary antibody for 1 hour at room temperature. Membranes were washed extensively (10 times, 2 minutes per wash) in PBS containing 0.05% Tween-20.

Membranes were incubated with the following primary antibody or antisera: anti-Flu, 1:1000 (12CA5; Invitrogen) mAb, rabbit pre-immunization serum, or *GPI8-132* post-immunization serum (*GPI8-132* antiserum). For preliminary selection of a starting dilution range, the *GPI8-132* post-immunization serum and pre-immunization serum from the matching rabbit were screened via Western blot analysis using dilutions of pre-immunization and matching bleeds in the range of 1:500 to 1:5000 using protein lysates from wild type *T. cruzi* and untransfected BHK21 cells. For additional optimization purposes, e.g., to achieve low background with maximal sensitivity of detection of TcGPI8, dilutions in the range of 1:200 to 1:2000 were tested using additional positive and negative control lysates (Figures 8 and 9). NHS-peptide purified *GPI8-132* antiserum was subsequently used at a dilution of 1:1000 for Western blot analysis of wild type *T. cruzi* and stable *T. cruzi*/pTEX transfectants.

The following secondary antibodies were used: goat anti-mouse IgG-conjugated to horseradish peroxidase (HRP), 1:10,000 (Biorad) or goat anti-mouse IgG-HRP (Sigma), 1:20,000. To detect bound antibody, membranes were incubated with chemiluminescence substrate (ECL; Amersham-Pharmacia) for one minute. Signal was then detected by 0.5-5 min exposure of membranes to x-ray film (Hyperfilm ECL; Amersham-Pharmacia).

FACS analysis of GPI-anchored proteins

Wild type and transfected *T. cruzi* were harvested and washed twice in ice cold PBS, and resuspended in 100 μ l PBS containing 0.1% BSA and 0.1% azide for staining. Parasites (10^6 per tube) were incubated for 30 minutes on ice with the following antibodies: C10, 2B10, 10D8, Y3, and anti-gp72 (1:50-1:200 dilutions). After washing with PAB, parasites were incubated with secondary antibody (1:200 dilution, goat anti-mouse IgG-FITC; Sigma) for 30 min at 4°C in the dark. Secondary antibody alone was used as an additional negative control. Finally, parasites were fixed in 1% paraformaldehyde. Flow cytometry was performed with Becton Dickinson FACScan and data analyzed using CellQuest (UTMB Flow Cytometry Core Facility). Forward (FSC) and side scatter (SSC) properties were used to gate out low FSC, SSC metacyclic forms in analysis of fluorescence histograms of epimastigotes. For each antibody, the average percentage of positive parasites was calculated from three independent experiments for pTEX transfectants. Statistical analysis was performed using one-way analysis of variance (ANOVA) with Bonferroni multiple comparison test for assessment of differences between wild type *T. cruzi* and pTEX transfectants.

***T. cruzi* development**

Fibroblast infection

T. cruzi epimastigotes transfectants were grown in LIT medium for >10 days to stationary-phase parasites (metacyclic trypomastigotes). Metacyclic trypomastigotes were then incubated in Dulbecco's Modified Eagle's Medium (DMEM; Gibco) containing 2% non-heat inactivated fetal bovine serum (FBS) for complement-mediated lysis of epimastigotes. A monolayer of fibroblasts (C2C12 and BHK21 cells) in tissue culture flasks was infected at a parasite to cell ratio of 50:1. At 24 hours after infection, medium containing free parasites was replaced and infection flasks monitored for trypomastigotes. At 6 days post-infection, trypomastigotes were harvested, counted and utilized for quantitative infection experiments.

Confocal microscopy

Parasites were harvested by centrifugation and washed in ice-cold PBS. To visualize kinetoplast and nuclear DNA, epimastigotes were incubated with Syto11 (Molecular Probes), a cell-permeant nucleic acid binding, green fluorescent dye. Parasites were incubated in Syto11 (1:200) on ice for 10 minutes. Confocal images of live parasites were captured on a Zeiss LSM 510 UV Meta Laser Scanning Confocal Microscope (UTMB Optical Imaging Core Facility). For Syto 11, the excitation λ_{Max} was 515 nm; emission λ_{Max} , 543 nm. For detection of the red fluorescent protein, RED-1, (from pDsRED1-C1, CLONTECH), the excitation λ_{Max} was 558 nm; emission λ_{Max} was 583 nm. Fluorescent signals were overlaid with Nomarski differential interference images using Zeiss AxioVision Viewer software.

RESULTS

Characterization of GPI8 in *T. cruzi*

Cloning of TcGPI8 and gene sequence analysis

To provide an approach to study the biological importance of GPI-anchored proteins in *T. cruzi*, the *T. cruzi* GPI8 (*TcGPI8*) gene was isolated, cloned and sequenced by utilizing available sequence information on known GPI8 genes. Alignment of *T. cruzi* GPI8 (*TcGPI8*) with yeast, human and *L. mexicana* GPI8 indicates that in *T. cruzi*, His198 and Cys156 correspond to the conserved active site residues (Figure 13). This observation suggested that TcGPI8 might have analogous catalytic activity. The function of *T. cruzi* GPI8 (TcGPI8) in GPI-anchoring activity and its essentiality to the survival of *T. cruzi* had not yet been elucidated prior to this proposal. Therefore, the objective of this study was to evaluate the effects of expressing TcGPI8 mutated in these conserved active site residues on GPI-anchoring activity in *T. cruzi* to determine whether the TcGPI8 analogously serves as the catalytic component of the GPI-anchoring machinery of *T. cruzi* and to evaluate the phenotypic effects of diminished or ablated GPI-anchoring on *T. cruzi*.

The open reading frame of *TcGPI8* is predicted to encode a protein of 325 amino acids with an isoelectric point (pI) of 6.14 and molecular mass of 37 kDa. iPSORT analysis further indicates a hydrophobic N-terminal signal peptide with a predicted cleavage site between residue number 26 and 27³⁰², suggesting that TcGPI8 is targeted to the endoplasmic reticulum. However, the ER retrieval sequence, KDEL³⁰³⁻³⁰⁴, is not present.

TcGPI8, as *Leishmania* and *T. brucei* GPI8, is likely to be a soluble protein, as there is no predicted transmembrane domain, unlike that identified for human and *S. cerevisiae* GPI8. It is postulated that interaction of these soluble GPI8s with other endoplasmic reticulum-localized proteins retains GPI8 in the proper site and orientation for its enzymatic function in association with the translocated precursor protein and the GPI-anchors, which are embedded in the ER membrane (Illustration 5). Recently, *T. cruzi* homologues of TTA1 and TTA2, two proteins involved in the TAM mechanism of *T. brucei*²⁵⁵, and of GAA1 could be identified in the *T. cruzi* genome public sequence database, which was completed on July 15, 2005²⁵⁹. However, no homologues of *PIG-S/gpi17*, *PIG-T/gpi16*, or *PIG-U/cdc91* could be identified²⁵⁹. It is possible that TcGAA1, TcTTA1 and/or TcTTA2 may serve to tether TcGPI8 to the endoplasmic reticulum membrane, facilitating its GPI-anchoring function (discussed in *Chapter 2, Other proteins involved in the TAM mechanism*).

At the amino acid level, TcGPI8 exhibits significant homology to GPI8 in *S. cerevisiae* (41%), *Leishmania* (55%) and *T. brucei* (68%). RT-PCR amplification of *GPI8* mRNA (Figure 14) demonstrated that *TcGPI8* is expressed at similar rates in all three life cycle stages. Southern blot analysis of *T. cruzi* chromosomal DNA indicated that *TcGPI8* was a single copy gene (Figure 15) and was thus amenable to targeted disruption. The significant homology of TcGPI8 to other characterized GPI8s and to plant endopeptidases, e.g., legumain, further provided a rationale for investigation of the essentiality of TcGPI8 and its role in the GPI-anchoring mechanism of *T. cruzi*.

Detection of TcGPI8 in T. cruzi

Screening of *GPI8-132* antisera

Preliminary optimization procedures were performed to select a dilution *GPI8-132* antisera (ProSci) to determine a dilution that achieved low background in Western blot (WB) analysis using wild type *T. cruzi* and control BHK21 lysates (Figure 16A). When matching control preimmunization serum was used at 1:1000 and 1:5000, there was the least non-specific binding of serum to proteins in experiments performed in parallel using identical lysates. Purification of *GPI8-132* antiserum by affinity chromatography using peptide-coupled NHS-activated sepharose resulted in two predominant elution fractions. Additional Western blot optimization was performed using dilutions in the range of 1:200 to 1:2000 (Figure 16B). In Western blot analysis to detect TcGPI8_{FH} expressed in bacteria, mammalian cells and *T. cruzi* transfectants, *GPI8-132* antiserum obtained from the pooled dialyzed fractions was used at 1:1000, as determined from these optimization procedures.

Detection of TcGPI8 expression by WB analysis

WB analysis did not detect expression of native TcGPI8 in wild type *T. cruzi* in 2×10^7 parasite equivalents using *GPI8-132* antisera at dilutions of 1:400-1:2000. Purification of *GPI8-132* antisera did not improve the sensitivity of detection. In addition, further efforts to concentrate, purify or immunoprecipitate native protein did not improve detection of protein at the predicted size of 36 kDa. Following Centricon concentration and trichloroacetic acid precipitation, an approximately 66 kDa band was seen in *T. cruzi* lysates that was not reactive with preimmunization serum (data not shown). To compare the level of detection for other *T. cruzi* proteins for which antibody was available, WB analysis was performed using available antibodies to *T. cruzi* proteins. Faint detection of the predicted 50-55 kDa band was achieved at a dilution of 1:1000 using anti-gp50/55 antibody (C10; ³⁰⁵, data not shown). At dilutions ranging from 1:1000 to 1:8000, anti-gp72 antibody²⁹¹ failed to detect the 72 kDa protein in 2×10^7 parasite equivalents (data not shown). These results suggested that the amount of TcGPI8 in total parasite lysate was a limiting factor in detection by WB analysis.

Specificity of *GPI8-132* for TcGPI8_{FH} detection

To provide positive controls for WB experiments of pTEX transfectants, to additionally confirm the expression of the predicted open reading frame (ORF) for the epitope-tagged *TcGPI8* construct, and to assess the specificity of the *GPI8-132* antiserum, *TcGPI8_{FH}* was cloned into pCDNA3 and into pET21b and expressed in mammalian cells (Figure 8) and in bacteria (Figure 9), respectively. GFP was expressed in pET21b.GFP and in pREP10.GFP expression controls in bacteria and in BHK21 cells, respectively, as indicated by *in situ* visualization under ultraviolet light. Therefore,

Western blot (WB) analysis was performed using protein lysates prepared from recombinant protein expression experiments performed in BHK21 cells and bacteria.

WB analysis using bacterial lysates was performed for triplicate membranes, which were incubated in parallel with *GPI8-132* antiserum, anti-Flu mAb, or the control preimmunization serum; WB detected expression of a protein of apparent molecular mass of 45 kDa in the lysate from *HMS174/DE3* bacteria/pET21b.*TcGPI8_{FH}* (Figure 16C, lane 3), which was not visible in the lysate from GFP-expressing bacteria (Figure 16C, lane 2). No bands at this apparent molecular mass were detected in the lysate of untransfected BHK21 cells, which was used as an additional negative control (Figure 16C, lane 1).

The expression of epitope tagged TcGPI8 was further evaluated in mammalian cells using protein lysates from transiently transfected BHK21 cells (Figure 8). As shown in Figure 16D, WB analysis using the anti-Flu antibody detected a band of apparent molecular mass of 45 kDa in lysates from BHK21 cells transfected with pCDNA3.*TcGPI8_{FH}* (lane 1), which was not present in lysates from either of the negative controls, e.g., BHK21/pCDNA3 lysates (Figure 16D, lane 8), or BHK21/pCDNA3.*GFP* (Figure 16D, lane 9). This increased size from the predicted 37 kDa for TcGPI8 would be expected based on the addition of a one hundred base pair epitope tag. For the positive control lysate, BHK21/pCDNA3.*MCAT_{FH}*, a protein of apparent molecular mass of 75 kDa was detected via anti-Flu mAb (Figure 16D, lane 10). For bacterial expression lysates used as additional controls in this WB analysis (Figure 16D, lanes 2-7), a protein migrating at an apparent molecular mass of 45 kDa was detected by the anti-Flu mAb in lysates of *HMS174/DE3* bacteria containing pET21b.*TcGPI8_{FH}* induced with IPTG (Figure 16D, lane 5 and 7). A faint band of the same molecular mass also could be seen in uninduced cultures grown in parallel (Figure 16D, lane 4 and 6). It is likely that this band represents "leaky" expression of TcGPI8 via the T7 promoter, since weak

expression of GFP was also observed under ultraviolet light in uninduced pET21b.*GFP*-transformed bacteria (data not shown). No band of this size was detected in lysates of pET21b.*GFP*-transformed bacteria (Figure 16D, lane 9). Together, these experiments indicate that an open-reading frame for TcGPI8_{FH} was expressed in bacteria and in mammalian cells and that *GPI8-132* antiserum was specific for detection of recombinant TcGPI8_{FH}.

OVER-EXPRESSION OF TCGPI8 PUTATIVE ACTIVE SITE MUTANTS

Selection of *T. cruzi* transfectants

To facilitate detection of over-expressed protein, *TcGPI8* was cloned in fusion with a carboxyl-terminal epitope tag, Flu₃His₆ (*TcGPI8_{FH}*) to generate pBSKII.*TcGPI8_{FH}* (Table 2). Mutant alleles of *TcGPI8* were created, and the respective ORFs were cloned into the *T. cruzi* expression vector, pTEX (Figure 1, Table 3) and confirmed by DNA sequencing (Figure 17A). pTEX containing the unmutated or mutated alleles of *TcGPI8* were electroporated into *T. cruzi* (*SylvioX10/4* strain) epimastigotes and cultivated in the selective drug, G418. After 2.5 months of incubation in medium containing G418, mock-electroporated wild type parasites died, indicative of successful drug selection. Subsequently, these transformants were cultured continuously in the presence of 200 µg/ml G418.

Screening of transformants by PCR analysis

The presence of the electroporated plasmid in transfectants was confirmed by PCR amplification of the *GAPDH-IR/neo^r* cassette present in pTEX (Figure 10, 17B).

The predicted ~1.3 kilobase *GAPDH-IR/neo^r* fragment could be amplified from all pTEX.*TcGPI8_{FH}* transfectants but not from the wild type control parasites (Figure 17B). The PCR amplification of a 780 base pair fragment representing the genomic copy of the *T. cruzi* *GAPDH* gene demonstrated that an equal amount of DNA was used in each reaction and confirmed the DNA quality used in all reactions (data not shown).

Detection of TcGPI8_{FH} protein expression in pTEX transformants

In *T. cruzi* transfectants, expression of TcGPI8_{FH} was demonstrated in WB analysis using both *GPI8-132* antisera (Figure 18A) and α -Flu mAb (Figure 18B). The density of the bands suggested that TcGPI8_{FH} was expressed at similar levels for pTEX.*TcGPI8_{FH}*, pTEX.*TcGPI8_{FH}^{C198A}* and pTEX.*TcGPI8_{FH}^{H156A}* transfectants. The level of expression was similar for transfectants cultivated at 100 or 200 μ g/ml G418, whereas it appeared to be marginally increased at 400 μ g/ml G418 (data not shown). However, at 800 μ g/ml G418, no detectable increase in protein expression over that achieved at a concentration of 400 μ g/ml was observed. Therefore, transfectants cultivated for >2 weeks in 400 μ g/ml G418 were used for subsequent phenotypic analyses.

Surface expression of GPI-anchored proteins in pTEX transformants

Surface expression of GPI-anchored proteins was investigated by immunostaining followed by flow cytometric analysis of epimastigote-stage transfectants using antibodies to mucins (2B10, 10D8) and to gp50/55 (C10) (Figure 19). Three independent FACS experiments of transfectants cultured in 400 μ g/ml G418 were performed comparing pTEX.*TcGPI8_{FH}*, pTEX.*TcGPI8_{FH}^{C198A}*, and pTEX.*TcGPI8_{FH}^{H156A}* transfectants to untransfected wild type parasites. These experiments were performed on stable transfectants. Stable transfection was defined by the death of mock-transfected *T. cruzi* in

G418 and the consistent detection of TcGPI8_{FH} expression when evaluated via WB analysis. For mock-transfected parasites continuously cultured in LIT medium containing 200, 400 or 800 µg/ml G418, no outgrowth of parasites was observed when monitored on a bi-weekly basis. For all parasites evaluated, live epimastigote stage parasites were successfully isolated by Ficoll-Paque gradient, and metacyclic trypomastigote forms were eliminated, based upon morphological observation under light microscope; these epimastigotes were recultured for over three weeks prior to FACS experiments. To maintain consistent growth and sampling, parasites were split at a ratio of 1 volume of parasite culture to 4 volumes of fresh parasite growth medium (liver infusion tryptose) three days prior to FACS staining experiments, which were performed once per week. The average percentage of positive staining events, which was calculated for each parasite type and antibody tested, is indicated in Figure 19. In testing using antibodies to any of the three GPI-anchored proteins (C10, 2B10, 10D8), there was no statistically significant difference in the mean percentage of positive events in pairwise comparisons of wild type parasites and transfectants ($p>0.05$). Importantly, no significant differences in mean percentage of positive events were detected between parasite types for the transmembrane protein control, GP72, or for the negative control, Y3. Thus, the surface expression of the GPI-anchored proteins GP50/55 (C10 antibody) or mucins (2B10 or 10D8 antibodies) was not reduced in pTEX.*TcGPI8_{FH}*^{C198A} or pTEX.*TcGPI8_{FH}*^{H156A} transfectants.

Life cycle development in pTEX transformants

The pattern of growth of pTEX transfectants as epimastigotes was similar to that of wild type *T. cruzi* (Figure 20). The mean parasite density on each day was calculated from three independent experiments, in which parasite density was determined by

counting on eight consecutive days following inoculation of 5×10^5 parasites into 5 ml growth medium. There was no statistically significant difference in mean parasite density (number of parasites/ml) comparing the *T. cruzi* control transfectant, pTEX.*TcGPI8*, with pTEX.*TcGPI8*^{H156A} or pTEX.*TcGPI8*^{C198A} ($p > 0.05$). For subsequent *in vitro* infection experiments, *T. cruzi* epimastigote transfectants were maintained at 400 µg/ml G418 in LIT medium for >10 days to obtain stationary-phase trypomastigotes that were utilized to pTEX.*TcGPI8*_{FH}^{H156A} transfectants were capable of infecting and replicating to similar levels as the wild type parasites and the pTEX.*TcGPI8*_{FH} transfectant in both fibroblast lines. Extracellular trypomastigotes were observed at 6 days post-infection for the transfectants as well as for wild type, untransfected parasites. Extracellular amastigotes also appeared at the same time points for all transfectants as for the wild type (data not shown). Thus, infectivity and *in vitro* development did not appear to be impaired in pTEX.*TcGPI8*_{FH}^{C198A} or pTEX.*TcGPI8*_{FH}^{H156A} transfectants, as compared to either the wild type parasites or the pTEX.*TcGPI8*_{FH} transfectant. Consistent with the lack of dominant-negative effect on GPI-anchoring, no phenotypic effects were observed for the aspects of *T. cruzi* life cycle evaluated.

Targeted disruption of TcGPI8

Generation of transformants

Transformants were obtained from electroporation and drug selection of *neo*^r-based *TcGPI8* disruption construct designed for disruption of one allele of *TcGPI8*. Only two of five replicate electroporations with the *neo*^r- *TcGPI8* construct resulted in selection of G418 transformants, suggesting that loss of *TcGPI8* may be unfavorable to parasite growth. The amount of DNA used in electroporation and the drug concentration

used in selection were varied to potentially improve transfection and/or selection efficiency, with no enhancement of selection timing or outcome.

Effects of neo^r -TcGPI8 transformation on *T. cruzi* development

The neo^r -TcGPI8 transfectants showed unusual morphologies, first with the appearance of extended thin forms that appeared reduced in motility. Confocal microscopy analysis of these transfectants demonstrated that *T. cruzi* development was defective (Figure 21B) in transfectants, whereas wild type, untransformed parasites cultured in parallel showed typical morphology (Figure 21A). The nucleic acid staining pattern observed in these “doublet” parasites using the green fluorescent dye, syto11, indicated that duplication of kinetoplast and nuclear DNA was not impaired²⁸⁹. Epimastigotes died and could not further be maintained in culture for >5 months after selection.

Evaluation of life cycle development in neo^r -TcGPI8 transformants

Three independent *in vitro* infection experiments were performed in two different fibroblast lines, C2C12 and BHK21 cells, using stationary-phase cultures of wild type and neo^r -TcGPI8 transfectants. Transfectants did not convert to the typical morphology of the infective metacyclic form following ≥ 10 days of cultivation without addition of new growth medium. No extracellular trypomastigotes were seen when monitoring cells infected with stationary-phase culture for up to 10 days. As a positive control for infection, *in vitro* infection experiments were performed with wild type parasites. These parasites infected both fibroblast lines, as indicated by the appearance of extracellular trypomastigotes and amastigotes at the anticipated time points following infection (data not shown).

Transformation with ble^r-TcGPI8 construct

Experiments were performed to disrupt the first allele of *TcGPI8* using the *ble^r*-based disruption construct. Upon transfection of wild type *T. cruzi* with the *ble^r-TcGPI8* disruption construct, no transformants were obtained from selection in phleomycin (ble). The first experimental set, in which drug selection in 50-100 µg/ml ble was performed, indicated that the concentration of ble was inadequate to select for transformants, as wild type parasites were capable of replicating for >3 months in this concentration range. At a later time point post-transfection, the ble dosage was increased to 500 µg/ml but did not improve selection. Subsequent electroporations were followed by selection using drug concentrations ranging from 250-750 µg/ml of ble. By 6 weeks, all transfected parasites cultured at 750 µg/ml died; by 8 weeks, those at 250 and 500 µg/ml ble died. These experiments indicate, mostly likely, that the efficacy of ble as a selective drug for *T. cruzi* is poor.

In attempt to disrupt the second copy of *TcGPI8*, G418-resistant parasites obtained from electroporation of the *neo^r-TcGPI8* disruption construct were subsequently electroporated with the *ble^r-TcGPI8* disruption construct or with pTEX_{ble}, or pTEX_{ble}-*TcGPI8_{FH}* as controls. Several combined G418/ble concentrations were used to select transformants (concentrations: 0, 50, 100 µg/ml G418/0, 250, 500 µg/ml ble). However, no clear trend in selection could be surmised, with the continued survival of mock-transfected parasites at 10 weeks following electroporation. Therefore, this set of electroporated parasites was no longer maintained in culture.

Stable *neo^r-TcGPI8* transfectants, in which the integration of the *neo^r* gene into the parasite genome was demonstrated (see *Evaluation of integration of neo^r via PCR and Southern blot analysis*), were subsequently electroporated with the *ble^r-TcGPI8*

disruption construct. During cultivation in 500 µg/ml ble, drastic changes from normal epimastigote morphology in axenic cultures were observed over time (Figure 22A) that were not observed in the wild type parasites cultured in parallel with the selective drug (Figure 22B). Amastigote-like forms with short, retracted flagella were abundant among the transfected population (Figure 22A)²⁸⁹. Uptake of propidium iodide in these forms indicated that parasite membranes were disrupted (data not shown).

Evaluation of integration of neo^r via PCR and Southern blot analysis

PCR amplification was performed to confirm the presence of the *GAPDH-IR/neo^r* cassette in the transfectants. The ~1.3 kilobase fragment was consistently amplified from gDNA of transfectant but not from wild type parasites, as expected (Figure 23A). This result confirmed the integration of the construct into the chromosomal DNA of transfectants. For the second set of transformants, the *GAPDH-IR-neo^r* cassette could not be PCR-amplified from gDNA after long-term cultivation (data not shown). This suggested that they were not stable transformants. Therefore, no further evaluation was performed for the second set. As shown in Figure 23B, in SB analysis of *neo^r-TcGPI8* transfectants, hybridization occurred with the *neo^r* probe; for wild type gDNA, no hybridization with the *neo^r* probe was observed; this result indicated that *neo^r* was present in the transfectant genome²⁸⁹.

Evaluation of targeted disruption of *TcGPI8* via PCR analysis

To determine whether *TcGPI8* was disrupted by the *neo^r-TcGPI8* construct, four independent PCR experiments were performed. First, to confirm whether the primers corresponding to the 5' or 3' flanking sequence were able to bind and amplify the predicted 2 kilobase (kb) fragment, PCR was performed using chromosomal DNA

(gDNA) obtained from either the SylvioX10/4 (Sylvio) or the Cl-Brener (CL) strain of *T. cruzi*. (Figure 24A, lanes 4 and 7). A 2 kb PCR fragment was detected for both strains. No product resulted from reactions in which only one primer was used (Figure 24A, lanes 5, 6, 8, and 9) or from matching PCR reactions using DNA from BHK21 cells as a negative control with both primers (Figure 24A, lane 10) or with a single primer (Figure 24A, lane 11 and 12). Thus, further experiments to evaluate disruption of the *TcGPI8* gene were performed using these primers (Figure 11). As shown in Figure 24B, no PCR product of the expected size for either of the confirmatory fragment C or D was amplified from gDNA of transfectants, although the expected *GAPDHIR-neo^r* cassette (fragment A1) as well as a 780 bp product using *GAPDH* gene-specific primers (fragment G) could be amplified. As additional positive controls, fragments A3 and A1 were amplified successfully from plasmid, as the indicated reactions P1 and P2, respectively resulted in the predicted 2.2 and 1.3 kb products. Three independent PCR experiments were performed, including one experiment utilizing a less stringent primer annealing temperature to improve the likelihood of successful primer binding. All PCR results were consistent for all control and test products, indicating that TcGPI8 was not specifically disrupted in these stable *neo^r-TcGPI8* transfectants. Further, these PCR results indicated that the 5' segment of *TcGPI8*, represented as fragment E, was not maintained during integration of the *GAPDHIR-neo^r* cassette into the genome (Figure 24B, lane 13). Additional experiments indicated that neither the 3' nor the 5' segment of *TcGPI8* was present adjacent to the integrated *GAPDHIR-neo^r* cassette (Figure 24C, lanes 1 and 3). These results were confirmed in three independent PCR experiments.

Identification of the site of integration of GAPDHIR-neo^r cassette in T. cruzi genome

Genome walking via an arbitrarily primed PCR approach to determine the site of integration resulted in three informative PCR-clones in which the expected *GAPDHIR/neo^r* portions were present (Figure 25A), and provided additional 5' flanking sequence of approximately 200 bases for Blast search. TcruziDB Blast search indicated that this insertion is located adjacent to the 3' end of one of the *GAPDH* genes (CL-Brener strain locus tag nos. Tc00.1047053506943 and Tc00.1047053509065; *GAPDH* of SylvioX10/6 strain, accession # X52898³⁰⁶) (Figure 25B)²⁸⁹.

CHAPTER 4:

CONCLUSIONS

Over-expression of TcGPI8 mutants

GPI-anchoring was neither diminished nor lost by over-expression of TcGPI8 C198 and H156 mutant alleles at the level of expression achieved at selective drug pressure of 400 µg/ml. Despite the lack of significant reduction in gp50/55 or mucins in this study, it remains possible that changes in other GPI-anchored proteins may have occurred. In other trypanosomes, e.g., *L. mexicana* and *T. brucei*, relatively few highly dominant GPI-anchored proteins have been described that play significant roles in their life cycle development. However, in *T. cruzi*, a greater variety of GPI-anchored proteins have been described, many of which have been ascribed roles in host cell attachment and/or the complex process of infection. In *T. cruzi*, the hierarchy of the transamidase's preference for anchoring of specific precursor proteins is unknown. This study was limited by the availability of reagents to detect a wider number of GPI-anchored proteins expressed in *T. cruzi* and does not exclude the hypothesis that subtle turnover of GPI-anchored protein expression could not be detected and that small changes may significantly impair the life cycle development of *T. cruzi*. Thus, it is conceivable that quantitatively small changes in the level of different GPI-anchored proteins among the transfectant population could collectively contribute to a net developmental impairment. However, in accordance with the lack of GPI-anchoring defect of these mutants, no impairment of *in vitro* infectivity, differentiation and replication was observed in this study. Collectively, these results suggest that the active site of TcGPI8 differs from that described for yeast, human and *Leishmania* GPI8^{253,277-278}.

In conclusion, these results suggest that the active site of TcGPI8 may not be comprised of H198A and C156A and, therefore, differs from the conserved residues in yeast, human and *Leishmania* GPI8. The approach used in this study, namely, the over-expression of mutant alleles in the presence of continued expression of native TcGPI8, does not rule out several alternative explanations for the lack of dominant negative effect on GPI-anchoring. First, the level of over-expression achieved in this system may not be sufficient to produce a dominant negative effect on GPI-anchoring. In this scenario, expression of mutant TcGPI8 alleles would be insufficient to out-compete native TcGPI8 for precursor proteins and thus, complete anchors remain available as substrate for native TcGPI8 to provide for wild type level of anchoring. A precedent is provided by prior studies where yeast GPI8 (yGPI8) mutant alleles were expressed via the physiological (native) yGPI8 promoter or the GAL1-10 promoter, resulting in only ~4-10 fold overexpression of yGPI8 alleles. This level did not produce a dominant-negative effect on anchoring. However, when yGPI8 expressed via the *CUP1* promoter was >20 fold over-expressed, a phenotypic effect was observed for the hypothesized active site mutants of yGPI8²⁷⁷.

In *T. cruzi* with the pTEX episomal expression system, increased expression of the exogenous protein is achieved via increasing the concentration of G418²⁹⁰. In this study, analysis of transfectants under further increased drug pressure did not appear to be warranted, as WB indicated that the level of TcGPI8_{FH} was not markedly increased at concentration of 800 µg/ml G418 as compared to that of transfectants maintained at 400 µg/ml. In yGPI8 studies, the level of over-expression of mutated yGPI8 to the same level as unmutated yGPI8 could not be achieved via any of the tested yeast over-expression systems. This was interpreted as evidence of the organism's selection against mutant alleles, as loss of GPI-anchoring is lethal for yeast²⁷⁷. In this study, it appears that an

overall threshold may exist when using pTEX, independent of the TcGPI8 allele expressed.

Second, mutation of C198 and H156 individually may be insufficient to disrupt the catalytic activity of TcGPI8, as the TAM active site may show plasticity that has been described for other enzyme homologues³⁰⁷. Specifically, neighboring histidine and cysteine residues present in TcGPI8 may provide equivalent functions and could be investigated by over-expression of TcGPI8 with mutations in both C198 and H156 (double mutants, DM).

Theoretically, it is possible that the Flu₃His₆ epitope-tag used in this study may inadvertently hinder the interaction of TcGPI8 with other putative TAM components or may interfere with correct protein folding. Prior studies have suggested that misfolded proteins are targeted for degradation in the proteosome³⁰⁸, and elements of this proteosomal pathway have been described in *T. cruzi*³⁰⁹⁻³¹³. Further, this epitope-tag has been used effectively in other expression systems³⁰⁰. Since TcGPI8_{FH} was consistently detected in transfectants maintained at G418 concentrations of 200, 400 and 800 µg/ml, degradation or secretion does not appear to have occurred.

The lack of a transmembrane domain in TcGPI8 suggests that, as a soluble protein, interaction with other proteins is required to tether it to the inner ER membrane for function in attaching the GPI-anchors, which are known to be embedded in the ER membrane, to the translocated precursor proteins³¹⁴. It is possible that the epitope tag interferes with binding to other TAM or prevents the requisite association with the ER membrane. Two approaches are possible to investigate this alternative explanation for a lack of dominant negative effect on anchoring: 1) co-immunoprecipitation of TAM components, and 2) expression of TcGPI8 and mutated forms that lack epitope-tags.

To evaluate the first point, co-immunoprecipitation of TcGPI8 along with interacting proteins, using either *GPI8-132* antiserum or, in transfectants, anti-Flu antibody, was attempted. However, the co-immunoprecipitation reactions resolved on SDS-PAGE followed by detection using silver staining were insufficiently clean to identifying putative TAM complex proteins, e.g., the *T. cruzi* homologues of the TbGPI8 interacting proteins, e.g., TTA1 and TTA2, that have recently been reported in the public database²⁵⁵, although TcGPI8_{FH} could be detected by WB following immunoprecipitation (data not shown). This limitation has been reported in other studies, and TAM complexes containing GPI8 have exclusively been detected when epitope-tagged proteins are over-expressed^{255,278-281}, rather than identification of native complexes expressed at physiological levels.

Homologues to yeast or mammalian proteins demonstrated to participate in the TAM mechanism, e.g., gaa1, PIG-T (gpi17), PIG-S (gpi16), or PIG-U (cdc91)^{246,251,278,280-281,284}, could not be identified by continued Blast search of the *T. cruzi* database throughout this study. To address the issue of epitope tag interference with TAM complex activity, *TcGPI8* constructs that lack any epitope-tag could be cloned and expressed in *T. cruzi* using pTEX. However, this was not attempted in this study, as the absence of the epitope-tag would make it impossible to distinguish the over-expressed mutant form from that expressed from the chromosomal copy of *TcGPI8*.

It remains possible, but unlikely, that TcGPI8 itself is not the catalytic subunit required for GPI-anchoring via transamidation in *T. cruzi*. Studies designed to complement the class K GPI8-deficient cell line by over-expression of TcGPI8 and of mutant TcGPI8 alleles have the potential to address this question. The hypothesis is that GPI-anchoring in class K cells will be restored by TcGPI8, provided that TcGPI8 interacts with the other mammalian TAM complex proteins and that TcGPI8 recognizes

the C-terminal anchoring signal sequence of mammalian GPI-precursor proteins. Provided that TcGPI8 can complement hGPI8 function, if H198 and/or C156 are the active site residues, then over-expression of these mutant alleles in class K cells would be unable to restore GPI-anchoring.

Integration of *GAPDHIR-neo^r* adjacent to the *GAPDH* gene

A marked cytokinesis defect was observed in *neo^r-TcGPI8* transformants at the epimastigote stage. At the time this phenotype became apparent, growth of transformants declined, indicating they were unable to complete their replication cycle. This phenotype was similarly demonstrated in *T. brucei* when *TbGPI8* expression was depleted by double stranded RNA interference and loss of GPI-anchoring occurred¹⁸⁰, although the precise mechanism of this cytokinesis defect has not been established. The morphological transformation of epimastigotes into metacyclic trypomastigotes in culture conditions of "starvation" did not occur for these *neo^r-TcGPI8* transformants, unlike for wild type parasites. These *neo^r-TcGPI8* transformants were unable to infect mammalian cells *in vitro*.

Name	Purpose	DNA Sequence (5-'3')
<i>GPI8F-SpeI</i>	Epitope-tag cloning in pRD67	ACTAGTATGAAGCGCCAGATGGG
<i>GPI8R-XhoI</i>	Epitope-tag cloning in pRD67	ATCCTCGAGAGCAAGTCATATTGTACAT CCACTGG
<i>GPI8^rTAG-F</i>	SDM (TAG184 ^r GAG)	GATGATGTGGGAGCAACGACGG
<i>GPI8^rTAG-R</i>	SDM (TAG184 ^r GAG)	CCGTCGTTGCTCCACACATC
<i>GPI8QC(C/A+XhoI)-F</i>	SDM (C198A)	ATGTGGACACAGCTCGAGCATTGTC
<i>GPI8QC(C/A+XhoI)-R</i>	SDM (C198A)	AGACAATGCTCGAGCTGTGTCCAGC
<i>GPI8QC(H/A+NaeI)-F</i>	H156A	CGCGGCCGGCGCCGCCGCAAAGAG
<i>GPI8QC(H/A+NaeI)-R</i>	H156A	CTCTTTGCGGCGGCGCCGCCGCG
<i>M13F</i>	DNA sequencing	GTAAAACGACGGCCAGT
<i>M13R</i>	DNA sequencing	GGAAACAGCTATGACCATG
<i>T7</i>	DNA sequencing	GTAATACGACTCACTATAGGGC
<i>Sp6</i>	DNA sequencing	GATTTAGGTGACACTATAG
<i>GAPDHIR-F</i>	<i>GAPDHIR-neo^r</i> , <i>GAPDHIR-ble^r</i> amplification from pTEX	GCGAGATCTGCGTGGCGATGACT
<i>neo^r-R</i>	<i>GAPDHIR-neo^r</i> from pTEX	GCGGATATCTCAGAAGAACTCGTC
<i>ble^r-R</i>	<i>GAPDHIR-ble^r</i> from pTEX	CATGCCATGGTCAGTCCTGCTCCTCGG
<i>GAPDH-F</i>	SB probe	CGGCTTTGGCCGCATCGGACGC
<i>GAPDH-R</i>	SB probe	CGGACACGTCCGGGGTGGGG
<i>5'FS-F</i>	PCR to confirm disruption	ATGCTGCGGATGTATTCTAAACGGG
<i>3'FS-R</i>	PCR to confirm disruption	GGGTCCACTTGCAGTCCCATTGTTG
<i>neo^r-R1</i>	TAIL-PCR	TTTCGCTTGGTGGTGAATGGGCAGGTA
<i>neo^r-R2</i>	TAIL-PCR	GCACAGCTGCGCAAGGAACGCC
<i>neo^r-R3</i>	TAIL-PCR	GCCGCGCTGCCTCG
<i>neo^r-F1</i>	TAIL-PCR	TACCTGCCCATTTCGACCACCAAGCGAA CAT
<i>neo^r-F2</i>	TAIL-PCR	AACGTGTCGCCAGGCTCAAGGCGCG
<i>neo^r-F3</i>	TAIL-PCR	GCCGCGCTGCCTCG
<i>AD1</i>	TAIL-PCR	TG(A/T)GNAG(A/T)ANCA(G/C)AGA
<i>AD2</i>	TAIL-PCR	AG(A/T)GNAG(A/T)ANCA(A/T)AGG
<i>AD3</i>	TAIL-PCR	CA(A/T)CGICNGAIA(G/C)GAA
<i>AD4</i>	TAIL-PCR	TC(G/C)TICGNACIT(A/T)GGA

Table 1: Primers. All primers used to perform PCR, cloning, site-directed mutagenesis, DNA sequencing and for screening of transfectants by PCR and Southern blot analysis are listed. The *neomycin resistance* gene (neomycin phosphotransferase, Accession # AAC08734) confers resistance to the drug, G418. The *ble resistance* gene (*Streptoalloteichus hindustans* phleomycin-ble binding protein, Accession # X52869), confers resistance to the drug, phleomycin (ble)²⁹¹. Abbreviations: F, forward primer; R, reverse primer; SDM, site-directed mutagenesis; GAPDH, glyceraldehyde phosphate dehydrogenase; IR, intergenic region; *neo^r*, *neomycin resistance gene*; *ble^r*, *ble resistance gene*; SB, Southern blot; FS, flanking sequence; TAIL-PCR, thermal asymmetric interlaced-PCR.

Plasmid	Gene	Selection marker	Epitope tag	Description	Bacterial strain
pSTBlue1	-	<i>amp^r</i>	-	PCR product cloning vector (Novagen)	<i>E. coli NovaBlue</i> TM
pSTBlue1. <i>SpeI</i> - <i>TcGPI8</i> - <i>XhoI</i>	<i>TcGPI8</i>	<i>amp^r</i>	-	Subcloning of <i>TcGPI8</i> into pRD67	<i>E. coli NovaBlue</i> TM
pRD67	-	<i>amp^r</i>	<i>FH</i>	Cloning in fusion with <i>FH</i> via <i>XhoI</i> site	<i>E. coli DH5α, XL-1Blue</i>
pRD67. <i>TcGPI8</i> _{FH}	<i>TcGPI8</i>	<i>amp^r</i>	<i>FH</i>	<i>SpeI/HindIII</i> for cloning	<i>E. coli DH5α, XL-1Blue</i>
pBSKII(SK+/-)	-	<i>amp^r</i>	-	Cloning vector (Stratagene)	<i>E. coli DH5 α, XL-1Blue</i>
pBSKII. <i>TcGPI8</i> _{FH}	<i>TcGPI8</i>	<i>amp^r</i>	<i>FH</i>	Subclone for site-directed mutagenesis- <i>SpeI/NsiI</i> fragment containing <i>TcGPI8</i> ORF	<i>E. coli DH5 α, XL-1Blue</i>

Table 2: *TcGPI8* cloning constructs. Constructs for cloning of *TcGPI8* in fusion with the Flu₃His₆ (FH) epitope tag sequence³⁰⁰ and for subsequent site-directed mutagenesis of *TcGPI8* are listed. Plasmids were transformed in the indicated bacterial strain for cloning purposes. All plasmids contain the *ampicillin resistance* (*amp^r*) gene for selection with ampicillin.

Plasmid	Gene	Selection marker	Epitope tag	Description	Transformation
pTEX	-	<i>neo^r</i>	-	<i>T. cruzi</i> expression vector	<i>T. cruzi</i>
pTEX. <i>TcGPI8</i> _{FH}	<i>TcGPI8</i>	<i>neo^r</i>	<i>FH</i>	<i>TcGPI8</i> , unmutated	<i>T. cruzi</i>
pTEX. <i>TcGPI8</i> _{FH} C198A	<i>TcGPI8</i>	<i>neo^r</i>	<i>FH</i>	C198A mutant allele of <i>TcGPI8</i>	<i>T. cruzi</i>
pTEX. <i>TcGPI8</i> _{FH} H156A	<i>TcGPI8</i>	<i>neo^r</i>	<i>FH</i>	H156A mutant allele of <i>TcGPI8</i>	<i>T. cruzi</i>

Table 3: *T. cruzi* expression vectors. The *T. cruzi* expression vector, pTEX²⁹⁰, was used for expression of *TcGPI8*_{FH}, the mutant alleles, C198A and H156A of *TcGPI8*_{FH}. Drug selection of pTEX transformants in *T. cruzi* using G418 is conferred by expression of the selection marker, *neo^r*. pTEX also contains the *ampicillin resistance* (*amp^r*) gene for plasmid cloning in bacteria. Abbreviations: FH, Flu₃His₆

Plasmid	Gene	Selection marker	Epitope tag	Description	Transformation
pCDNA3	-	<i>amp^r</i>	-	Mammalian expression vector (Invitrogen); transfection control	BHK21
pCDNA3. <i>TcGPI8</i> _{FH}	<i>TcGPI8</i>	<i>amp^r</i>	<i>FH</i>	Unmutated gene	BHK21
pREP10. <i>GFP</i>	<i>GFP</i>	<i>amp^r</i>	-	Transfection control (Invitrogen)	BHK21
pCDNA3.MCAT _{FH}	<i>MCAT</i>	<i>amp^r</i>	<i>FH</i>	Transfection control (R. Davey)	BHK21

Table 4: Mammalian expression vectors. pCDNA3 contains the cytomegalovirus (CMV) promoter and poly-A addition signals for expression of cloned genes in mammalian cells. pCDNA3 contains the *ampicillin resistance* (*amp^r*) gene for plasmid cloning in bacteria. *MCAT*_{FH}³⁰⁰ encodes a 70-75 kDa protein. Abbreviations: GFP, green fluorescent protein; FH, Flu₃His₆ epitope-tag; BHK21; baby hamster kidney cell line.

Plasmid	Gene	Selection marker	Epitope tag	Description	Transformation
pET21b	-	<i>amp^r</i>	-	Bacterial expression vector (Novagen)	<i>DH5α, XL-1Blue</i> (cloning); <i>HMS174/DE3</i> (expression)
pET21b. <i>TcGPI8</i> _{FH}	<i>TcGPI8</i>	<i>amp^r</i>	<i>FH</i>	Recombinant TcGPI8 (rTcGPI8) expression	<i>HMS174/DE3</i>
pET21b.MCAT _{FH}	<i>MCAT</i>	<i>amp^r</i>	<i>FH</i>	Transfection control	<i>HMS174/DE3</i>
pET21b. <i>GFP</i>	<i>GFP</i>	<i>amp^r</i>	-	Transfection control (Invitrogen)	<i>HMS174/DE3</i>

Table 5: Bacterial expression vectors. pET21b contains the T7lac promoter for the IPTG-inducible expression of cloned genes in bacteria. *MCAT*_{FH}³⁰⁰ encodes an ~70-75 kDa protein. pET21b contains the *ampicillin resistance* (*amp^r*) gene for plasmid cloning in bacteria. Abbreviations: FH, Flu₃His₆; GFP, green fluorescent protein.

Plasmid	Selection marker	Description	Transformation
pCR2.1	<i>amp^r</i>	TA cloning vector (Invitrogen)	<i>E. coli Topo10F'</i> (cloning, Invitrogen)
pCR2.1. <i>GAPDHIR-neo^r</i>	<i>amp^r</i>	cloning of PCR product	-
pBSKII.5' <i>TcGPI8-GAPDHIR-neo^r-3'TcGPI8</i>	<i>neo^r</i>	<i>neo^r</i> -based <i>TcGPI8</i> disruption cassette (<i>ScaI/HindIII</i> fragment)	<i>T. cruzi</i>
pTEX _{ble}	<i>amp^r, ble^r</i>	PCR amplification of <i>GAPDHIR/ble^r</i> ; electroporation control	<i>T. cruzi</i>
pSTBlue1. <i>GAPDHIR-ble^r</i>	<i>amp^r</i>	clone of PCR product	<i>E. coli NovaBlueTM</i> (cloning, Novagen)
pBSKII.5' <i>TcGPI8-GAPDHIR-neo^r-3'TcGPI8</i> ^{<i>BamHI</i>}	<i>amp^r</i>	cloning of construct	<i>E. coli DH5α, XL-1 Blue</i>
pBSKII.5' <i>TcGPI8-GAPDHIR-ble^r-3'TcGPI8</i>	<i>ble^r</i>	<i>ble^r</i> -based <i>TcGPI8</i> disruption cassette (<i>ScaI</i> fragment)	<i>T. cruzi</i>

Table 6: Cloning vectors and constructs for targeted disruption of *TcGPI8*. All plasmids contain the *ampicillin resistance* (*amp^r*) gene for selection in ampicillin. Abbreviations as listed in Table 1.

FIGURES

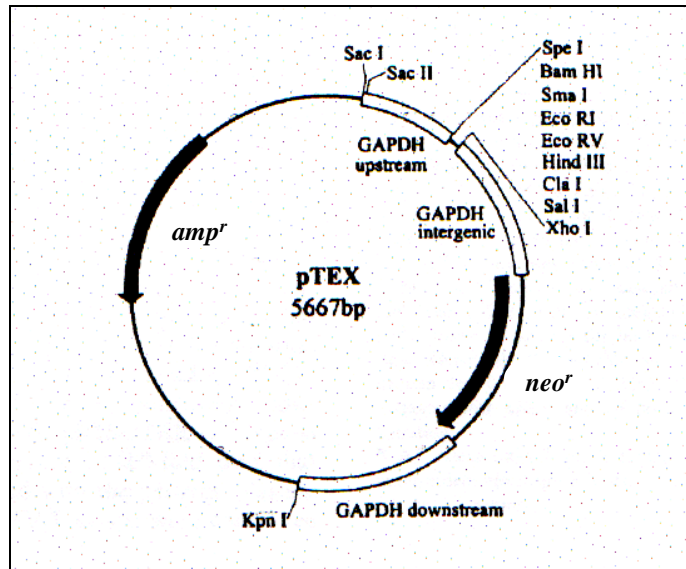


Figure 1: The *T. cruzi* expression vector, pTEX. The *T. cruzi* expression vector, pTEX²⁹⁰ has been used effectively for extra-chromosomal expression of a variety of exogenous genes in *T. cruzi*^{57, 315-316}. pTEX has a multiple cloning site flanked by upstream- and intergenic-region sequences of the *T. cruzi* GAPDH gene²⁹³ to allow for constitutive expression of the cloned gene of interest. In addition, pTEX contains the neomycin resistance (*neo^r*) gene to facilitate stable selection of transformants using the antibiotic G418 following electroporation of parasites. For cDNA cloning, the ampicillin resistance gene (*amp^r*) allows for selection of recombinant plasmids. Diagram reprinted with permission from Martinez-Calvillo, S., I. Lopez, and R. Hernandez, *pRIBOTEX expression vector: a pTEX derivative for a rapid selection of Trypanosoma cruzi transfectants*. Gene, 1997. 199(1-2): p. 71-6.

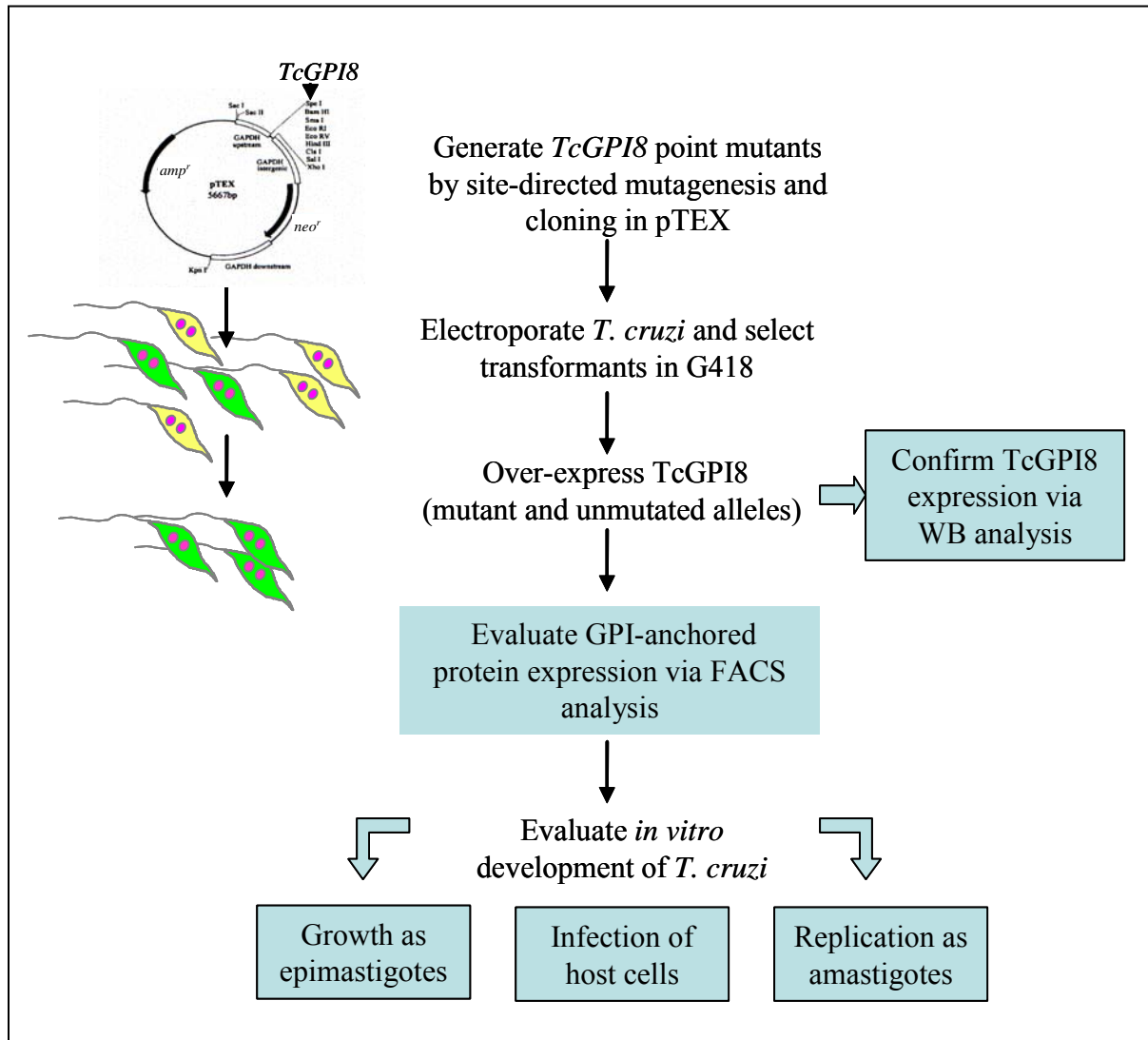


Figure 2: Experimental approach to over-expression of TcGPI8 in *T. cruzi*.

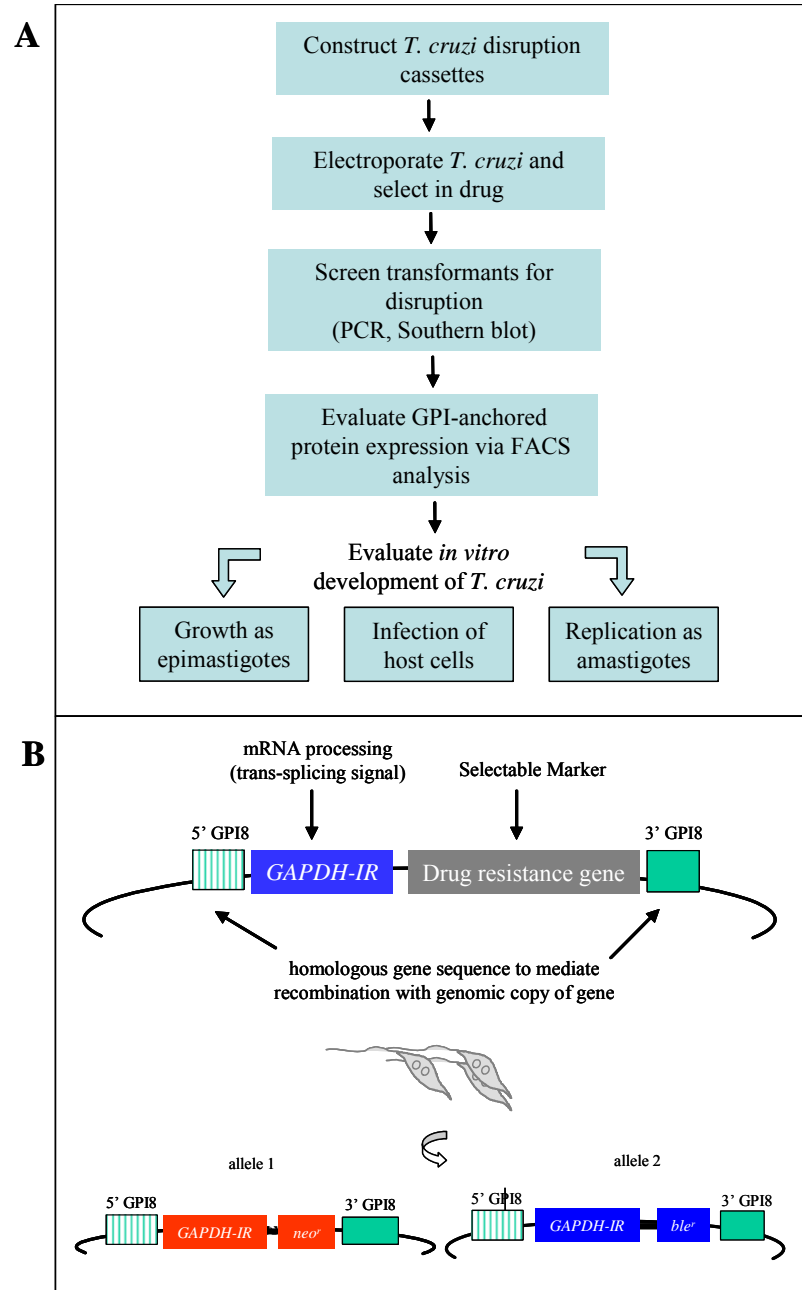


Figure 3: Experimental approach to targeted disruption of *TcGPI8* in *T. cruzi*. A) Experimental flow chart. B) Schematic of disruption constructs.

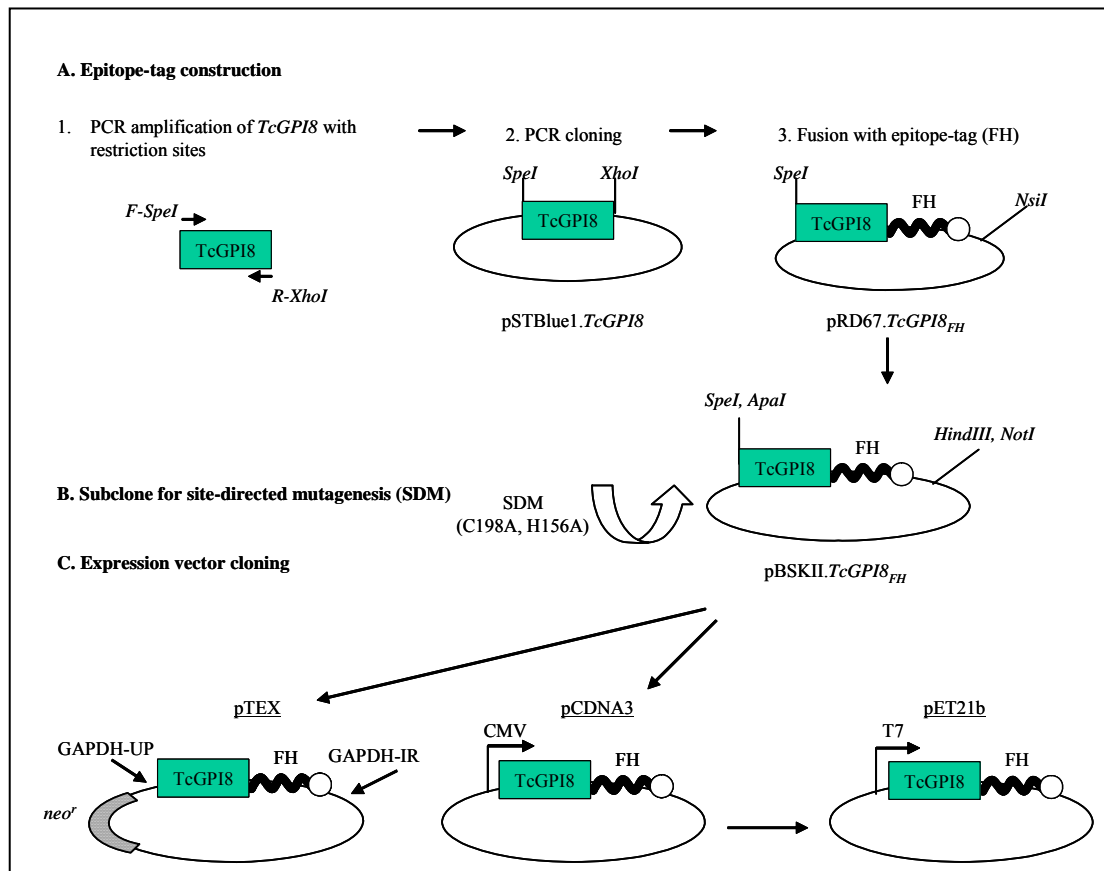


Figure 4: Cloning of *TcGPI8* in expression vectors. A) *TcGPI8* was cloned in fusion with the Flu₃His₆ (FH) epitope-tag, as follows. 1) PCR amplification of *TcGPI8* was performed using primers that incorporated an *SpeI* restriction enzyme site adjacent to the ATG (start) codon of *TcGPI8* and an out-of-frame *XhoI* site at the 3' end of *TcGPI8* (primer pair: *GPI8F-SpeI* and *GPI8R-XhoI*). 2) The PCR product was cloned into pSTBlue1 via blunt end ligation. 3) The *SpeI/XhoI* insert containing *TcGPI8* was then cloned in fusion with the epitope-tag in pRD67³⁰⁰. Screening of plasmid DNA clones was performed using restriction enzyme digestion. DNA sequence was obtained using plasmid-based primers (SP6, T7, M13F, or M13R primers). B) For the purpose of site directed mutagenesis (SDM) and subsequent cloning, *TcGPI8_{FH}* was cloned into pBSKII via *SpeI/NsiI* (cohesive to *SpeI/PstI*). C) After SDM, the *TcGPI8_{FH}* open reading frame was cloned into the *T. cruzi*, mammalian and bacterial expression vectors: pTEX, pCDNA3 and pET21b, respectively. For pTEX.*TcGPI8_{FH}*, the *SpeI/HindIII* insert from pBSKII.*TcGPI8_{FH}* was cloned into pTEX. For pCDNA3.*TcGPI8_{FH}*, the *ApaI/NotI* insert was used. For pET21b.*TcGPI8_{FH}*, the *SpeI/HindIII* insert from pCDNA3.*TcGPI8_{FH}* (cohesive to *NheI/HindIII* in pET21b) was used.

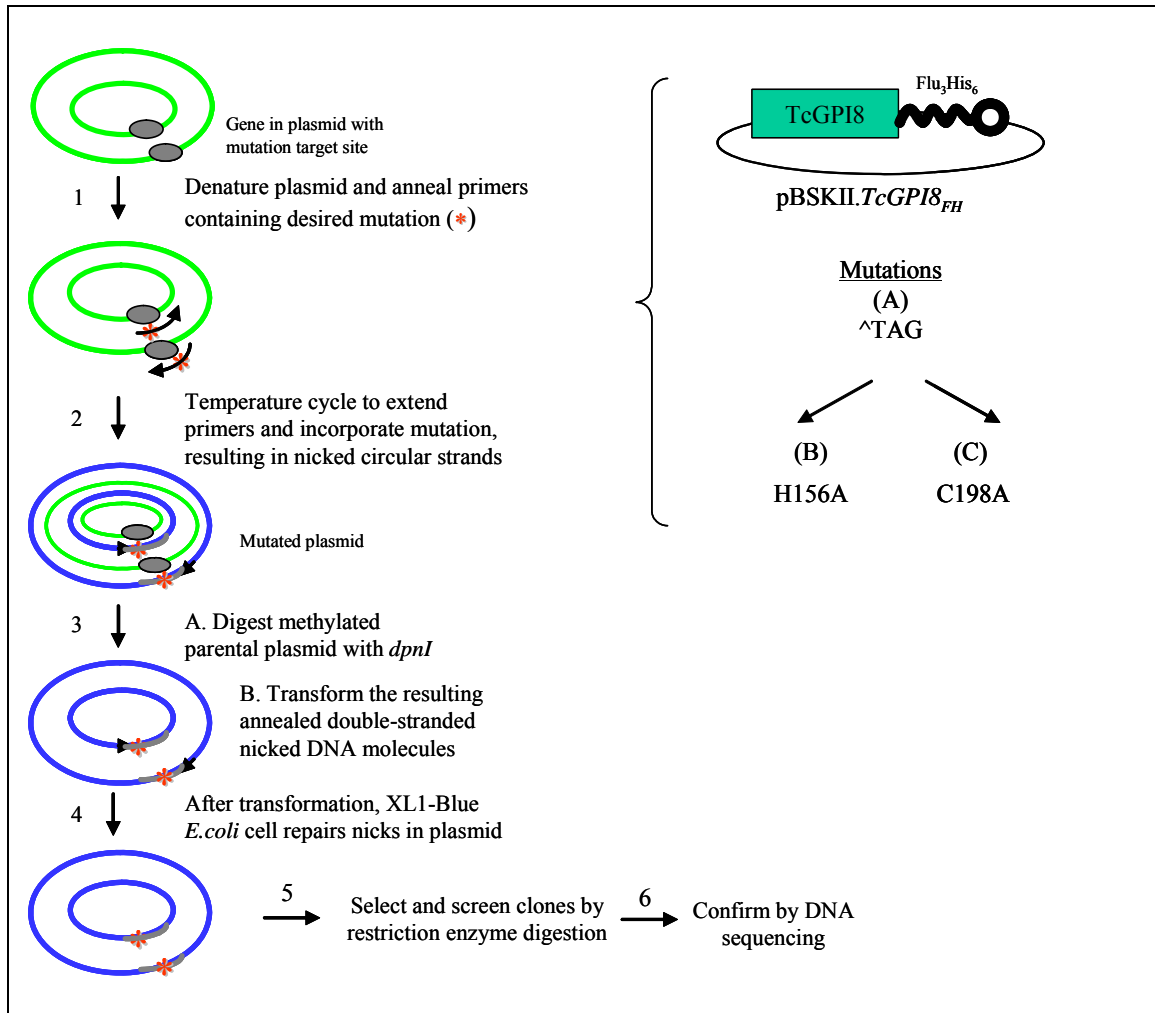


Figure 5: Site-directed mutagenesis of TcGPI8. Stratagene QuickChange™ Site Directed Mutagenesis method was used to: A) recreate the open-reading frame sequence for TcGPI8 using the primer pair GPI8^{^TAG}-F, GPI8^{^TAG}-R and to mutate the putative active site residues, B) H156A using primers GPI8QC(H/A+NaeI)-F, GPI8QC(H/A+NaeI)-R, and C) C198A using primers GPI8QC(C/A+XhoI)-F, GPI8QC(C/A+XhoI)-R. Source: Modified and reprinted with permission from Stratagene QuikChange™ Site Directed Mutagenesis Kit: Instruction Manual (Catalog#200518, Revision #100007).

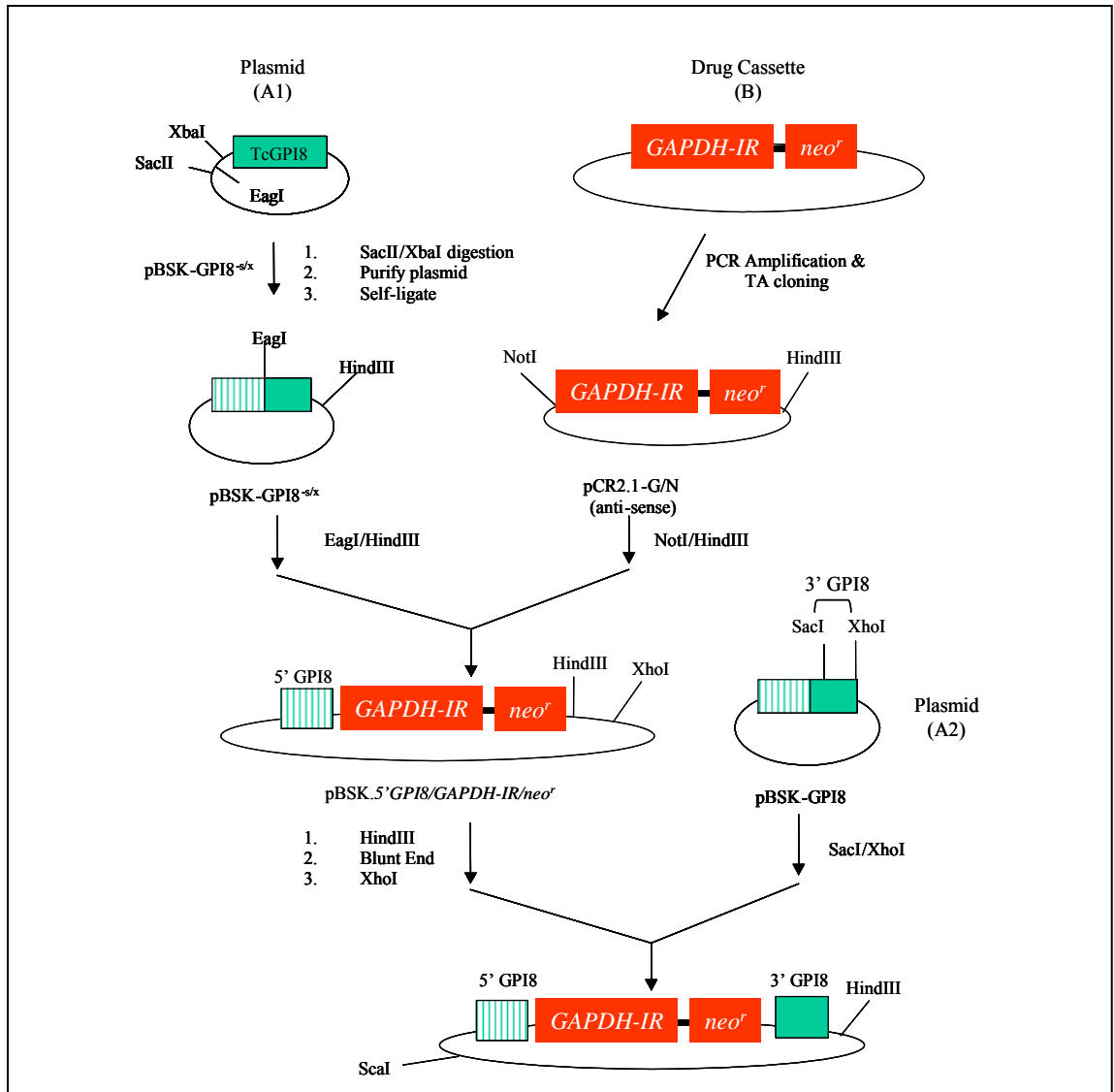


Figure 6: Cloning strategy for neomycin-resistance (*neo*^r) based *TcGPI8* disruption construct. *GAPDH-IR/neo*^r was PCR amplified from pTEX using LA *taq* polymerase (Takara Corp). The amplicon was cloned into pCR2.1 (Invitrogen). The *EagI* site was removed from pBSKII.*TcGPI8* via self-ligation of Klenow-treated *SacII/XbaI* fragment. This plasmid was then utilized to clone the 5' portion of *TcGPI8* adjacent to the *GAPDH-IR/neo*^r fragment of pCR2.1-*GAPDH-IR/neo*^r (*NotI/HindIII*; cohesive to *EagI/HindIII*). The 3' end of *TcGPI8* was then cloned adjacent to the 3' end of *neo*^r (5' blunt ends, 3' *XhoI*). For electroporation of *T. cruzi*, this final construct was linearized with *ScaI/HindIII*.

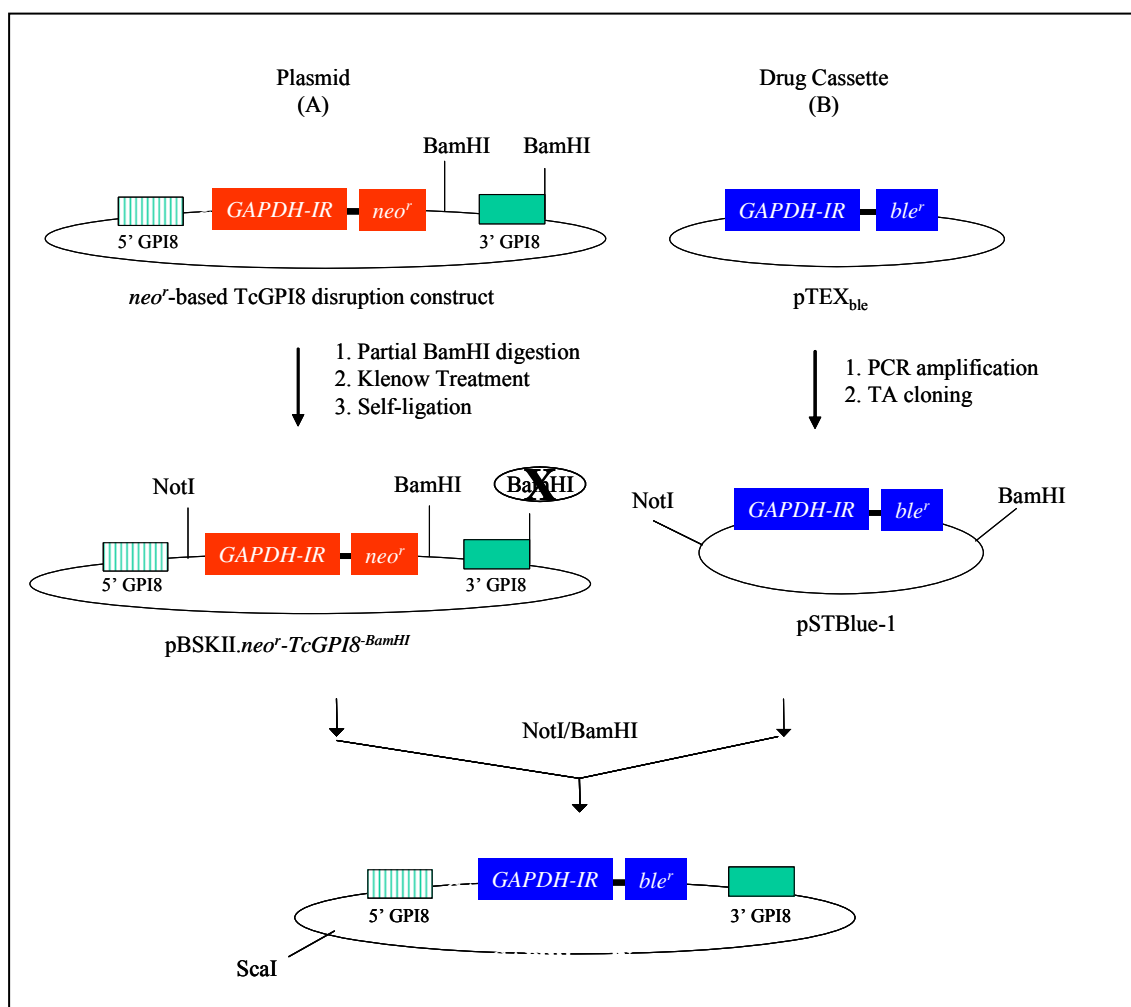


Figure 7: Cloning strategy for phleomycin resistance (*ble^r*)-based *TcGPI8* disruption construct. The *GAPDH-IR/neo^r* gene in the *neo^r*-based *TcGPI8* disruption construct was replaced with the *GAPDH-IR/ble^r* gene, as follows. The *GAPDH-IR-ble^r* cassette was PCR amplified from pTEX_{ble} using the primer pair *GAPDH-IR-F* and *ble^r-R* and cloned into pSTBlue1. The *Bam*HI site at the 3' end of *TcGPI8* was removed from the *neo^r*-based *TcGPI8* disruption construct by self-ligation of the Klenow-treated partial *Bam*HI digest fragment. The *GAPDH-IR-ble^r* insert from pSTBlue1.*GAPDH-IR-ble^r* was then ligated to the *Not*I/*Bam*HI vector from pBSKII.*neo^r*-*TcGPI8*^{-BamHI}. For electroporation of *T. cruzi*, the pBSKII.*TcGPI8/ble^r* construct was linearized with *Sca*I.

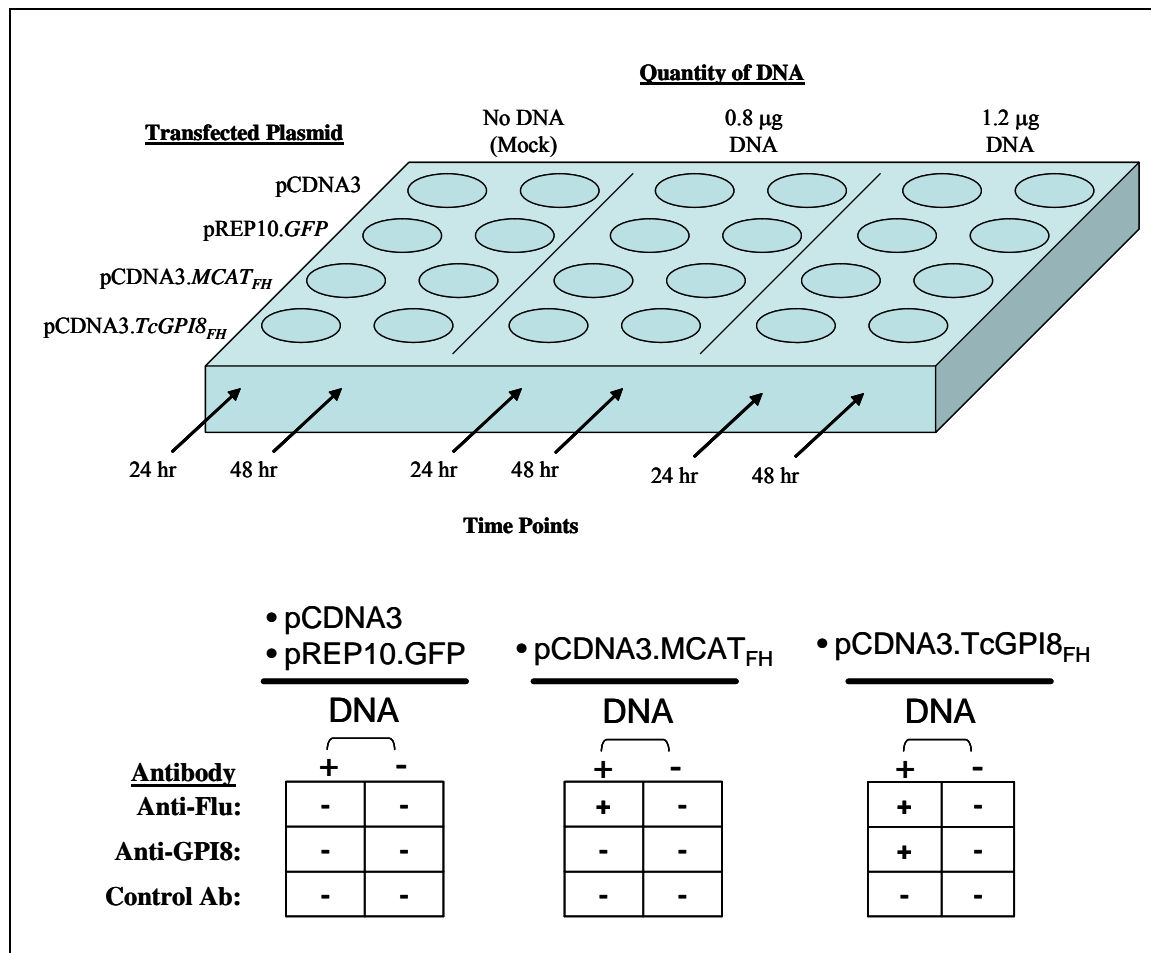


Figure 8: Experimental design for expression of TcGPI8_{FH} in mammalian cells. BHK21 cells were plated at 90% confluency and allowed to adhere overnight. The following day, plasmid DNA (0.8 μ g or 1.2 μ g)-Lipofectamine2000 mixtures, were added to wells, as indicated. Cells were harvested for protein analysis at 24 and 48 hr post-transfection.

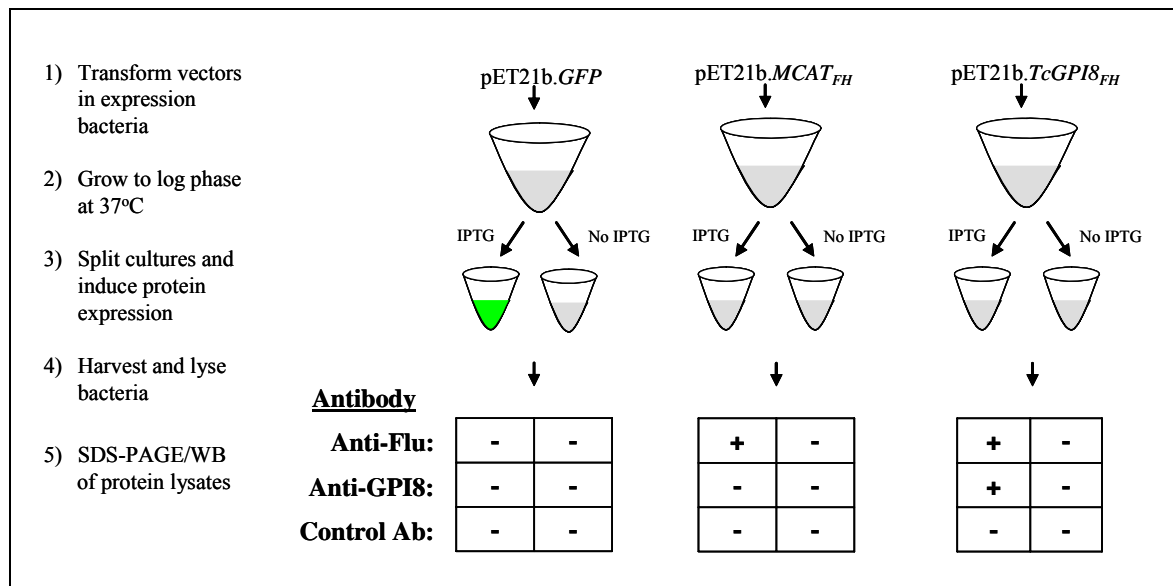


Figure 9: Expression of *TcGPI8_{FH}* in bacteria. Experiments were performed to confirm expression of the *TcGPI8_{FH}* open reading frame and as a positive control protein for screening of *GPI8-132* antiserum (α -GPI8) in Western blot analysis. pET21b.*TcGPI8_{FH}*, pET21b.*MCAT_{FH}³⁰⁰* and pET21b.*GFP* were transformed in *HMS174/DE3* bacteria and day cultures (8-12 hours growth at 37°C, 250 rpm) were used to inoculate LB medium containing ampicillin. Cultures were grown to log phase and split into two equivalent volumes. One portion was induced with 1 mM IPTG and all bacteria incubated for 3 hours at 37°C. A_{600} was measured. Bacteria were harvested and lysed for use in SDS-PAGE/Western blot analysis.

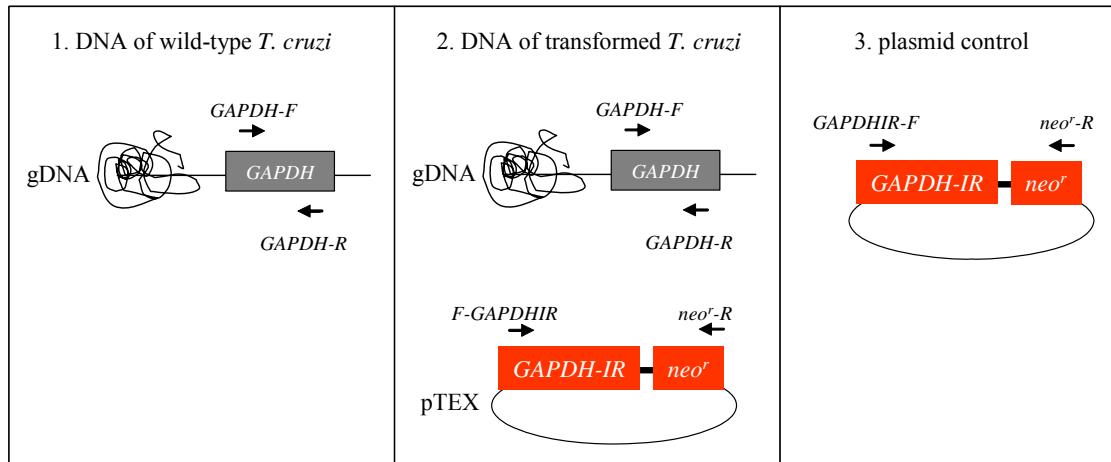


Figure 10: Experimental design for screening of *T. cruzi* pTEX transformants by PCR analysis. The *GAPDHIR-neo^r* cassette, present in pTEX, was PCR amplified using the primer pair, *F-GAPDHIR* and *R-neo^r*. To control for gDNA quantity, control reactions were performed to amplify the 780 bp chromosomal copy of the *T. cruzi* *GAPDH* gene using the primer pair, *F-GAPDH* and *R-GAPDH*. Individual primers were also used as negative controls.

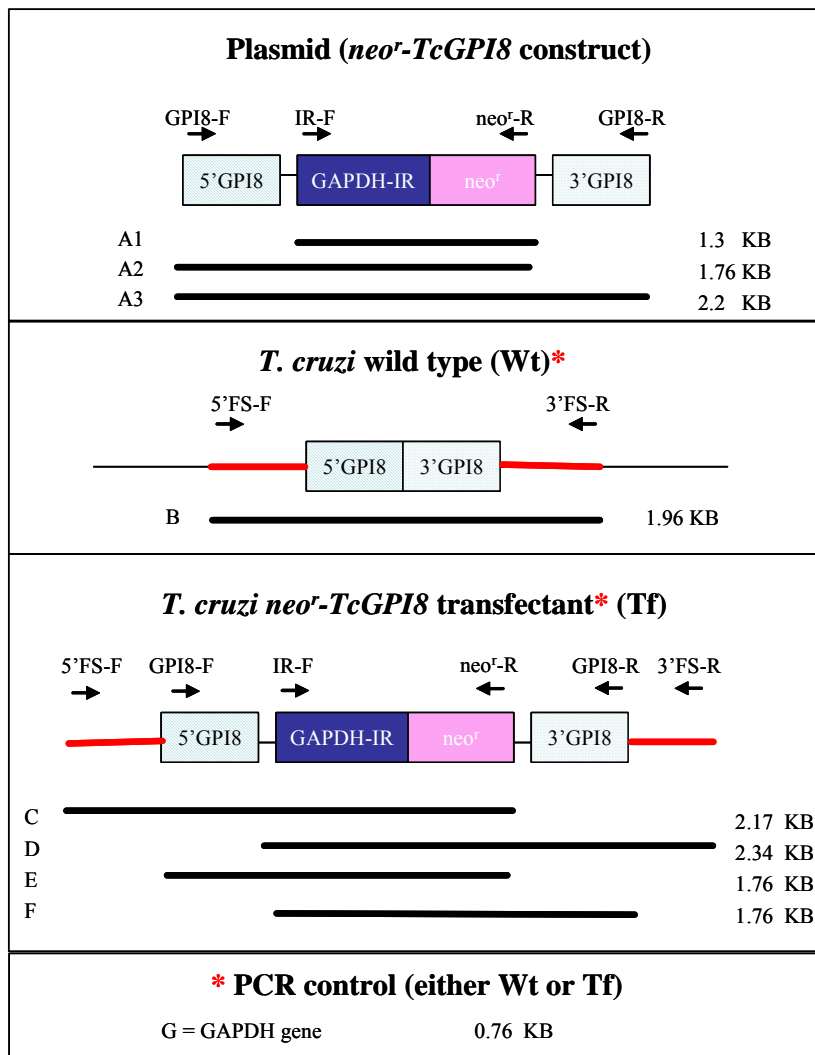


Figure 11: Experimental design for evaluation of *TcGPI8* disruption with *neo^r-TcGPI8* construct. A) For PCR-based confirmation of specific targeting of the *TcGPI8* gene via insertion of the *GAPDH-IR-neo^r* fragment, primers were designed 458 bp upstream (5' flanking sequence-forward, 5'FS-F) and 573 bp downstream (3' flanking sequence-reverse, 3'FS-R) of the *TcGPI8* locus identified in public genome sequence of the CL-Brener strain of *T. cruzi* (8643|Tc00.1047053511277|Trypanosoma cruzi|Location=106868..109045). In addition, to evaluate the segments of the *neo^r-TcGPI8* construct that were integrated into the gDNA of transformants, PCR was performed using the indicated primers pairs. Fragments are labeled A1, A2, A3, B, C, D, E and F and the expected PCR amplicon sizes in kilobases (kb) are indicated to the right.

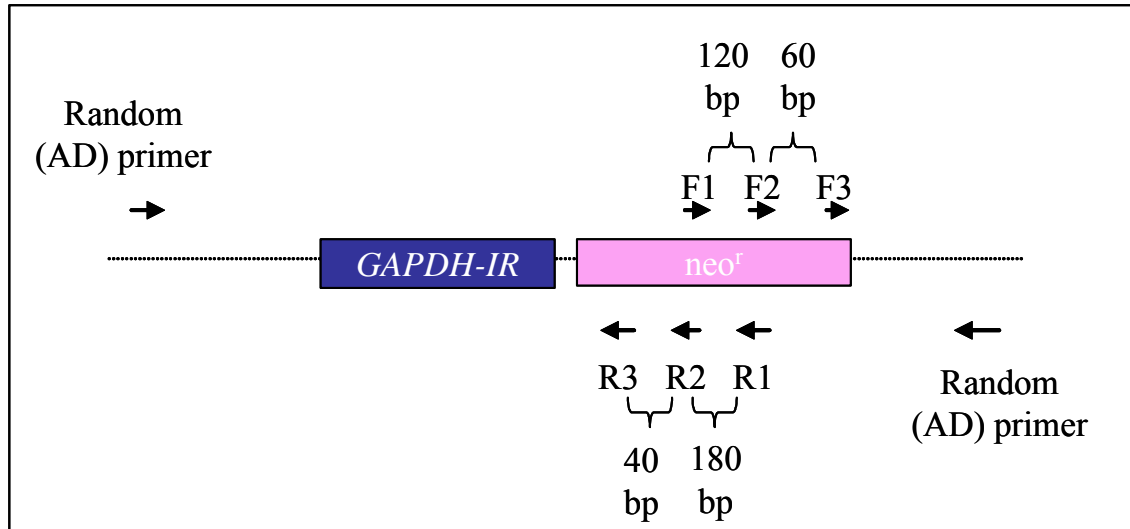


Figure 12: Experimental design for identification of the site of integration of the *GAPDH-IR-neo^r* cassette into the *T. cruzi* genome. A set of nested, specific primers were designed based on the *neo^r* gene of pTEX derived from pMC1neo (Stratagene)²⁹⁰, with sufficient product size difference to detect nested PCR products via agarose gel electrophoresis. Thermal asymmetric interlaced (TAIL)-PCR reactions²⁹⁴⁻²⁹⁵ were performed using a *neo^r*-specific primer (forward, F: F1, F2 or F3; reverse, R: R1, R2, or R3) in combination with one of four arbitrary degenerate (AD) primers (cycling conditions modified from²⁹⁴). The size difference between nested PCR products in base pairs (bp) is shown.

<i>T. cruzi</i>	-----MKR-----QMGFLWCCCI	13
<i>T. brucei</i>	-----MLPMLLWLVA	10
<i>L. mexicana</i>	-----MRTTAYVMTSPTRCIATLIVFAFL	25
<i>S. cerevisiae</i>	-----MRIAMHLP---LLLLYIF	15
<i>H. sapiens</i>	-----MAVTDLSLRAATVLATVL	18
<i>T. gondii</i>	MATSEPLAPAAASSSSSPSSFSSSSFSASLASLCAASAPVASGSSSHISPRLRFFFLSLL	60
<i>P. falciparum</i>	-----MGIKIIIIYIFFLSWAKWVCGSVNFTGFDNKNMI	33
Legumain	-----MVMMLVMLS LHGTAAARLN	18
<i>T. cruzi</i>	LFFLLT-----TVDTVIASSNKTNTLWAVILSSSRYYFFNIRHTSNA	55
<i>T. brucei</i>	NLFLAP-----AAEGFHGMN---KTNTWAVILSSSRYYFFNLRHTTNA	49
<i>L. mexicana</i>	VLTAAG-----AASAPLGATGKGQSNWAVIVSSSRYLFNRYHTANA	67
<i>S. cerevisiae</i>	LLPLS-----GANNTDAAHEVIAT-NTNNWAVLVSTSRFWFNRYRHMANV	58
<i>H. sapiens</i>	LLSFGS-----VAASHIEDQAEQFFRSGHNTNNWAVLVCTSRFWFNRYRHVANT	65
<i>T. gondii</i>	SLCLSSPVCFSRASSAPSASSRSSSSPSLSSFFSGDFRNNWAVIVNTSRYYNRYHTANA	120
<i>P. falciparum</i>	GKHVELEG-----RYKKEYIDRFLEELRKHNMYNNNVILLSTSRHYFNRYHTTNL	84
Legumain	RREWDS-----VIQLPTEPVDDVGTWAVLVAGSNGYGNRYHQADV	60
<i>T. cruzi</i>	LTIIYHLCKRHG-IDDDHILLVGDSSYACDPRNPYPAAIYST---LSGPD-----RINLY	105
<i>T. brucei</i>	LAMYHLCKRHG-MDDDHILVFLSDSYACDPRKPNPATIYGA---PAQAE-----QPNLY	99
<i>L. mexicana</i>	LTMYHLLRQHG-IDDDHILLFLSDSFACDPRNVYPAEIFSQ---PPGAHDADGRASMNLY	123
<i>S. cerevisiae</i>	LSMYRTVKRLG-IPDSQIILMLSDDVACNSRNLFPGSVFNN---KDHAIDL---Y-----	106
<i>H. sapiens</i>	LSVYRSVKRLG-IPDSHIVLMLADDMACNPRNPKPATVFSH---KNMELNVY-----	113
<i>T. gondii</i>	LSIYHTVKRLG-IPDSQIILMLSDDHACSPRNFFPGRIFND---HTRTLNLYGAGDRSGG	176
<i>P. falciparum</i>	LIAYKYLKYGFDTHDKNILLMIPFDQACDNRNIREGQIFREYELFPSSSHNKETKIENINL	144
Legumain	CHAYQLLIKGG-VKEENIVVFMYDDIAYNAMNPRPGVINH---PQGPDVY-----	107
<i>T. cruzi</i>	GCSVEIDYAGYDVDVRRFLGVLQGRYDAYTPPSRRLNTDENS--HILIIYAAGHAAKSFFK	163
<i>T. brucei</i>	GCNIRVDYASYDVGVRFLGVLQGRYDENTPPSRRLDNTDENS--NIIIIYAAGHSAEKFFK	157
<i>L. mexicana</i>	GCSAQVDYAGSDVDVRRFLSVLQGRYDENTPPTRRLLSDNTS--NIIIIYVAGHGAKSFFK	181
<i>S. cerevisiae</i>	GDSVEVDYRGYEVTVENFIRLLTDRTWEDHPKSKRLLTDENS--NIFIYMTGHGGDDFLK	164
<i>H. sapiens</i>	GDDVEVDYRSYEVTVENFLRVLTGRIPPSTPRSKRLLSDDRS--NIIIIYMTGHGGNGFLK	171
<i>T. gondii</i>	GSSVEVDYRGDEVQVATLLQLLAGRHNPATPRGKRLLTDENS--QVLLYLSGHGGDGFLK	234
<i>P. falciparum</i>	YENLNIDYKNNNVDRDEQIRRVLRHRYDAFTPKKNRLYNNGNNEKNLFLYMTGHGGVNFLK	204
Legumain	-AGVPKDYTGEDVTPENLVAVILGDKSKVKGGSGKVINSPED-RIFIFYSIHGPGVGLG	165
<i>T. cruzi</i>	FQDSEFLSSMDIADTLMMMWQRRYRKVVFLMDTCRALSMCLEIK-----APNVICT	216
<i>T. brucei</i>	FQDSEFMSSTDIAADTLMMMWQRRYRKLVFLVDTCRALSLCLEIK-----APNVVCLA	210
<i>L. mexicana</i>	FQDTEFLSSSDISETLTMMHQRRYGRVVFADTCHAIALCEHVE-----APNVVCLA	234
<i>S. cerevisiae</i>	FQDAEEIASEDIAADFQMYEKKRYNEIFFMIDTCQANTMYSKFY-----SPNIIAVG	217
<i>H. sapiens</i>	FQDSEEITNIELADAFEQMWQKRRYNELLFIIDTCQGASMYERFY-----SPNIMALA	224
<i>T. gondii</i>	FQDWEIISVLDADAVAQMKARFRFREMIIAETCQGSTLLDAMA-----TAGVLGLA	287
<i>P. falciparum</i>	IQEFNIISSSEFNIIYIQELLIKNFYKYIFVIIDTCQGYSFYDDILNFVYKKKINNIFFLS	264
Legumain	MPNAPFVYAMDFIDVLKKKHASGGYKEMVIYIEACESGSIFEGIMP-----KDLNIYVT	220

Fig. 13 (page 1)

<i>T. cruzi</i>	SSD	ATLESYSHHL	---	PLTGLTVISRWSLES	KLLEHAKCE	-----	VGPKETTALQM	266
<i>T. brucei</i>	SSE	AHLDSYSHHL	---	PPSGFTVITRWTFE	FLEVLKDSKCR	-----	PENG	260
<i>L. mexicana</i>	ASD	AESYSCQYD	---	EQLGTHMVSFWMNEM	YLLNGTSCSNPLTRRIGDD	---	AVSVLHQ	290
<i>S. cerevisiae</i>	SSEM	DESSYSHHS	---	VEIGVAVIDRFTYYCL	DLEQID	---	KNSTLTLDLFDSTFE	271
<i>H. sapiens</i>	SSQ	VGEDSLSHQPD	---	PAIGVHLMDRYTFYV	LEFLEEIN	---	PASQTNMNDLFQVCPKS	278
<i>T. gondii</i>	SSG	PKESSYSHHAD	---	GFLGVAVIDRWYTYTL	QFFEKSVRD	---	ASSSATFEQLMNSYSRK	343
<i>P. falciparum</i>	SSK	RNENSYSLFSS	---	SYLSVSTVDRFTYHFF	NYLQQIHKIYEKPSKNIKAFSLYNI	---		320
Legumain	ASNA	QENSFGTYCPGMNPPPEEY	VTCLGD	LYSVSWMEDSE	THNLKRET	VQ	QYQSVRK	280
	:	*		.	*	.	:	:
<i>T. cruzi</i>	SW	YNFN	-----					272
<i>T. brucei</i>	SF	YDFN	-----					266
<i>L. mexicana</i>	SW	YNFN	-----					296
<i>S. cerevisiae</i>	KIH	SHVGVRTDLFDRNPSEVLITDFFANVQNVIPDD	-----					307
<i>H. sapiens</i>	LCV	STPGHRTDLFQRDPKNVLITDFFGSVR	-----					308
<i>T. gondii</i>	QLL	STASVTELFGRPLGETKLEFFATASSLHATHGLYPIKTQRRVSWRMCRDRPAQDT						403
<i>P. falciparum</i>	LNY	LKTQHIMSEPTTNNSKFNSSIFLHDKNILFFNSN	-----					357
Legumain	TSNS	NSYRFGSHVMQYGD	TNITAEKLYLYHGFD	PATVN	-----			318
<i>T. cruzi</i>			-----	YGEERASLPPPRSVPPHFDAVN	DPKAIHKWKLEEFFCDHKQDPVPVDV			320
<i>T. brucei</i>			-----	YGPERSLPQPLSEPAHFDAVN	RPNIREWKMDFFCEQDRDKIPVEL			314
<i>L. mexicana</i>			-----	YHPYRVEASRNRSPKAHRDAVN	DPALREWIVADFVCGQVSAAVPVDV			344
<i>S. cerevisiae</i>			-----	SKPLSVSHYHHYKDHIDTAQYELNNNVLDLALETYRKNNQSSKIEKKIKDIKSTSV				363
<i>H. sapiens</i>			-----	KVEITTEITIKLQQDS-EIMESSYKEDQ	MDKLMPLKYAEQLPV			351
<i>T. gondii</i>	QHK	RGN	SRAGGENSSEREENSIEREETENS	SEREENS	SEREENS	SEREENS	SEREENS	463
<i>P. falciparum</i>			-----	LLIIHKDDVSIYQDKQ	THNHKYICLDNLSKCGHIKNNVHKMQLTYEQTL			408
Legumain			-----	FPPHNGNLEAKMEVVNRDAELLFMQMYQ	RSNHQPEKKTHILEQITETV			368
				.		:		
<i>T. cruzi</i>	QY	DLL	-----					325
<i>T. brucei</i>	RY	DLF	-----					319
<i>L. mexicana</i>	RY	DLE	-----					349
<i>S. cerevisiae</i>	LDV	DIDSNECFFTSFKQS	-----					381
<i>H. sapiens</i>	AQ	IIHQKPK--LKDWHPP	-----					367
<i>T. gondii</i>	RE	ENSSEREENS	SEREENS	SEREENS	SEREENS	SEREENS	SEREENS	523
<i>P. falciparum</i>	YY	NNNQNF	FSNHMSNFTDYFFTHDIYNIYNIY	NVYNIY	NVYNIY	NVYNIY	NVYNIY	454
Legumain	KH	RNHL	DGSVELIGVLLYGP	GKSSSVLH	SVRAPGLPLVDDW	TCLKSMVR	-----	417
<i>T. cruzi</i>			-----					
<i>T. brucei</i>			-----					
<i>L. mexicana</i>			-----					
<i>S. cerevisiae</i>			-----	ATIILALIVTILWFMLRGNTAKATYD				407
<i>H. sapiens</i>			-----	GGFILGLWALIIMVFFKTYG	IKHMKF			393
<i>T. gondii</i>	EFD	QGRNAGKAGRTETD	GQAEKAREEAGRPEAEGASVKQAVETL	VERIWGGREEKFQST				583
<i>P. falciparum</i>			-----	VYDIYNVYSFLILLLSLFFIMCSLLTYI				483
Legumain			-----	VFETHCGSLTQYGMKHMRAFGNV	CNSGVSKA			448

Fig. 13 (page 2)

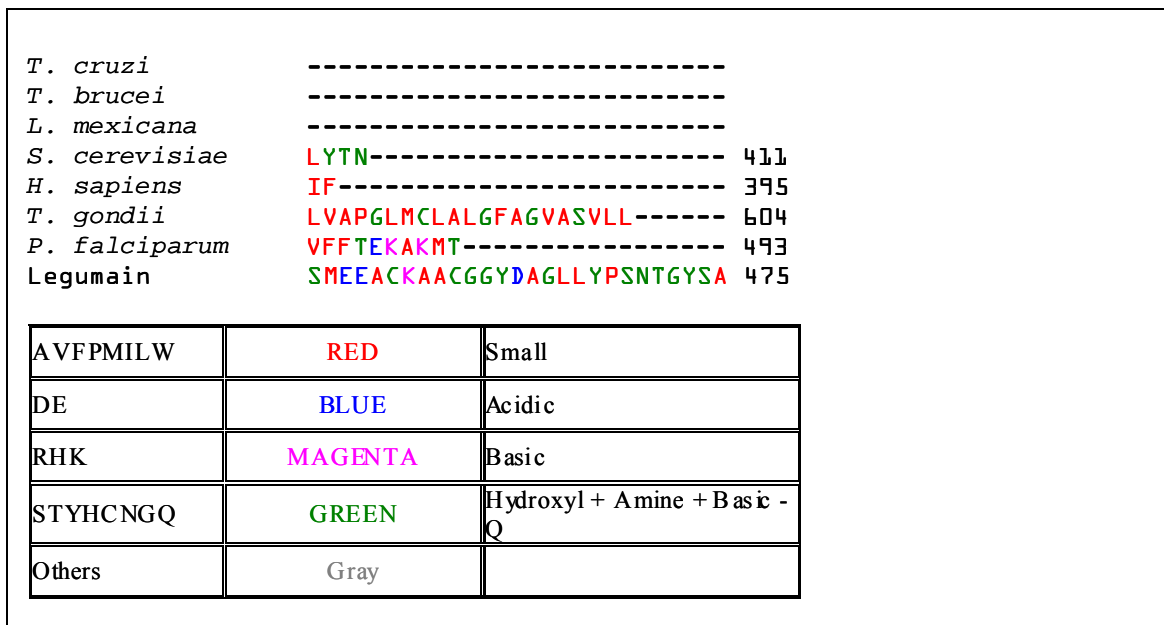


Fig. 13 (page 3)

Figure 13: CLUSTAL W (1.82) multiple sequence alignment of GPI8 in *T. cruzi*, *T. brucei*, *L. mexicana*, *S. cerevisiae* (yeast), *H. sapiens* (human), *T. gondii*, and *P. falciparum*, and legumain in *C. ensiformis*. GenBank accession numbers: TbGPI8: AJ308106; LmGPI8: AJ242865; yGPI8: P49018; hGPI8: Q92643; TgGPI8: AJ507036; PfGPI8: AJ401201; Legumain: JX0344. Legend: red, small amino acid (AA); blue, acidic AA; magenta, basic AA; green, Hydroxyl + Amine + Basic AA; *, identical AA; :, conserved AA (see color table); ., semi-conserved; -, indicates gap in the DNA sequence.

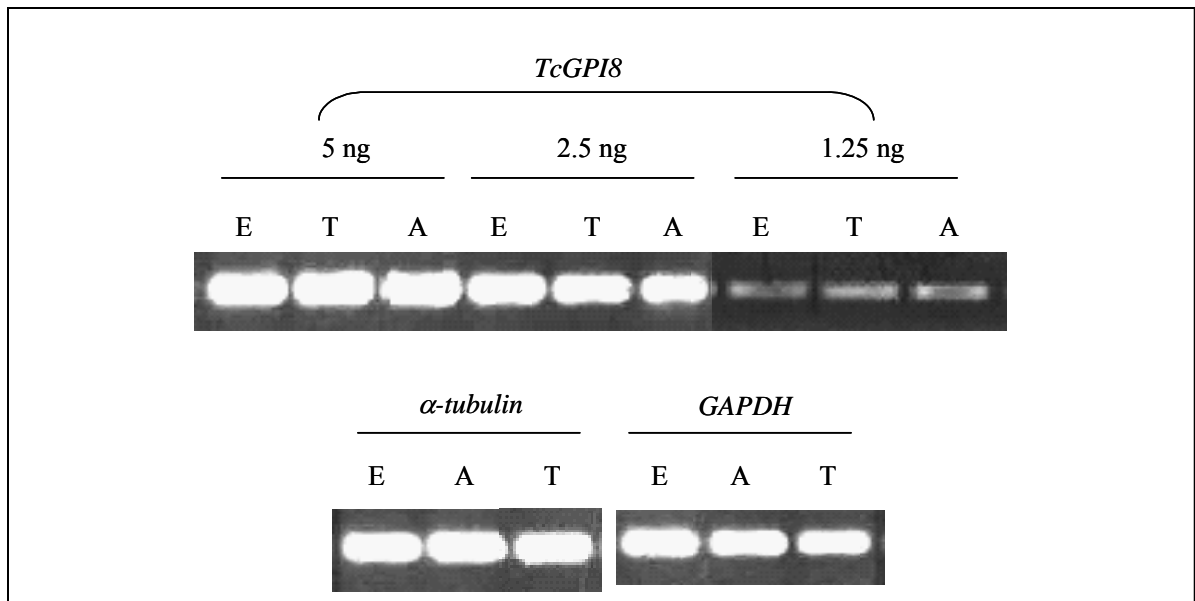


Figure 14: RT-PCR analysis of *GPI8* mRNA in *T. cruzi*. mRNA obtained from *T. cruzi* epimastigotes (lane 1, 4, 7, 10, 13), trypomastigotes (lanes 2, 5, 8, 11, 13) and amastigotes (lanes 3, 6, 9, 12, 15) was reverse transcribed to make cDNA. cDNA was used in PCR reaction with oligonucleotides specific for gene encoding *TcGPI8* (lanes 1-9), α -tubulin (lanes 10-12) and glyceraldehyde dehydrogenase (GAPDH, lanes 13-15). The amount of cDNA used per reaction: 5 ng (lanes 1-3, 10-15), 2.5 ng (lanes 4-6) and 1.25 ng (lanes 7-9).



Figure 15: Southern blot analysis of *T. cruzi* GPI8 (*TcGPI8*). Agarose gel electrophoresis of *T. cruzi* genomic DNA was performed following restriction enzyme digestion. The digested DNA was transferred to membranes, which were then probed with ^{32}P -labeled *T. cruzi* *TcGPI8*. The hybridization of *TcGPI8* probe with one genomic fragment suggests that *TcGPI8* is present as a single copy gene. Abbreviations used: B, *Bam*HI; X, *Xho*I; H, *Hind*III; S, *Sal*I; E, *Eco*RI.

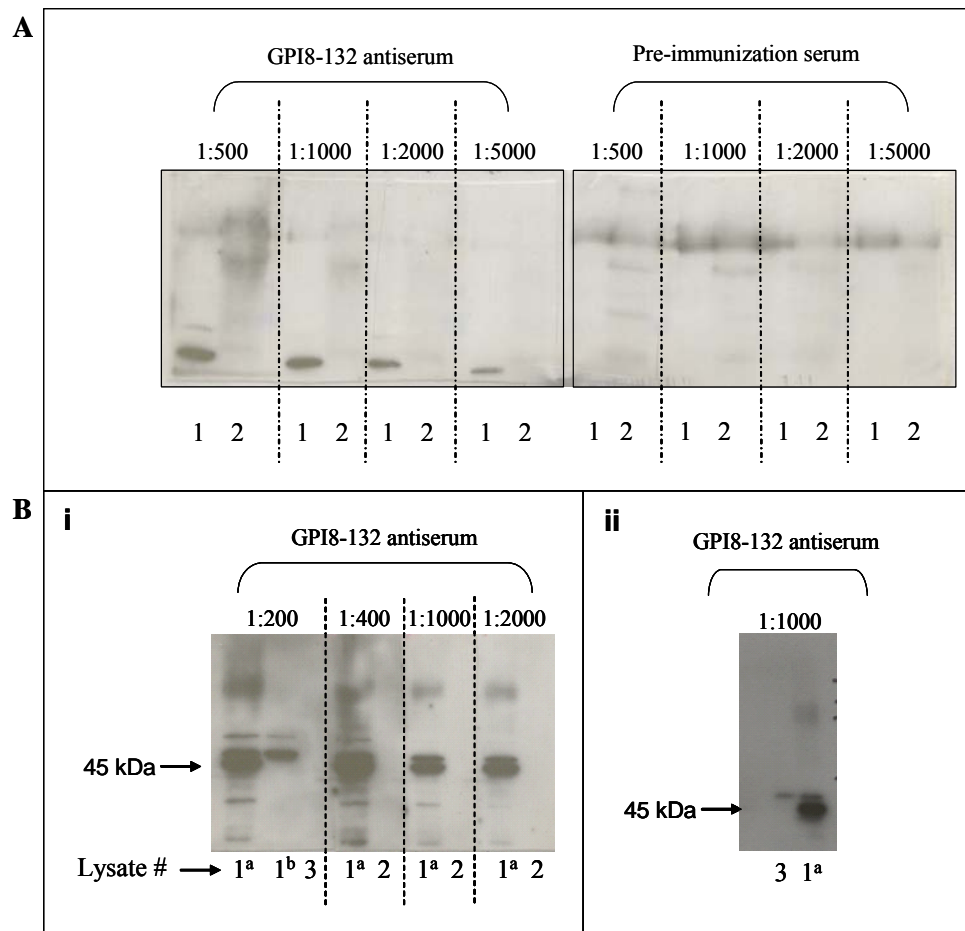


Figure 16 (A-B): Antibody optimization and specificity screening by detection of over-expression of epitope-tagged TcGPI8 in mammalian and bacterial cells. A) Preliminary optimization of *GPI8-132* antiserum. To select a preliminary range of dilutions in which background is minimal for use of the *GPI8-132* antiserum, protein lysates from wild type *T. cruzi* (indicated as 1) and untransfected BHK21 cells (indicated as 2) were resolved via SDS-PAGE, and transferred to PVDF membrane. Western blot analysis was performed using dilutions in the range of 1:500 to 1:5000, as indicated, for the *GPI8-132* antiserum and, in parallel, for the matching pre-immunization serum. B) Secondary optimization of *GPI8-132* antiserum. To select the optimal dilution for use of the *GPI8-132* antiserum to detect TcGPI8, while achieving low background, protein lysates from pET21b.*TcGPI8_{FH}*-transformed, IPTG induced bacteria (indicated as 1^a and 1^b; ^b represents an alternative preparation of the pET21b.*TcGPI8_{FH}*-transformed bacteria than 1^a) and wild type *T. cruzi* (indicated as 2) from were resolved via SDS-PAGE, and transferred to PVDF membrane. Western blot analysis was performed using dilutions in the range of 1:200 to 1:2000, as indicated, for the *GPI8-132* antiserum.

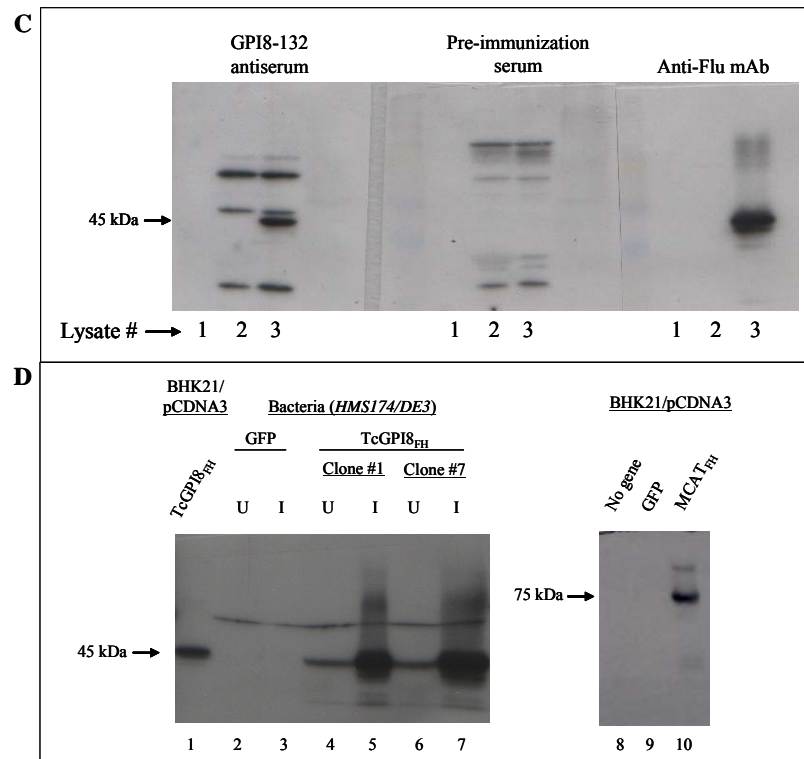


Figure 16 (C-D): Antibody optimization and specificity screening by detection of over-expression of epitope-tagged TcGPI8 in mammalian and bacterial cells. C) Specificity screening of GPI8-132 antiserum. HMS174/DE3 bacteria were transformed with the indicated bacterial expression vector, protein expression was induced with 1 mM IPTG, and the respective protein lysates harvested, as follows: lane 2: pET21b.GFP, lane 3: pET21b.TcGPI8_{FH}. Lysate prepared from BHK21 cells was used as an additional negative control (lane 1). D) TcGPI8_{FH} expression in mammalian cells. Expression of TcGPI8_{FH} was evaluated using lysates prepared from transiently transfected BHK21 cells. BHK21 were transformed via lipid-mediated method (0.8 µg DNA). Cells were harvested at 24 hr and protein lysates were prepared, resolved via SDS-PAGE, and transferred to PVDF membrane, as follows: lane 1, pCDNA3.TcGPI8_{FH}; lane 8, pCDNA3; lane 9, pREP10.GFP; and lane 10, pCDNA3.MCAT_{FH}³⁰⁰. In addition, bacterial expression lysates (as described for A, above) were used as controls, as follows: lane 2, pET21b.GFP without IPTG induction (uninduced, U); lane 3, pET21b.GFP with IPTG induction (induced, I); lane 4 and 6, pET21b.TcGPI8_{FH} without IPTG induction (U); lane 5 and 7, pET21b.TcGPI8_{FH} with IPTG induction (I). Antiserum raised against the GPI8-132 peptide detects a protein of apparent molecular mass of 45 kDa, which is not seen in the parallel blot incubated with the matching control preimmunization serum. Antibody to the Flu₃His₆ (FH) epitope tag (anti-Flu mAb) detects a band of this same size in bacteria or mammalian cells transformed with pET21b.TcGPI8_{FH} or pCDNA3.TcGPI8_{FH}, respectively, but not in the control pCDNA transfected cell lysate. A protein migrating at 75 kDa is detected in pCDNA3.MCAT_{FH}³⁰⁰ lysate.

A (page 1)

TcGPI8-FH	ATGAAGCGCCAGATGGGTTTTTTGTGGTGTGTTGCATCCTTTTTTTTCT	50
TcGPI8-FH-H156A	ATGAAGCGCCAGATGGGTTTTTTGTGGTGTGTTGCATCCTTTTTTTTCT	50
TcGPI8-FH-C198A	ATGAAGCGCCAGATGGGTTTTTTGTGGTGTGTTGCATCCTTTTTTTTCT	50

TcGPI8-FH	GCTGACAACAGTCGACACCGTCATCGCCAGCAGCAACAAAACAAAGACAA	100
TcGPI8-FH-H156A	GCTGACAACAGTCGACACCGTCATCGCCAGCAGCAACAAAACAAAGACAA	100
TcGPI8-FH-C198A	GCTGACAACAGTCGACACCGTCATCGCCAGCAGCAACAAAACAAAGACAA	100

TcGPI8-FH	ACTTGTGGGCTGTCAATTTTGTCTTCCTCACGCTACTTCTTTAATATACGC	150
TcGPI8-FH-H156A	ACTTGTGGGCTGTCAATTTTGTCTTCCTCACGCTACTTCTTTAATATACGC	150
TcGPI8-FH-C198A	ACTTGTGGGCTGTCAATTTTGTCTTCCTCACGCTACTTCTTTAATATACGC	150

TcGPI8-FH	CACACCTCCAATGCACTGACAATTTACCATCTCTGCCGCAAGCATGGAAT	200
TcGPI8-FH-H156A	CACACCTCCAATGCACTGACAATTTACCATCTCTGCCGCAAGCATGGAAT	200
TcGPI8-FH-C198A	CACACCTCCAATGCACTGACAATTTACCATCTCTGCCGCAAGCATGGAAT	200

TcGPI8-FH	AGACGACGACCATATCATTCTCTTAGTTGGTGACAGCTATGCCTGTGACC	250
TcGPI8-FH-H156A	AGACGACGACCATATCATTCTCTTAGTTGGTGACAGCTATGCCTGTGACC	250
TcGPI8-FH-C198A	AGACGACGACCATATCATTCTCTTAGTTGGTGACAGCTATGCCTGTGACC	250

TcGPI8-FH	CACGCAATCCCTACCCGGCTGCCATTTACAGCACTCTTTTCAGGCCCGGAT	300
TcGPI8-FH-H156A	CACGCAATCCCTACCCGGCTGCCATTTACAGCACTCTTTTCAGGCCCGGAT	300
TcGPI8-FH-C198A	CACGCAATCCCTACCCGGCTGCCATTTACAGCACTCTTTTCAGGCCCGGAT	300

TcGPI8-FH	CGAATAAACTTGTATGGCTGCAGCGTTGAAATAGACTATGCCGGATACGA	350
TcGPI8-FH-H156A	CGAATAAACTTGTATGGCTGCAGCGTTGAAATAGACTATGCCGGATACGA	350
TcGPI8-FH-C198A	CGAATAAACTTGTATGGCTGCAGCGTTGAAATAGACTATGCCGGATACGA	350

Figure 17 (A)

A (page 2)

TcGPI8-FH	TGTGGATGTGCGCCGCTTTCTTGGTGTTCTGCAGGGACGCTATGATGCCT	400
TcGPI8-FH-H156A	TGTGGATGTGCGCCGCTTTCTTGGTGTTCTGCAGGGACGCTATGATGCCT	400
TcGPI8-FH-C198A	TGTGGATGTGCGCCGCTTTCTTGGTGTTCTGCAGGGACGCTATGATGCCT	400

TcGPI8-FH	ATACTCCGCCTTCGCGGCGCCTCAACACGGATGAAAACTCTCATATCTTG	450
TcGPI8-FH-H156A	ATACTCCGCCTTCGCGGCGCCTCAACACGGATGAAAACTCTCATATCTTG	450
TcGPI8-FH-C198A	ATACTCCGCCTTCGCGGCGCCTCAACACGGATGAAAACTCTCATATCTTG	450

TcGPI8-FH	ATTTACGCGGCCGGTCACGCCGAGAGAGTTTTTTTAAATTTCAAGACTC	500
TcGPI8-FH-H156A	ATTTACGCGGCCGGTCACGCCGAGAGAGTTTTTTTAAATTTCAAGACTC	500
TcGPI8-FH-C198A	ATTTACGCGGCCGGTCACGCCGAGAGAGTTTTTTTAAATTTCAAGACTC	500

TcGPI8-FH	GGAATTTTGTAGCTCCATGGATATCGCGGATACACTCATGATGATGTGGG	550
TcGPI8-FH-H156A	GGAATTTTGTAGCTCCATGGATATCGCGGATACACTCATGATGATGTGGG	550
TcGPI8-FH-C198A	GGAATTTTGTAGCTCCATGGATATCGCGGATACACTCATGATGATGTGGG	550

TcGPI8-FH	AGCAACGACGGTATCGTAAGGTGGTTTTTATGCTGGACACATGCCGAGCA	600
TcGPI8-FH-H156A	AGCAACGACGGTATCGTAAGGTGGTTTTTATGCTGGACACATGCCGAGCA	600
TcGPI8-FH-C198A	AGCAACGACGGTATCGTAAGGTGGTTTTTATGCTGGACACATGCCGAGCA	600

TcGPI8-FH	TTGTCTATGTGCCTTGAAATTAAAGCACCCAATGTGATCTGCCTCACCTC	650
TcGPI8-FH-H156A	TTGTCTATGTGCCTTGAAATTAAAGCACCCAATGTGATCTGCCTCACCTC	650
TcGPI8-FH-C198A	TTGTCTATGTGCCTTGAAATTAAAGCACCCAATGTGATCTGCCTCACCTC	650

TcGPI8-FH	ATCGGATGCGACATTGGAGAGTTATTCGCATCATTTAGATCCATTGACAG	700
TcGPI8-FH-H156A	ATCGGATGCGACATTGGAGAGTTATTCGCATCATTTAGATCCATTGACAG	700
TcGPI8-FH-C198A	ATCGGATGCGACATTGGAGAGTTATTCGCATCATTTAGATCCATTGACAG	700

Figure 17 (A)

A (page 3)

TcGPI8-FH	GGTTGACTGTTATCTCACGCTGGTCAC'TGAATCTTTGAAACTTCTGGAG	750
TcGPI8-FH-H156A	GGTTGACTGTTATCTCACGCTGGTCAC'TGAATCTTTGAAACTTCTGGAG	750
TcGPI8-FH-C198A	GGTTGACTGTTATCTCACGCTGGTCAC'TGAATCTTTGAAACTTCTGGAG	750

TcGPI8-FH	CATGCAAAGTGTGAAGTCGGACCCAAAGAGACGACGCTCTGCAGATGTC	800
TcGPI8-FH-H156A	CATGCAAAGTGTGAAGTCGGACCCAAAGAGACGACGCTCTGCAGATGTC	800
TcGPI8-FH-C198A	CATGCAAAGTGTGAAGTCGGACCCAAAGAGACGACGCTCTGCAGATGTC	800

TcGPI8-FH	GTGGTACAAC'TTCAATTATGGTGAAGAACGCGCGAGTCTTCTCTCTCCGA	850
TcGPI8-FH-H156A	GTGGTACAAC'TTCAATTATGGTGAAGAACGCGCGAGTCTTCTCTCTCCGA	850
TcGPI8-FH-C198A	GTGGTACAAC'TTCAATTATGGTGAAGAACGCGCGAGTCTTCTCTCTCCGA	850

TcGPI8-FH	GGTCGGTGCCGTCACACTTTGATGCAGTGAATGATCCGAAGGCTATTTCAT	900
TcGPI8-FH-H156A	GGTCGGTGCCGTCACACTTTGATGCAGTGAATGATCCGAAGGCTATTTCAT	900
TcGPI8-FH-C198A	GGTCGGTGCCGTCACACTTTGATGCAGTGAATGATCCGAAGGCTATTTCAT	900

TcGPI8-FH	AAATGGAAATTGGAGGAGT'TTTTTGTGATCGCAAACAGGATCCCGTTCC	950
TcGPI8-FH-H156A	AAATGGAAATTGGAGGAGT'TTTTTGTGATCGCAAACAGGATCCCGTTCC	950
TcGPI8-FH-C198A	AAATGGAAATTGGAGGAGT'TTTTTGTGATCGCAAACAGGATCCCGTTCC	950

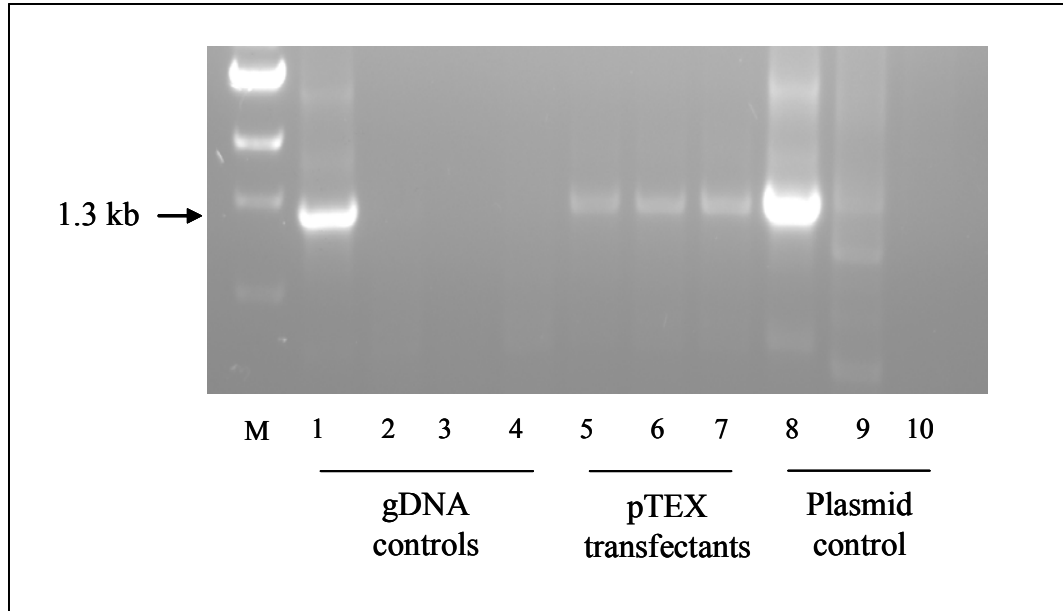
TcGPI8-FH	AGTGGATGTACAATATGACTTGCTCTCGAGCATCGAGGGCAGATACCCAT	1000
TcGPI8-FH-H156A	AGTGGATGTACAATATGACTTGCTCTCGAGCATCGAGGGCAGATACCCAT	1000
TcGPI8-FH-C198A	AGTGGATGTACAATATGACTTGCTCTCGAGCATCGAGGGCAGATACCCAT	1000

TcGPI8-FH	ACGATGTTCC'TGACTATGCGGGCTATCCCTATGACGTCCCGGACTATGCA	1050
TcGPI8-FH-H156A	ACGATGTTCC'TGACTATGCGGGCTATCCCTATGACGTCCCGGACTATGCA	1050
TcGPI8-FH-C198A	ACGATGTTCC'TGACTATGCGGGCTATCCCTATGACGTCCCGGACTATGCA	1050

TcGPI8-FH	GGCTATCCATATGACGTTCCAGATTACGCAGGAGCTCACCATCACCATCA	1100
TcGPI8-FH-H156A	GGCTATCCATATGACGTTCCAGATTACGCAGGAGCTCACCATCACCATCA	1100
TcGPI8-FH-C198A	GGCTATCCATATGACGTTCCAGATTACGCAGGAGCTCACCATCACCATCA	1100

TcGPI8-FH	CCATGGCTAG	1110
TcGPI8-FH-H156A	CCATGGCTAG	1110
TcGPI8-FH-C198A	CCATGGCTAG	1110

Figure 17 (A)

B**Figure 17 (B)****Figure 17: Characterization of pTEX constructs and *T. cruzi*/pTEX transfectants.**

A) Sequence of pTEX clones utilized for transfection of *T. cruzi*. Confirmation of TcGPI8 open reading frame, the presence of the mutation (indicated by box) introduced by QuikChange™ site directed mutagenesis of TcGPI8 corresponding to the three pTEX clones used for electroporation of *T. cruzi*. The epitope-tag, Flu₃His₆ (FH), is highlighted in yellow. B) PCR analysis of *T. cruzi* pTEX transfectants. DNA was extracted from transfectant and wild type parasites (*T. cruzi*) and PCR amplification was performed using *GAPDH-IR* and *neo^r* specific primers (30 or 400 ng/reaction for plasmid or gDNA, respectively). M, molecular weight marker; lane 1: positive gDNA control, stable *neo^r*-TcGPI8 *T. cruzi* transfectants; lanes 2-4: negative gDNA control (2, both primers; 3, forward primer; 4, reverse primer); lane 5: wild type gDNA of *T. cruzi*; lane 6: *T. cruzi* transfectant, pTEX.TcGPI8; lane 7: *T. cruzi* transfectant, pTEX.TcGPI8^{C198A}; lane 8: *T. cruzi* transfectant, pTEX.TcGPI8^{H156A} lanes 8-10: pTEX._{neo}, plasmid DNA was used as control: (8, both primers; 9, forward primer; 10, reverse primer). The expected ~1.3 kilobase product, indicated by the arrow, was amplified from parasites transfected with pTEX.TcGPI8 (lane 5), pTEX.TcGPI8^{C198A} (lane 6), pTEX.TcGPI8^{H156A} (lane 7) indicating the presence of pTEX, which is also amplified from the pTEX control (lane 9) as well as the positive gDNA control (lane 1). No product was observed in untransfected wild type *T. cruzi* or for the single primer controls (lanes 9-10).

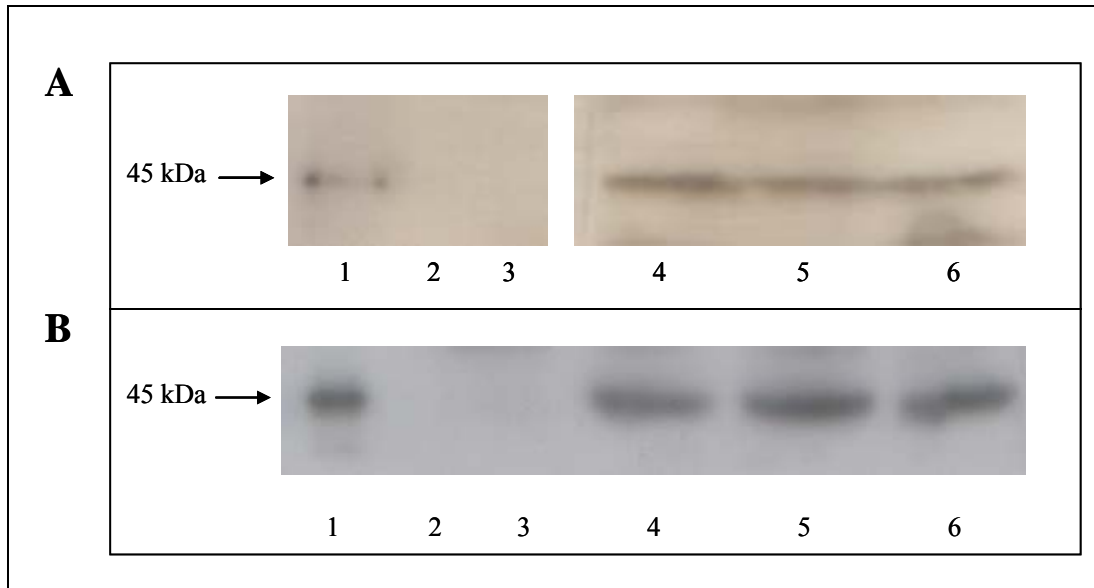


Figure 18: Detection of expression of epitope-tagged TcGPI8 in *T. cruzi* transfectants.

pTEX transfectants were generated as described in *Materials and Methods* and were cultivated in G418 concentration of 400 $\mu\text{g}/\text{ml}$ for subsequent protein analysis. Parasite protein lysates (2×10^7 parasite equivalents per lane) were resolved via SDS-PAGE and transferred to membranes. Western blot analysis of TcGPI8 was performed using: A) *GPI8-132* antiserum, and B) anti-Flu monoclonal antibody. For both panels A and B, control bacterial lysates were used, as follows: induced pET21b.*TcGPI8_{FH}* (lane 1) and pET21b.*GFP* (lane 2). *T. cruzi* lysates: wild type (lane 3) and pTEX.TcGPI8 (lane 4), pTEX.*TcGPI8^{CI98A}* (lane 5), pTEX.*TcGPI8^{HI56A}* (lane 6) transfectants. All TcGPI8 alleles contain the Flu₃His₆ (FH) epitope tag, which was recognized by the anti-Flu mAb, as indicated by the arrow; *GPI8-132* recognized a protein of this same apparent molecular mass. All epitope-tagged TcGPI8 alleles were expressed at a similar level in all transfectants cultured at 200 $\mu\text{g}/\text{ml}$ G418. Native TcGPI8 is undetectable under these assay conditions.

		ANTIBODY				
		Y3	GP72	C10	2B10	10D8
Wild type	Av. % Pos.	0.26	85.37	94.91	51.23	34.97
	SD	0.23	9.11	3.68	12.46	15.08
Tc/pTEX.TcGPI8	Av. % Pos.	0.22	89.91	97.77	56.82	39.39
	SD	0.16	10.74	2.50	5.65	12.41
Tc/pTEX.TcGPI8 ^{C198A}	Av. % Pos.	0.14	88.65	96.38	49.09	60.44
	SD	0.10	6.42	2.52	9.73	20.56
Tc/pTEX.TcGPI8 ^{H156A}	Av. % Pos.	0.13	86.15	97.24	56.55	60.69
	SD	0.08	8.88	1.53	14.31	31.49

Figure 19: Surface expression of GPI-anchored proteins in *T. cruzi* pTEX transfectants. Stable transfectants were obtained as described in *Materials and Methods*. To eliminate dead parasites and metacyclic forms, live epimastigote stage wild type and transfectant parasites were isolated via Ficoll Paque-Plus density gradient and cultured in liver infusion tryptose medium. Parasites (1×10^6) were stained with antibody to the epimastigote stage-specific GPI-anchored protein: GP50/55 (C10) and mucins (2B10, 10D8) followed by incubation with FITC-conjugated secondary antibody (goat anti-mouse IgG-FITC; Sigma). Antibody to GP72, a transmembrane protein, was used as a positive control. The Y3 antibody, which recognizes mouse H-2 molecules (major histocompatibility complex), was used as an irrelevant antibody control. The average percentage of positive events (Av. % Pos.) for each antibody used, and the corresponding standard deviation (SD), was calculated from three independent experiments. No significant difference in surface expression of GPI-anchored proteins was detected for C10, 2B10 or 10D8, when comparing transfectants expressing either the C198A or the H156A allele of TcGPI8 to wild type, untransfected *T. cruzi* or to the pTEX.TcGPI8 transfectants.

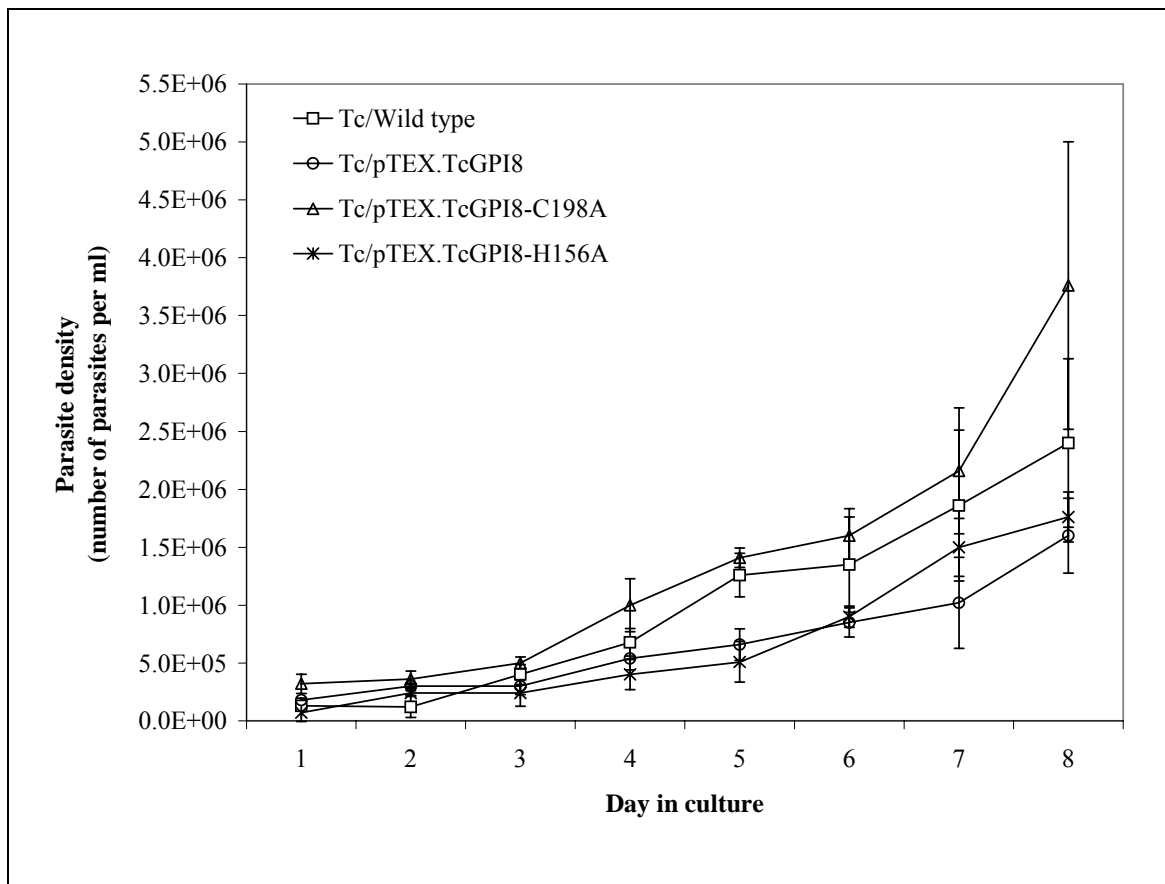


Figure 20: Growth of *T. cruzi* transfectants as epimastigotes. Epimastigote-stage wild type and stable pTEX transfectants, as indicated in legend, were grown at 28°C in liver infusion tryptose medium (LIT) supplemented with 0.01 mg/ml hemin, 10% FBS and antibiotics. Growth curves were obtained by monitoring the density of wild type *T. cruzi* and pTEX transfectants, as follows: 5×10^5 parasites were inoculated into 5 ml of LIT; transfectants were cultured in LIT containing 400 µg/ml G418. Ten microliter of parasite suspension was removed for daily counting on a hemacytometer. The average density, in number of parasites per ml, and the corresponding standard deviation, was calculated from three independent experiments.

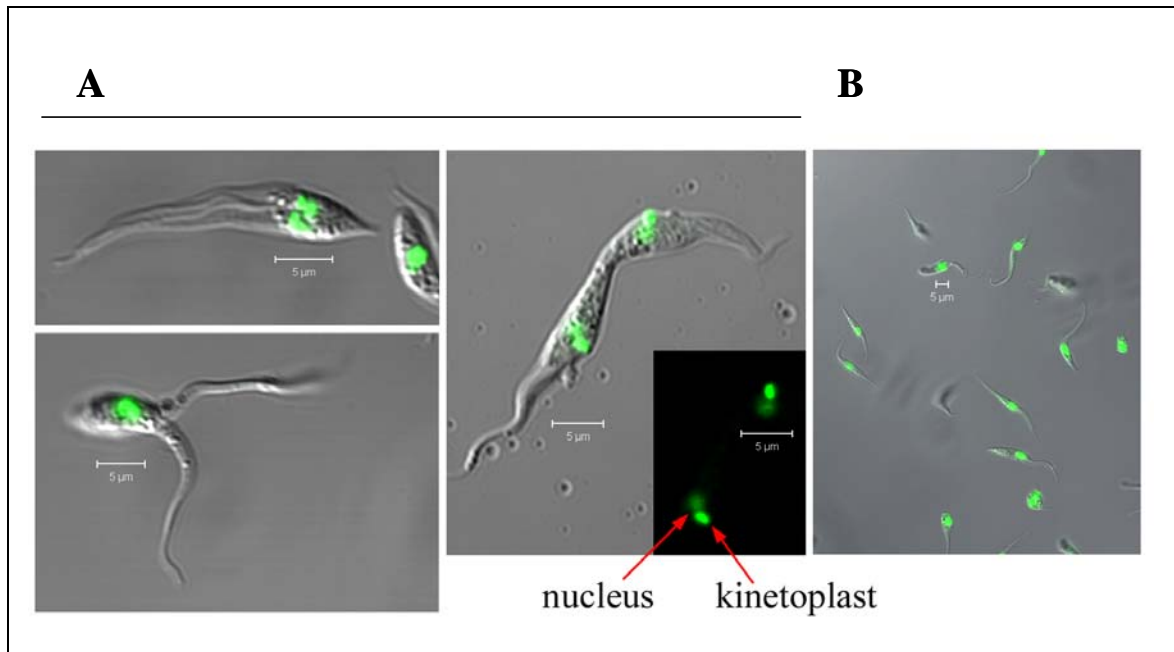


Figure 21: Confocal analysis of *neo^r-TcGPI8* transformants. Parasites (10^6) were harvested by centrifugation and washed in ice-cold PBS. Epimastigote morphology was documented via confocal microscopy of live parasites. To visualize kinetoplast and nuclear DNA, epimastigotes were incubated on ice for 10 min with Syto11 (Molecular Probes, 1:200 dilution), a cell-permeant nucleic acid binding fluorescent dye (excitation λ_{Max} , 515 nm; emission λ_{Max} , 543 nm). Confocal images were captured on a Zeiss LSM 510 UV Meta Laser Scanning Confocal Microscope (UTMB Optical Imaging Core Facility) at a magnification of 63X. Signals were overlaid with Nomarski differential interference images using Zeiss AxioVision Viewer software. A) Stable *neo^r-TcGPI8* transfectants; B) Wild type untransfected parasites. Reprinted with permission from Zacks MA. 2007. *Impairment of cell division of Trypanosoma cruzi epimastigotes*. Mem Inst Oswaldo Cruz 102(1): p. 113.

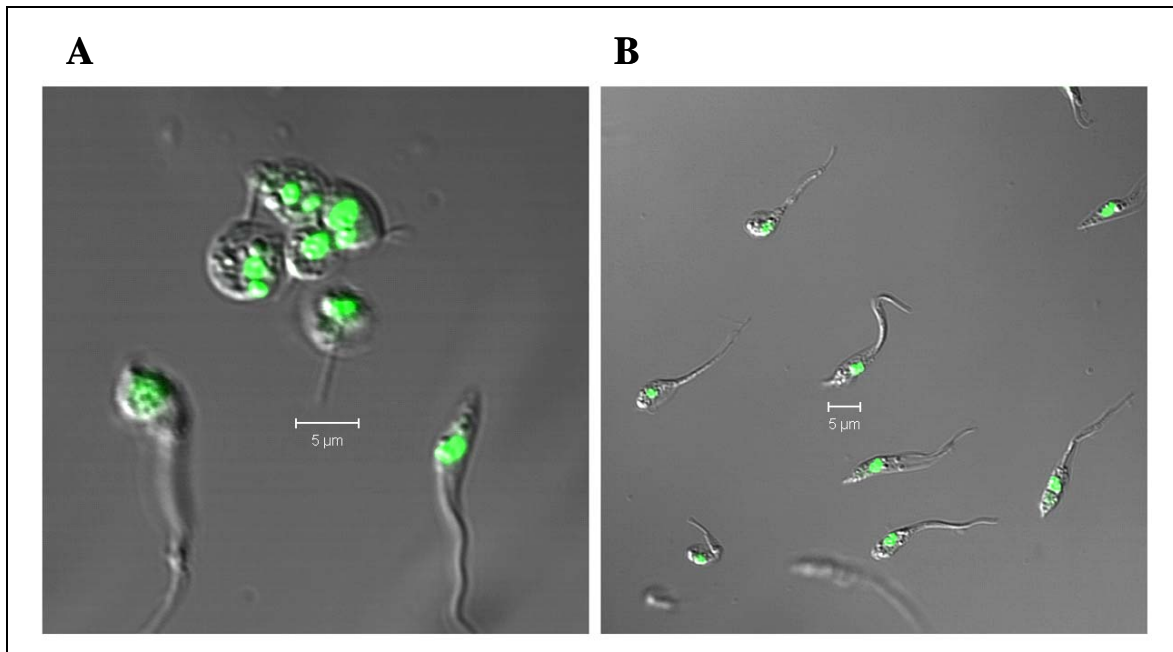


Figure 22: Confocal analysis of *neo'*-*TcGPI8* transformants following electroporation with *ble'*-*TcGPI8*. Parasites (10^6) were incubated with Syto11 stain in PBS on ice for 10 minutes. Images were collected and analyzed as described in Figure 23. A) *T. cruzi neo'*-*TcGPI8* transformants that were electroporated with *ble'*-*TcGPI8* construct to target the second copy of *TcGPI8*; B) Wild type untransfected parasites. Reprinted with permission from Zacks MA. 2007. *Impairment of cell division of Trypanosoma cruzi epimastigotes*. Mem Inst Oswaldo Cruz 102(1): p. 113.

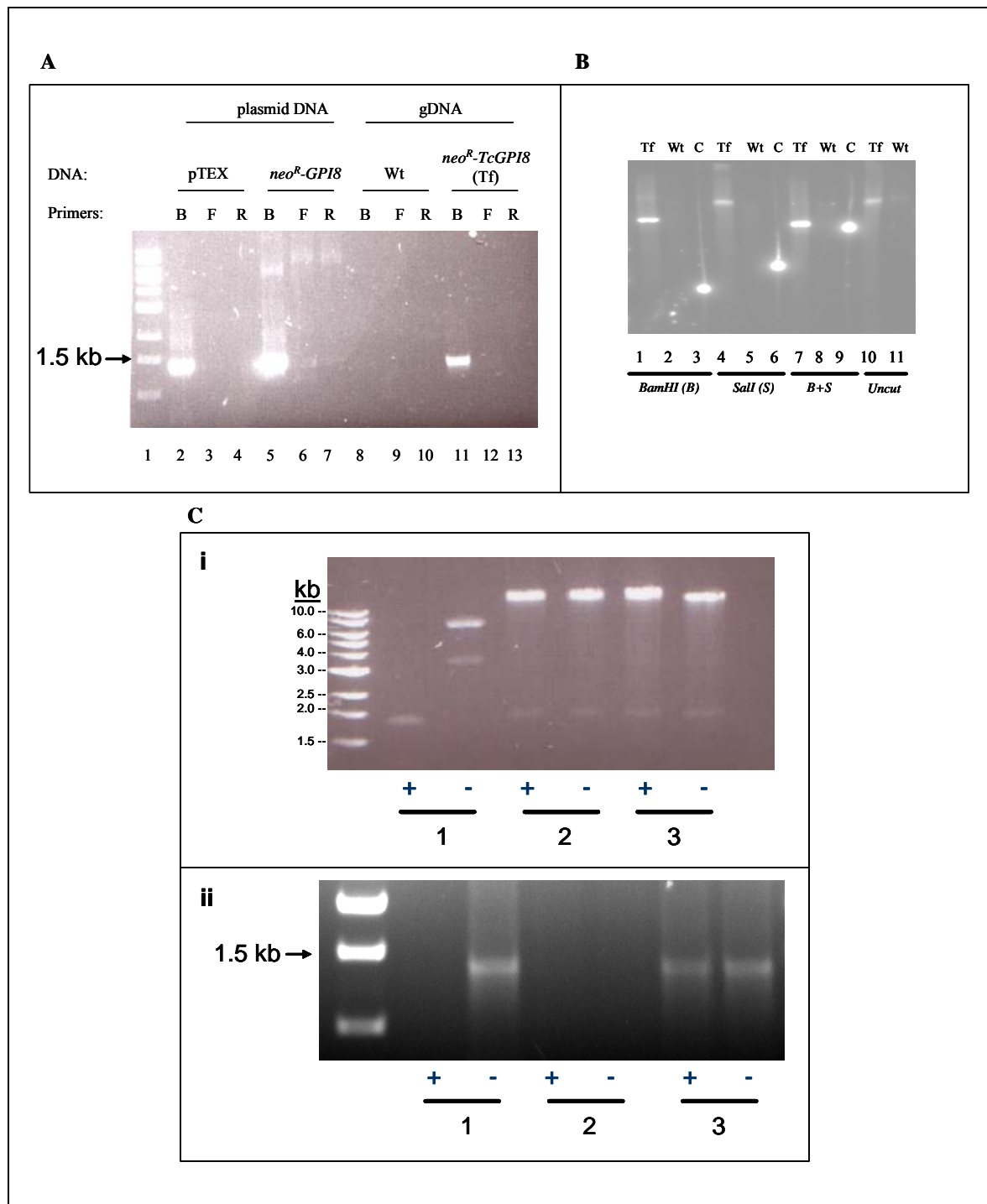


Figure 23

Figure 23: Evaluation of *neo^r* integration into genome of *neo^r-TcGPI8 T. cruzi* transfectants. Wild type *T. cruzi* was electroporated with the *neo^r-TcGPI8* disruption cassette. Parasites were then selected for >3 months in G418. Chromosomal DNA (gDNA) was extracted from *neo^r-TcGPI8* transfectants as well as from wild type *T. cruzi* for use in PCR or Southern blot analysis. A) PCR amplification of the *GAPDH-IR/neo^r* cassette from gDNA of *neo^r-TcGPI8 T. cruzi* transfectants. gDNA from wild type, untransfected *T. cruzi* was used as a control. Negative controls: forward (F) primer only (*GAPDH-IR-F*) or reverse (R) primer (*neo^r-R*) only. Both the pTEX and pBSK.*neo^r-TcGPI8*, plasmids containing the *GAPDH-IR/neo^r* cassettes were used in positive control reactions. Abbreviations: B, both primers; F, forward primer; R, reverse primer; Tf, transfectant; Wt, wild type. The expected 1.3 kilobase (kb) fragment, as indicated by the arrow, was PCR amplified from gDNA of *neo^r-TcGPI8* transfectants but not from the wild type control. B) Southern blot analysis. gDNA of *neo^r-TcGPI8* was digested with restriction enzymes (*Bam*HI and/or *Sall*) and resolved via agarose gel electrophoresis. Following transfer of DNA to nylon membrane, hybridization was performed using a ³²P-labeled *neo^r* probe (Amersham Megaprime, random primer labeling) at 68°C. After 6 days exposure, the image was scanned by phosphorimager. gDNA from *neo^r-TcGPI8* transfectants hybridized with the *neo^r* probe (lanes 1, 4, and 7), indicating the presence of *neo^r* in the genome of the *neo^r-TcGPI8* transfectant. As expected, no hybridization with the *neo^r* probe is observed for wild type gDNA (lanes 2, 5, and 8). Bands were detected at the expected size for plasmid (*neo^r-TcGPI8*) DNA (positive control, lanes 3, 6, and 9). Panel B is reprinted with permission from: Zacks MA. 2007. *Impairment of cell division of Trypanosoma cruzi epimastigotes*. Mem Inst Oswaldo Cruz 102(1): p. 111. C) PCR amplification of the *GAPDH-IR/neo^r* cassette from gDNA of *neo^r-TcGPI8 T. cruzi* transfectants following *dpn*I digestion. To exclude the possibility that the PCR amplification in panel B was due to the continued presence of the 4.2 kb linearized *neo^r-TcGPI8* cassette in parasites following electroporation, PCR amplification of the *GAPDH-IR/neo^r* cassette from *neo^r-TcGPI8* transfectants was performed using *dpn*I-digested DNA. Equal quantities of the indicated DNA were incubated for 24 hours with (+) or without (-) the restriction enzyme, *dpn*I to digest DNA obtained from preparation in *dam*⁺ bacteria (plasmid DNA). PCR was performed using *neo^r*-specific primers, as described in panel B. The *dpn*I treated DNA (500 mg/lane, panel i) and PCR products (5 µl of 50 µl reaction, panel ii) obtained from the following were resolved via agarose gel electrophoresis: 1: gDNA of stable *neo^r-TcGPI8* transfectants; 2: plasmid control DNA, *neo^r-TcGPI8* construct; 3: gDNA of wild type *T. cruzi*.

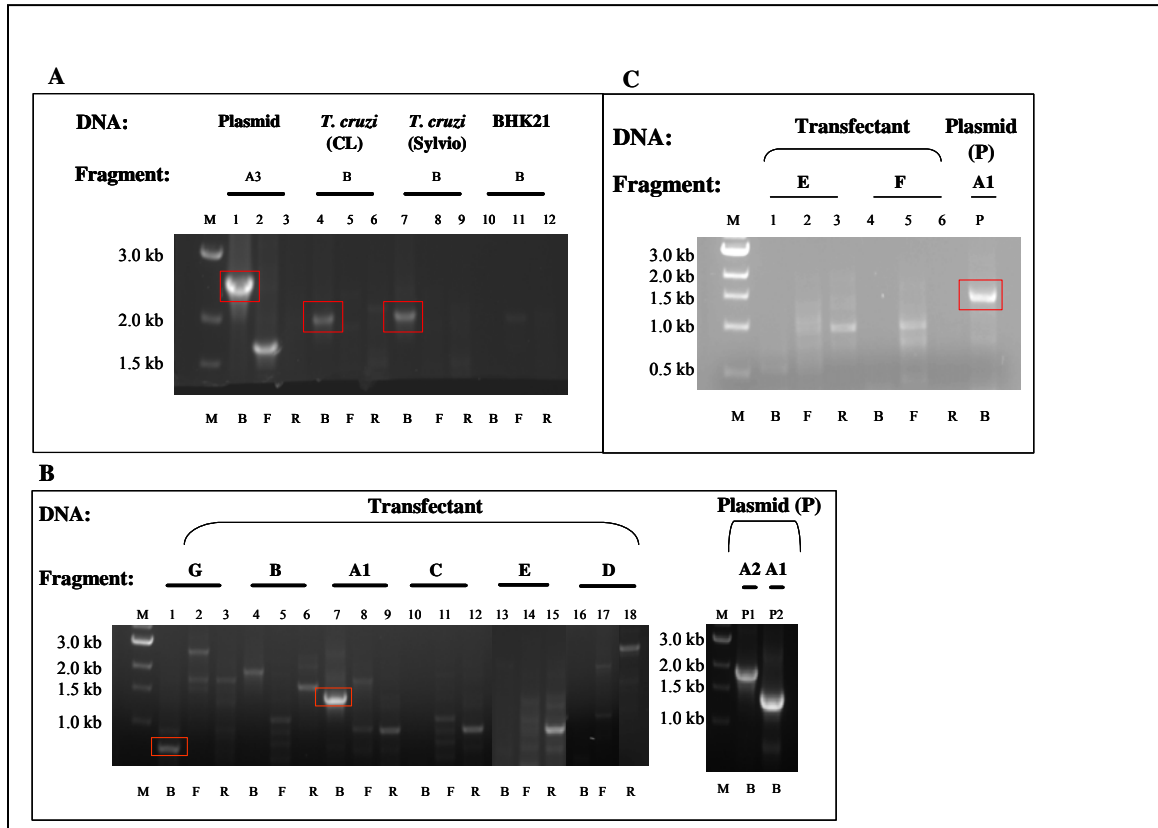


Figure 24: Evaluation of targeted disruption of *TcGPI8* in *neo^r-TcGPI8* transformants. PCR reactions were performed using combinations of *TcGPI8* gene specific primers with 5'FS-F or 3'FS-R primer, as shown in Figure 11. A) To confirm the similarity of the region flanking *TcGPI8* for Sylvio X10/4 (the strain that was used to generate transformants) in comparison to the CL-Brener strain (the *T. cruzi* sequencing strain from which *TcGPI8* flanking sequence was obtained), PCR was performed in parallel (as described for *T. cruzi* gDNA) for both strains. PCR reactions were resolved via agarose gel electrophoresis. Products of the expected size for fragment B (primer pair: 5'FS-F/3'FS-R) from gDNA of *T. cruzi* CL-Brener (CL, lane 4) and SylvioX10/4 (Sylvio, lane 7) strains and for fragment A3 (primer pair: GPI8-F/GPI8-R) for the *neo^r-TcGPI8* construct (plasmid control) were amplified. B) To determine whether *TcGPI8* was disrupted by the *neo^r-TcGPI8* construct, PCR analysis was performed using gDNA of *neo^r-TcGPI8* transfectants. Primer pairs for fragments A1, A2, B, C, D, E, F, and G are GAPDHIR-F/*neo^r*-R, GPI8-F/*neo^r*-R, 5'FS-F/3'FS-R, 5'FS-F/*neo^r*-R, GAPDHIR-F/3'FS-R, GPI8-F/*neo^r*-R, GAPDHIR-F/GPI8-R, GAPDH-F/GAPDH-R, respectively (Table 1). C) To determine whether the 5' and 3' segments of the *TcGPI8* disruption cassette were retained in the insertion, PCR was performed using gDNA of *neo^r-TcGPI8* transfectants. No PCR product of the expected size resulted from amplification using the primer pairs, GPI8-F/*neo^r*-R (fragment E) or GAPDHIR-F/GPI8-R (fragment F). The expected product was obtained in plasmid control reactions using the *neo^r-TcGPI8* cassette (fragment A1, primer pairs: GAPDHIR-F/*neo^r*-R). Abbreviations: M, molecular weight marker (1 kb DNA ladder); B, Both primers; F, Forward primer only; R, Reverse primer only.

A	GAPDHIR	CGTGGCGATGAC	12
	c1-8_-4	CGTGGCGATGAC	268
	C3-2topo_10	CGTGGCGATGAC	299

	GAPDHIR	TTCAGGTCTTTCTTTTGCGAATAGGGATCTTATAATACACGATGCGTGTCCCGTGATGAT	72
	c1-8_-4	TTCAGGTCTTTCTTTTGCGAATAGGGATCTTATAATACACGATGCGTGTCCCGTGATGAT	328
	C3-2topo_10	TTCAGGTCTTTCTTTTGCGAATAGGGATCTTATAATACACGATGCGTGTCCCGTGATGAT	359

	GAPDHIR	CGTTACCGGTGCTGCCACGATCCAATTGACACAGCGTCAAGAGCAAAACAATTTTACTTT	132
	c1-8_-4	CGTTACCGGTGCTGCCACGATCCAATTGACACAGCGTCAAGAGCAAAACAATTTTACTTT	388
	C3-2topo_10	CGTTACCGGTGCTGCCACGATCCAATTGACACAGCGTCAAGAGCAAAACAATTTTACTTT	419

	GAPDHIR	TCCCTTTAAGGACAACAACAAAAAATATATAACTTTTTTCTTTTTTTTTTTTTTTG	192
	c1-8_-4	TCCCTTTAAGGACAACAACAATAAATATATAACTTTTTTCTTTTTTTTTTTTTTT-G	447
	C3-2topo_10	TCCCTTTAAGGACAACAACAATAAATATATAACTTTTTTCTTTTTTTTTTTTTTT--G	476
		*****	*
	GAPDHIR	AAATTATATTTATGGTCATCTTTGGGAAACAAAAGCAGCAATTTAATGATGCGGAAGGA	252
	c1-8_-4	AAATTATATTTATGGTCATCTTCGGGAAACAAAAGCAGCAATTTAATGATGCGGAAGGA	507
	C3-2topo_10	AAATTATATTTATGGTCATCTTTGGGAAACAAAAGCAGCAATTTAATGATGCGGAAGGA	536

	GAPDHIR	TGAGTGAATAATGTTTAATCAATGTACGAGGATTGGGGTATTGCAAGGAAAATGTAGA	312
	c1-8_-4	TGAGTGAATAATGTTTAATCAATGTACGAGGATTGGGGTATTGCAAGGAAAATGTAGA	567
	C3-2topo_10	TGAGTGAATAATGTTTAATCAATGTACGAGGATTGGGGTATTGCAAGGAAAATGTAGA	596

	GAPDHIR	TGATTTAATTGGGTGTGTGATGCAGCTTGTGGTAATTTTGCTCACTTCCCTTTTGGCA	372
	c1-8_-4	TGATTTAATTGGGTGTGTGATGCAGCTTGTGGTAATTTTGCTCACTTCCCTTTTGGCA	627
	C3-2topo_10	TGATTTAATTGGGTGTGTGATGCAGCTTGTGGTAATTTTGCTCACTTCCCTTTTGGCA	656

	GAPDHIR	CATCTTTTTAGTTTTTCTGCTTTTCTTTCCCATTTATCCACTTGCTCTCTCTTTCCAC	432
	c1-8_-4	CATCTTTTTAGTTTTTCTGCTTTTCTTTCCCATTTATCCACTTGCTCTCTCTTTCCAC	687
	C3-2topo_10	CATCTTTTTAGTTTTTCTGCTTTTCTTTCCCATTTATCCACTTGCTCTCTCTTTCCAC	716

	GAPDHIR	GTTTCCTGCACGAATGCAGAAAGTGATATTTTACTTTGAAAGCCATCTACCAACAACAA	492
	c1-8_-4	GTTTCCTGCACGAATGCAGAAAGTGATATTTTACTTTGAAAGCCATCTACCAACAACAA	747
	C3-2topo_10	GTTTCCTGCACGAATGCAGAAAGTGATATTTTACTTTGAAAGCCATCTACCAACAACAA	776

	GAPDHIR	TTACATTGAACAGAATTT	510
	c1-8_-4	TTACATTGAACAGAATTT	806
	C3-2topo_10	TTACATTGAACAGAATTT	836

Fig. 25 (page 1)

B

```
neor          ATGGGATCGGCCATTGAACAAGATGGATTGCACGC 35
c1-8_-4       ATGGGATCGGCCATTGAACAAGATGGATTGCACGC 867
C3-2topo_10   ATGGGATCGGCCATTGAACAA-ATGGATTGC-CGC 895
*****

neor          AGGTTCTCCGCCGCTTGGG-TGGAGAGGCTATTCGGCTATGACTGGGCACAACAGACAA 94
c1-8_-4       AGGTTCACCGCCGCTTGGGGTGGAGAGGCTATTCGGCTATGACTGGGCACAACAGACAA 927
C3-2topo_10   AGGTTCTCCG-CCGCTCGGG-GGGAGAGGCTATTCGGCTATGACTGGGCACAACAAA--A 951
*****

neor          TCGGCTGCTCTGATGCCGCCGTGTTCCGGCTGTCAGCGCAGGGGCGCCCGGTTCTTTTGG 154
c1-8_-4       TCGGCTGCTCTGATGCCGCCGTGTTCCGGCTGTCAGCGCAGGGGCGCCCGGTTCTTTTGG 987
C3-2topo_10   TCGGCTGCTCTGATGCCCC--TGTTCCGGCTGTCACC--A-GGGC-CCCG--TCTTTTGG 1003
*****

neor          TCAAGACCGACCTGTCGGGTGCCCTGAATGAACTGCAGGACGAGGCAGC-----G-CGG 207
c1-8_-4       TCA-GACCGACCTGTCGGG-GCCCTGA-TGAACTGCAGGACGAGGCACC-----GGCTA 1038
C3-2topo_10   TCA--ACCGAC-TGTCCGG-G-CCTGAATGAACTGCAGGACAAGGCACCCCGGCAGGGCA 1058
***          *****
```

Fig. 25 (page 2)

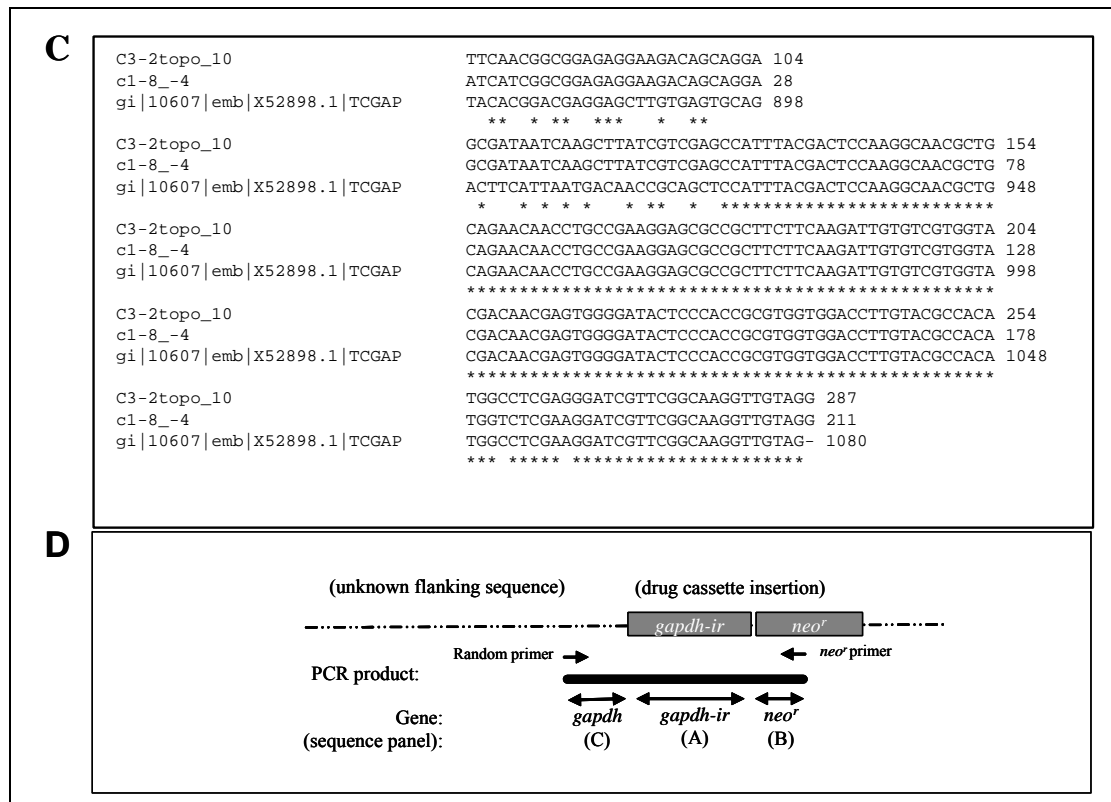


Fig. 25 (page 3)

Figure 25: Identification of the site of integration of GAPDHIR-*neo*^r cassette in the *T. cruzi* genome. Genome walking via an arbitrarily primed PCR approach was used to determine the site of integration²⁹⁴⁻²⁹⁵. Briefly, random, degenerate primers²⁹⁴ were used in pairs with *neo*^r-specific primers (nested primers R1, 5'-TTTCGCTTGGTGGTTCGA-ATGGGCAGGTA-3'; R2, 5'-GCACAGCTGCGCAAGGAACGCC-3'; R3, 5'-GCCGCGCTGCCTCG-3') to amplify fragments from gDNA of stable *neo*^r-*TcGPI8* transfectants containing the unknown sequence flanking *GAPDHIR-neo*^r using modified cycling parameters²⁹⁴. PCR fragments were cloned and sequenced (UTMB Protein Core Facility). Three informative clones were obtained, e.g., clones in which the DNA sequence matched to the expected *GAPDHIR*, and *neo*^r portions and in which additional flanking sequence was present. *T. cruzi* blast search was performed using these flanking sequences. The sequence of the third clone was identical to c1-8_-4. Sequence alignments of TAIL-PCR clones with A) *GAPDHIR*, B) *neo*^r, and C) *GAPDH* are shown. The *GAPDHIR* and *neo*^r portions of the disruption cassette were confirmed and *T. cruzi* blast search identified the sequence flanking the 5' end of the *GAPDHIR-neo*^r insertion as matching to the 3' end of the *T. cruzi* *GAPDH* gene (accession #X52898)³⁰⁶. Reprinted with permission from Zacks MA. 2007. *Impairment of cell division of Trypanosoma cruzi epimastigotes*. Mem Inst Oswaldo Cruz 102(1): p. 112.

Bibliography

1. Stevens JR, Noyes HA, Dover GA, Gibson WC, 1999. The ancient and divergent origins of the human pathogenic trypanosomes, *Trypanosoma brucei* and *T. cruzi*. *Parasitology* 118: 107-116.
2. Brener Z, 1973. Biology of *Trypanosoma cruzi*. *Annu Rev Microbiol* 27: 347-82.
3. Miles M, 2003. American trypanosomiasis (Chagas disease). Cook G, Zumla A, eds. *Manson's tropical disease*. London: Elsevier Science, 1325-1337.
4. World Health Organization, 2002. *The World Health Report*. Geneva: World Health Organization.
5. Barrett MP, Burchmore RJ, Stich A, Lazzari JO, Frasch AC, Cazzulo JJ, Krishna S, 2003. The trypanosomiasis. *Lancet* 362: 1469-1480.
6. Girones N, Fresno M, 2003. Etiology of Chagas disease myocarditis: autoimmunity, parasite persistence, or both? *Trends Parasitol* 19: 19-22.
7. Zacks MA, Wen JJ, Vyatkina G, Bhatia V, Garg N, 2005. An overview of chagasic cardiomyopathy: pathogenic importance of oxidative stress. *An Acad Bras Cienc* 77: 695-715.
8. Mott KE, Muniz TM, Lehman JS, Jr., Hoff R, Morrow RH, Jr., de Oliveira TS, Sherlock I, Draper CC, 1978. House construction, triatomine distribution, and household distribution of seroreactivity to *Trypanosoma cruzi* in a rural community in northeast Brazil. *Am J Trop Med Hyg* 27: 1116-1122.
9. Guzman-Bracho C, 2001. Epidemiology of Chagas disease in Mexico: an update. *Trends Parasitol* 17: 372-376.
10. Schofield CJ, Dias JC, 1999. The Southern Cone Initiative against Chagas disease. *Adv Parasitol* 42: 1-27.
11. Cuba CA, Abad-Franch F, Roldan Rodriguez J, Vargas Vasquez F, Pollack Velasquez L, Miles MA, 2002. The triatomines of northern Peru, with emphasis on the ecology and infection by trypanosomes of *Rhodnius ecuadoriensis* (Triatominae). *Mem Inst Oswaldo Cruz* 97: 175-183.
12. Aguilar VH, Abad-Franch F, Racines VJ, Paucar CA, 1999. Epidemiology of Chagas disease in Ecuador. A brief review. *Mem Inst Oswaldo Cruz* 94 Suppl 1: 387-393.
13. WHO Special Programme for Research and Training in Tropical Diseases, 2002. *Strategic Direction for Research*. TDR Strategic Direction: Chagas Disease. Geneva: World Health Organization.
14. Monteiro FA, Escalante AA, Beard CB, 2001. Molecular tools and triatomine systematics: a public health perspective. *Trends Parasitol* 17: 344-347.
15. Feliciangeli MD, Dujardin JP, Bastrenta B, Mazzarri M, Villegas J, Flores M, Munoz M, 2002. Is *Rhodnius robustus* (Hemiptera: Reduviidae) responsible for Chagas disease transmission in Western Venezuela? *Trop Med Int Health* 7: 280-287.
16. Beard CB, Cordon-Rosales C, Durvasula RV, 2002. Bacterial symbionts of the triatominae and their potential use in control of Chagas disease transmission. *Annu Rev Entomol* 47: 123-141.

17. Beard CB, Pye G, Steurer FJ, Rodriguez R, Campman R, Peterson AT, Ramsey J, Wirtz RA, Robinson LE, 2003. Chagas disease in a domestic transmission cycle, southern Texas, USA. *Emerg Infect Dis* 9: 103-105.
18. Meurs KM, Anthony MA, Slater M, Miller MW, 1998. Chronic *Trypanosoma cruzi* infection in dogs: 11 cases (1987-1996). *J Am Vet Med Assoc* 213: 497-500.
19. Yabsley MJ, Noblet GP, 2002. Seroprevalence of *Trypanosoma cruzi* in raccoons from South Carolina and Georgia. *J Wildl Dis* 38: 75-83.
20. Pietrzak SM, Pung OJ, 1998. Trypanosomiasis in raccoons from Georgia. *J Wildl Dis* 34: 132-136.
21. Karsten V, Davis C, Kuhn R, 1992. *Trypanosoma cruzi* in wild raccoons and opossums in North Carolina. *J Parasitol* 78: 547-549.
22. Bradley KK, Bergman DK, Woods JP, Crutcher JM, Kirchhoff LV, 2000. Prevalence of American trypanosomiasis (Chagas disease) among dogs in Oklahoma. *J Am Vet Med Assoc* 217: 1853-1857.
23. Woody NC, Woody HB, 1974. Letter: Possible Chagas's disease in United States. *N Engl J Med* 290: 749-750.
24. Navin TR, Roberto RR, Juranek DD, Limpakarnjanarat K, Mortenson EW, Clover JR, Yescott RE, Taclindo C, Steurer F, Allain D, 1985. Human and sylvatic *Trypanosoma cruzi* infection in California. *Am J Public Health* 75: 366-369.
25. Ochs DE, Hnilica VS, Moser DR, Smith JH, Kirchhoff LV, 1996. Postmortem diagnosis of autochthonous acute chagasic myocarditis by polymerase chain reaction amplification of a species-specific DNA sequence of *Trypanosoma cruzi*. *Am J Trop Med Hyg* 54: 526-529.
26. Herwaldt BL, Grijalva MJ, Newsome AL, McGhee CR, Powell MR, Nemec DG, Steurer FJ, Eberhard ML, 2000. Use of polymerase chain reaction to diagnose the fifth reported US case of autochthonous transmission of *Trypanosoma cruzi*, in Tennessee, 1998. *J Infect Dis* 181: 395-399.
27. Barnabe C, Yaeger R, Pung O, Tibayrenc M, 2001. *Trypanosoma cruzi*: a considerable phylogenetic divergence indicates that the agent of Chagas disease is indigenous to the native fauna of the United States. *Exp Parasitol* 99: 73-79.
28. Dodd RY, Leiby DA, 2004. Emerging infectious threats to the blood supply. *Annu Rev Med* 55: 191-207.
29. Kerndt PR, Waskin HA, Kirchhoff LV, Steurer F, Waterman SH, Nelson JM, Gellert GA, Shulman IA, 1991. Prevalence of antibody to *Trypanosoma cruzi* among blood donors in Los Angeles, California. *Transfusion* 31: 814-818.
30. Shulman IA, Appleman MD, Saxena S, Hiti AL, Kirchhoff LV, 1997. Specific antibodies to *Trypanosoma cruzi* among blood donors in Los Angeles, California. *Transfusion* 37: 727-731.
31. Leiby DA, Fucci MH, Stumpf RJ, 1999. *Trypanosoma cruzi* in a low- to moderate-risk blood donor population: seroprevalence and possible congenital transmission. *Transfusion* 39: 310-315.
32. MMWR. 2002. Chagas disease after organ transplantation--United States, 2001. *Morb Mortal Wkly Rep* 51: 210-212.

33. Schmunis GA, 1991. *Trypanosoma cruzi*, the etiologic agent of Chagas' disease: status in the blood supply in endemic and nonendemic countries. *Transfusion* 31: 547-557.
34. Schmunis GA, Zicker F, Cruz JR, Cuchi P, 2001. Safety of blood supply for infectious diseases in Latin American countries, 1994-1997. *Am J Trop Med Hyg* 65: 924-930.
35. Schmunis GA, Zicker F, Moncayo A, 1996. Interruption of Chagas' disease transmission through vector elimination. *Lancet* 348: 1171.
36. Schmunis GA, Zicker F, Pinheiro F, Brandling-Bennett D, 1998. Risk for transfusion-transmitted infectious diseases in Central and South America. *Emerg Infect Dis* 4: 5-11.
37. Schmunis GA, Zicker F, Segura EL, del Pozo AE, 2000. Transfusion-transmitted infectious diseases in Argentina, 1995 through 1997. *Transfusion* 40: 1048-1053.
38. Guzman B, 2001. The Hispanic Population, census 2000 brief. Washington, D.C.: US Census Bureau.
39. Kirchhoff LV, Gam AA, Gilliam FC, 1987. American trypanosomiasis (Chagas' disease) in Central American immigrants. *Am J Med* 82: 915-920.
40. Leiby DA, Herron RM, Jr., Read EJ, Lenos BA, Stumpf RJ, 2002. *Trypanosoma cruzi* in Los Angeles and Miami blood donors: impact of evolving donor demographics on seroprevalence and implications for transfusion transmission. *Transfusion* 42: 549-555.
41. McCarthy M, 2003. American Red Cross to screen blood for Chagas' disease. *Lancet* 362: 1988.
42. Alter HJ, Stramer SL, Dodd RY, 2007. Emerging infectious diseases that threaten the blood supply. *Semin Hematol* 44: 32-41.
43. Blood Products Advisory Committee, 2002. Transcripts of the Sept 12, 2002 Blood Products Advisory Committee Meeting. CBER, FDA.
44. Lab Tests Online, 2007. Screening U.S. Blood Supply for *Trypanosoma cruzi*, the Cause of Chagas' Disease: American Association for Clinical Chemistry.
45. United States Food and Drug Administration Press Office, December 13, 2006. FDA Approves First Test to Screen Blood Donors for Chagas Disease (Press Release): FDA News.
46. Leiby DA, Rentas FJ, Nelson KE, Stambolis VA, Ness PM, Parnis C, McAllister HA, Jr., Yawn DH, Stumpf RJ, Kirchhoff LV, 2000. Evidence of *Trypanosoma cruzi* infection (Chagas' disease) among patients undergoing cardiac surgery. *Circulation* 102: 2978-2982.
47. Urbina JA, 2001. Specific treatment of Chagas disease: current status and new developments. *Curr Opin Infect Dis* 14: 733-741.
48. Bhatia V, Wen J-J, Zacks M, Garg N, 2007 (in press). American trypanosomiasis and perspectives on vaccine development. Barrett A, Stanberry L, eds. *Vaccines Against Biothreats and Emerging Infections*: Elsevier Academic Press.
49. Nogueira N, Cohn Z, 1977. *Trypanosoma cruzi*: uptake and intracellular fate in normal and activated cells. *Am J Trop Med Hyg* 26: 194-203.
50. Sibley LD, Andrews NW, 2000. Cell invasion by un-palatable parasites. *Traffic* 1: 100-6.

51. Schenkman S, Robbins ES, Nussenzweig V, 1991. Attachment of *Trypanosoma cruzi* to mammalian cells requires parasite energy, and invasion can be independent of the target cell cytoskeleton. *Infect Immun* 59: 645-654.
52. Hall BF, 1993. *Trypanosoma cruzi*: mechanisms for entry into host cells. *Semin Cell Biol* 4: 323-333.
53. Tan H, Andrews NW, 2002. Don't bother to knock--the cell invasion strategy of *Trypanosoma cruzi*. *Trends Parasitol* 18: 427-428.
54. Woolsey AM, Sunwoo L, Petersen CA, Brachmann SM, Cantley LC, Burleigh BA, 2003. Novel PI 3-kinase-dependent mechanisms of trypanosome invasion and vacuole maturation. *J Cell Sci* 116: 3611-3622.
55. Burleigh BA, 2005. Host cell signaling and *Trypanosoma cruzi* invasion: do all roads lead to lysosomes? *Sci STKE* 2005: 36.
56. Schenkman S, Diaz C, Nussenzweig V, 1991. Attachment of *Trypanosoma cruzi* trypomastigotes to receptors at restricted cell surface domains. *Exp Parasitol* 72: 76-86.
57. Ramirez MI, Ruiz Rde C, Araya JE, Da Silveira JF, Yoshida N, 1993. Involvement of the stage-specific 82-kilodalton adhesion molecule of *Trypanosoma cruzi* metacyclic trypomastigotes in host cell invasion. *Infect Immun* 61: 3636-3641.
58. Ruiz Rde C, Rigoni VL, Gonzalez J, Yoshida N, 1993. The 35/50 kDa surface antigen of *Trypanosoma cruzi* metacyclic trypomastigotes, an adhesion molecule involved in host cell invasion. *Parasite Immunol* 15: 121-125.
59. Santori FR, Dorta ML, Juliano L, Juliano MA, da Silveira JF, Ruiz RC, Yoshida N, 1996. Identification of a domain of *Trypanosoma cruzi* metacyclic trypomastigote surface molecule gp82 required for attachment and invasion of mammalian cells. *Mol Biochem Parasitol* 78: 209-216.
60. Neira I, Silva FA, Cortez M, Yoshida N, 2003. Involvement of *Trypanosoma cruzi* metacyclic trypomastigote surface molecule gp82 in adhesion to gastric mucin and invasion of epithelial cells. *Infect Immun* 71: 557-561.
61. Rodriguez A, Rioult MG, Ora A, Andrews NW, 1995. A trypanosome-soluble factor induces IP3 formation, intracellular Ca²⁺ mobilization and microfilament rearrangement in host cells. *J Cell Biol* 129: 1263-1273.
62. Tardieux I, Nathanson MH, Andrews NW, 1994. Role in host cell invasion of *Trypanosoma cruzi*-induced cytosolic-free Ca²⁺ transients. *J Exp Med* 179: 1017-1022.
63. Low HP, Paulin JJ, Keith CH, 1992. *Trypanosoma cruzi* infection of BSC-1 fibroblast cells causes cytoskeletal disruption and changes in intracellular calcium levels. *J Protozool* 39: 463-470.
64. Dorta ML, Ferreira AT, Oshiro ME, Yoshida N, 1995. Ca²⁺ signal induced by *Trypanosoma cruzi* metacyclic trypomastigote surface molecules implicated in mammalian cell invasion. *Mol Biochem Parasitol* 73: 285-289.
65. Ruiz RC, Favoreto S, Jr., Dorta ML, Oshiro ME, Ferreira AT, Manque PM, Yoshida N, 1998. Infectivity of *Trypanosoma cruzi* strains is associated with differential expression of surface glycoproteins with differential Ca²⁺ signalling activity. *Biochem J* 330 (Pt 1): 505-511.

66. Burleigh BA, Andrews NW, 1998. Signaling and host cell invasion by *Trypanosoma cruzi*. *Curr Opin Microbiol* 1: 461-465.
67. Rodriguez A, Martinez I, Chung A, Berlot CH, Andrews NW, 1999. cAMP regulates Ca²⁺-dependent exocytosis of lysosomes and lysosome-mediated cell invasion by trypanosomes. *J Biol Chem* 274: 16754-16759.
68. Ming M, Ewen ME, Pereira ME, 1995. Trypanosome invasion of mammalian cells requires activation of the TGF beta signaling pathway. *Cell* 82: 287-296.
69. Burleigh BA, Caler EV, Webster P, Andrews NW, 1997. A cytosolic serine endopeptidase from *Trypanosoma cruzi* is required for the generation of Ca²⁺ signaling in mammalian cells. *J Cell Biol* 136: 609-620.
70. Caler EV, Vaena de Avalos S, Haynes PA, Andrews NW, Burleigh BA, 1998. Oligopeptidase B-dependent signaling mediates host cell invasion by *Trypanosoma cruzi*. *Embo J* 17: 4975-4986.
71. Burleigh BA, Andrews NW, 1995. A 120-kDa alkaline peptidase from *Trypanosoma cruzi* is involved in the generation of a novel Ca(2+)-signaling factor for mammalian cells. *J Biol Chem* 270: 5172-5180.
72. Tardieux I, Webster P, Ravesloot J, Boron W, Lunn JA, Heuser JE, Andrews NW, 1992. Lysosome recruitment and fusion are early events required for trypanosome invasion of mammalian cells. *Cell* 71: 1117-1130.
73. Soares MJ, Souto-Padron T, De Souza W, 1992. Identification of a large pre-lysosomal compartment in the pathogenic protozoon *Trypanosoma cruzi*. *J Cell Sci* 102 (Pt 1): 157-167.
74. Rodriguez A, Samoff E, Rioult MG, Chung A, Andrews NW, 1996. Host cell invasion by trypanosomes requires lysosomes and microtubule/kinesin-mediated transport. *J Cell Biol* 134: 349-362.
75. Rodriguez A, Webster P, Ortego J, Andrews NW, 1997. Lysosomes behave as Ca²⁺-regulated exocytic vesicles in fibroblasts and epithelial cells. *J Cell Biol* 137: 93-104.
76. McNeil PL, Steinhardt RA, 1997. Loss, restoration, and maintenance of plasma membrane integrity. *J Cell Biol* 137: 1-4.
77. Reddy A, Caler EV, Andrews NW, 2001. Plasma membrane repair is mediated by Ca(2+)-regulated exocytosis of lysosomes. *Cell* 106: 157-169.
78. Hall BF, Webster P, Ma AK, Joiner KA, Andrews NW, 1992. Desialylation of lysosomal membrane glycoproteins by *Trypanosoma cruzi*: a role for the surface neuraminidase in facilitating parasite entry into the host cell cytoplasm. *J Exp Med* 176: 313-325.
79. Andrews NW, Whitlow MB, 1989. Secretion by *Trypanosoma cruzi* of a hemolysin active at low pH. *Mol Biochem Parasitol* 33: 249-256.
80. Ley V, Robbins ES, Nussenzweig V, Andrews NW, 1990. The exit of *Trypanosoma cruzi* from the phagosome is inhibited by raising the pH of acidic compartments. *J Exp Med* 171: 401-413.
81. Andrews NW, Abrams CK, Slatin SL, Griffiths G, 1990. A *T. cruzi*-secreted protein immunologically related to the complement component C9: evidence for membrane pore-forming activity at low pH. *Cell* 61: 1277-1287.

82. Manning-Cela R, Cortes A, Gonzalez-Rey E, Van Voorhis WC, Swindle J, Gonzalez A, 2001. LYT1 protein is required for efficient in vitro infection by *Trypanosoma cruzi*. Infect Immun 69: 3916-3623.
83. Abe Y, Shirane K, Yokosawa H, Matsushita H, Mitta M, Kato I, Ishii S, 1993. Asparaginyl endopeptidase of jack bean seeds. Purification, characterization, and high utility in protein sequence analysis. J Biol Chem 268: 3525-3529.
84. de Carvalho TM, de Souza W, 1989. Early events related with the behaviour of *Trypanosoma cruzi* within an endocytic vacuole in mouse peritoneal macrophages. Cell Struct Funct 14: 383-392.
85. Stecconi-Silva RB, Andreoli WK, Mortara RA, 2003. Parameters affecting cellular invasion and escape from the parasitophorous vacuole by different infective forms of *Trypanosoma cruzi*. Mem Inst Oswaldo Cruz 98: 953-958.
86. Ley V, Andrews NW, Robbins ES, Nussenzweig V, 1988. Amastigotes of *Trypanosoma cruzi* sustain an infective cycle in mammalian cells. J Exp Med 168: 649-659.
87. McCabe RE, Remington JS, Araujo FG, 1984. Mechanisms of invasion and replication of the intracellular stage in *Trypanosoma cruzi*. Infect Immun 46: 372-376.
88. de Carvalho TU, de Souza W, 1986. Infectivity of amastigotes of *Trypanosoma cruzi*. Rev Inst Med Trop Sao Paulo 28: 205-212.
89. Zhang L, Tarleton RL, 1999. Parasite persistence correlates with disease severity and localization in chronic Chagas' disease. J Infect Dis 180: 480-486.
90. Garg N, Gerstner A, Bhatia V, DeFord J, Papaconstantinou J, 2004. Gene expression analysis in mitochondria from chagasic mice: alterations in specific metabolic pathways. Biochem J 381: 743-752.
91. Garg N, Popov VL, Papaconstantinou J, 2003. Profiling gene transcription reveals a deficiency of mitochondrial oxidative phosphorylation in *Trypanosoma cruzi*-infected murine hearts: implications in chagasic myocarditis development. Biochim Biophys Acta 1638: 106-120.
92. Nosjean O, Briolay A, Roux B, 1997. Mammalian GPI proteins: sorting, membrane residence and functions. Biochim Biophys Acta 1331: 153-186.
93. Garg N, 1998. Biological significance of glycosylphosphatidylinositols in protozoan parasites. Trends Glycosci Glycotech 10: 439-453.
94. Ferguson MA, 1999. The structure, biosynthesis and functions of glycosylphosphatidylinositol anchors, and the contributions of trypanosome research. J Cell Sci 112 (Pt 17): 2799-2809.
95. Zacks MA, Garg N, 2006. Recent developments in the molecular, biochemical and functional characterization of GPI8 and the GPI-anchoring mechanism [review]. Mol Membr Biol 23: 209-225.
96. Ferguson MAJ, 1994. What can GPI do for you? Parasitol Today 10: 48-52.
97. Ferguson MA, 1992. Colworth Memorial Lecture. Glycosyl-phosphatidylinositol membrane anchors: the tale of a tail. Biochem Soc Transactions 20: 243-256.
98. Reizman H, Conzelmann A, 1998. 256. Glycosylphosphatidylinositol: protein transamidase. Barrett AJ, Rawlings ND, Woessner JF, eds. The Handbook of Proteolytic Enzymes. London: Academic Press, 756-759.

99. McConville MJ, Ferguson MA, 1993. The structure, biosynthesis and function of glycosylated phosphatidylinositols in the parasitic protozoa and higher eukaryotes. *Biochem J* 294 (Pt 2): 305-324.
100. Ferguson MA, 1997. The surface glycoconjugates of trypanosomatid parasites. *Philos Trans R Soc Lond B Biol Sci* 352: 1295-1302.
101. Gazzinelli RT, Denkers EY, 2006. Protozoan encounters with Toll-like receptor signalling pathways: implications for host parasitism. *Nat Rev Immunol* 6: 895-906.
102. Alexander J, Russell DG, 1992. The interaction of *Leishmania* species with macrophages. *Adv Parasitol* 31: 175-254.
103. Beverley S, Turco S, 1998. Lipophosphoglycan (LPG) and the identification of virulence genes in the protozoan parasite *Leishmania*. *Trends Microbiol.* 6: 35-40.
104. Soares RP, Cardoso TL, Barron T, Araujo MS, Pimenta PF, Turco SJ, 2005. *Leishmania braziliensis*: a novel mechanism in the lipophosphoglycan regulation during metacyclogenesis. *Int J Parasitol* 35: 245-253.
105. Descoteaux A, Matlashewski G, Turco SJ, 1992. Inhibition of macrophage protein kinase C-mediated protein phosphorylation by *Leishmania donovani* lipophosphoglycan. *J Immunol* 149: 3008-3015.
106. Lodge R, Descoteaux A, 2005. Modulation of phagolysosome biogenesis by the lipophosphoglycan of *Leishmania*. *Clin Immunol* 114: 256-265.
107. Pimenta PF, Saraiva EM, Rowton E, Modi GB, Garraway LA, Beverley SM, Turco SJ, Sacks DL, 1994. Evidence that the vectorial competence of phlebotomine sand flies for different species of *Leishmania* is controlled by structural polymorphisms in the surface lipophosphoglycan. *Proc Natl Acad Sci U S A* 91: 9155-9159.
108. McConville MJ, Turco SJ, Ferguson MA, Sacks DL, 1992. Developmental modification of lipophosphoglycan during the differentiation of *Leishmania major* promastigotes to an infectious stage. *Embo J* 11: 3593-3600.
109. Pimenta PF, Turco SJ, McConville MJ, Lawyer PG, Perkins PV, Sacks DL, 1992. Stage-specific adhesion of *Leishmania promastigotes* to the sandfly midgut. *Science* 256: 1812-1815.
110. Eilam Y, El-On J, Spira DT, 1985. *Leishmania major*: excreted factor, calcium ions, and the survival of amastigotes. *Exp Parasitol* 59: 161-168.
111. Brittingham A, Chen G, McGwire BS, Chang KP, Mosser DM, 1999. Interaction of *Leishmania* gp63 with cellular receptors for fibronectin. *Infect Immun* 67: 4477-4484.
112. Puentes SM, Da Silva RP, Sacks DL, Hammer CH, Joiner KA, 1990. Serum resistance of metacyclic stage *Leishmania major* promastigotes is due to release of C5b-9. *J Immunol* 145: 4311-4316.
113. Liu X, Chang KP, 1992. Extrachromosomal genetic complementation of surface metalloproteinase (gp63)-deficient *Leishmania* increases their binding to macrophages. *Proc Natl Acad Sci U S A* 89: 4991-4995.
114. McGwire B, Chang KP, 1994. Genetic rescue of surface metalloproteinase (gp63)-deficiency in *Leishmania amazonensis* variants increases their infection of macrophages at the early phase. *Mol Biochem Parasitol* 66: 345-347.

115. Joshi PB, Sacks DL, Modi G, McMaster WR, 1998. Targeted gene deletion of *Leishmania major* genes encoding developmental stage-specific leishmanolysin (GP63). *Mol Microbiol* 27: 519-530.
116. Bouvier J, Schneider P, Etges R, 1995. Leishmanolysin: surface metalloproteinase of *Leishmania*. *Methods Enzymol* 248: 614-633.
117. Russell DG, 1987. The macrophage-attachment glycoprotein gp63 is the predominant C3-acceptor site on *Leishmania mexicana* promastigotes. *Eur J Biochem* 164: 213-221.
118. Russell DG, Wright SD, 1988. Complement receptor type 3 (CR3) binds to an Arg-Gly-Asp-containing region of the major surface glycoprotein, gp63, of *Leishmania* promastigotes. *J Exp Med* 168: 279-292.
119. Soteriadou KP, Remoundos MS, Katsikas MC, Tzinia AK, Tsikaris V, Sakarellos C, Tzartos SJ, 1992. The Ser-Arg-Tyr-Asp region of the major surface glycoprotein of *Leishmania* mimics the Arg-Gly-Asp-Ser cell attachment region of fibronectin. *J Biol Chem* 267: 13980-13985.
120. Chang CS, Chang KP, 1986. Monoclonal antibody affinity purification of a *Leishmania* membrane glycoprotein and its inhibition of *leishmania*-macrophage binding. *Proc Natl Acad Sci U S A* 83: 100-104.
121. Peters C, Kawakami M, Kaul M, Ilg T, Overath P, Aebischer T, 1997. Secreted proteophosphoglycan of *Leishmania mexicana* amastigotes activates complement by triggering the mannan binding lectin pathway. *Eur J Immunol* 27: 2666-2672.
122. Turco SJ, Descoteaux A, 1992. The lipophosphoglycan of *Leishmania* parasites. *Annu Rev Microbiol* 46: 65-94.
123. Proudfoot L, O'Donnell CA, Liew FY, 1995. Glycoinositolphospholipids of *Leishmania major* inhibit nitric oxide synthesis and reduce leishmanicidal activity in murine macrophages. *Eur J Immunol* 25: 745-750.
124. Proudfoot L, Nikolaev AV, Feng GJ, Wei WQ, Ferguson MA, Brimacombe JS, Liew FY, 1996. Regulation of the expression of nitric oxide synthase and leishmanicidal activity by glycoconjugates of *Leishmania* lipophosphoglycan in murine macrophages. *Proc Natl Acad Sci U S A* 93: 10984-10989.
125. Suzuki E, Tanaka AK, Toledo MS, Takahashi HK, Straus AH, 2002. Role of beta-D-galactofuranose in *Leishmania major* macrophage invasion. *Infect Immun* 70: 6592-6596.
126. Vickerman K, Luckins AG, 1969. Localization of variable antigens in the surface coat of *Trypanosoma brucei* using ferritin conjugated antibody. *Nature* 224: 1125-1126.
127. Zitzmann N, Mehlert A, Carrouee S, Rudd PM, Ferguson MA, 2000. Protein structure controls the processing of the N-linked oligosaccharides and glycosylphosphatidylinositol glycans of variant surface glycoproteins expressed in bloodstream form *Trypanosoma brucei*. *Glycobiology* 10: 243-249.
128. Cross GA, 1996. Antigenic variation in trypanosomes: secrets surface slowly. *Bioessays* 18: 283-291.
129. Homans SW, Edge CJ, Ferguson MA, Dwek RA, Rademacher TW, 1989. Solution structure of the glycosylphosphatidylinositol membrane anchor glycan of *Trypanosoma brucei* variant surface glycoprotein. *Biochemistry* 28: 2881-2887.

130. Masterson WJ, Raper J, Doering TL, Hart GW, Englund PT, 1990. Fatty acid remodeling: a novel reaction sequence in the biosynthesis of trypanosome glycosyl phosphatidylinositol membrane anchors. *Cell* 62: 73-80.
131. Doering TL, Raper J, Buxbaum LU, Adams SP, Gordon JI, Hart GW, Englund PT, 1991. An analog of myristic acid with selective toxicity for African trypanosomes. *Science* 252: 1851-1854.
132. Doering TL, Lu T, Werbovetz KA, Gokel GW, Hart GW, Gordon JI, Englund PT, 1994. Toxicity of myristic acid analogs toward African trypanosomes. *Proc Natl Acad Sci U S A* 91: 9735-9739.
133. Roditi I, Schwarz H, Pearson TW, Beecroft RP, Liu MK, Richardson JP, Buhring HJ, Pleiss J, Bulow R, Williams RO, et al., 1989. Procyclin gene expression and loss of the variant surface glycoprotein during differentiation of *Trypanosoma brucei*. *J Cell Biol* 108: 737-746.
134. Acosta-Serrano A, Cole RN, Englund PT, 2000. Killing of *Trypanosoma brucei* by concanavalin A: structural basis of resistance in glycosylation mutants. *J Mol Biol* 304: 633-644.
135. Mowatt MR, Wisdom GS, Clayton CE, 1989. Variation of tandem repeats in the developmentally regulated procyclic acidic repetitive proteins of *Trypanosoma brucei*. *Mol Cell Biol* 9: 1332-1335.
136. Acosta-Serrano A, Vassella E, Liniger M, Kunz Renggli C, Brun R, Roditi I, Englund PT, 2001. The surface coat of procyclic *Trypanosoma brucei*: programmed expression and proteolytic cleavage of procyclin in the tsetse fly. *Proc Natl Acad Sci U S A* 98: 1513-1518.
137. Maudlin I, Welburn SC, 1988. The role of lectins and trypanosome genotype in the maturation of midgut infections in *Glossina morsitans*. *Trop Med Parasitol* 39: 56-58.
138. Voyiatzaki CS, Soteriadou KP, 1992. Identification and isolation of the *Leishmania* transferrin receptor. *J Biol Chem* 267: 9112-9117.
139. Frasch AC, 2000. Functional diversity in the trans-sialidase and mucin families in *Trypanosoma cruzi*. *Parasitol Today* 16: 282-6.
140. Roggentin P, Rothe B, Kaper JB, Galen J, Lawrisuk L, Vimr ER, Schauer R, 1989. Conserved sequences in bacterial and viral sialidases. *Glycoconj J* 6: 349-353.
141. Zingales B, Carniol C, de Lederkremer RM, Colli W, 1987. Direct sialic acid transfer from a protein donor to glycolipids of trypomastigote forms of *Trypanosoma cruzi*. *Mol Biochem Parasitol* 26: 135-144.
142. Parodi AJ, Pollevick GD, Mautner M, Buschiazzi A, Sanchez DO, Frasch AC, 1992. Identification of the gene(s) coding for the trans-sialidase of *Trypanosoma cruzi*. *Embo J* 11: 1705-1710.
143. Previato JO, Andrade AF, Pessolani MC, Mendonca-Previato L, 1985. Incorporation of sialic acid into *Trypanosoma cruzi* macromolecules. A proposal for a new metabolic route. *Mol Biochem Parasitol* 16: 85-96.
144. Schenkman S, Kurosaki T, Ravetch JV, Nussenzweig V, 1992. Evidence for the participation of the Ssp-3 antigen in the invasion of nonphagocytic mammalian cells by *Trypanosoma cruzi*. *J Exp Med* 175: 1635-1641.

145. Schenkman S, Ferguson MA, Heise N, de Almeida ML, Mortara RA, Yoshida N, 1993. Mucin-like glycoproteins linked to the membrane by glycosylphosphatidylinositol anchor are the major acceptors of sialic acid in a reaction catalyzed by trans-sialidase in metacyclic forms of *Trypanosoma cruzi*. *Mol Biochem Parasitol* 59: 293-303.
146. Piras MM, Henriquez D, Piras R, 1987. The effect of fetuin and other sialoglycoproteins on the in vitro penetration of *Trypanosoma cruzi* trypomastigotes into fibroblastic cells. *Mol Biochem Parasitol* 22: 135-143.
147. Pereira ME, Zhang K, Gong Y, Herrera EM, Ming M, 1996. Invasive phenotype of *Trypanosoma cruzi* restricted to a population expressing trans-sialidase. *Infect Immun* 64: 3884-3892.
148. Schenkman RP, Vandekerckhove F, Schenkman S, 1993. Mammalian cell sialic acid enhances invasion by *Trypanosoma cruzi*. *Infect Immun* 61: 898-902.
149. Schenkman S, Jiang MS, Hart GW, Nussenzweig V, 1991. A novel cell surface trans-sialidase of *Trypanosoma cruzi* generates a stage-specific epitope required for invasion of mammalian cells. *Cell* 65: 1117-1125.
150. Lopez M, Huynh C, Andrade LO, Pypaert M, Andrews NW, 2002. Role for sialic acid in the formation of tight lysosome-derived vacuoles during *Trypanosoma cruzi* invasion. *Mol Biochem Parasitol* 119: 141-145.
151. Rubin-de-Celis SS, Uemura H, Yoshida N, Schenkman S, 2006. Expression of trypomastigote trans-sialidase in metacyclic forms of *Trypanosoma cruzi* increases parasite escape from its parasitophorous vacuole. *Cell Microbiol* 8: 1888-1898.
152. Cross GA, Takle GB, 1993. The surface trans-sialidase family of *Trypanosoma cruzi*. *Annu Rev Microbiol* 47: 385-411.
153. Magdesian MH, Giordano R, Ulrich H, Juliano MA, Juliano L, Schumacher RI, Colli W, Alves MJ, 2001. Infection by *Trypanosoma cruzi*. Identification of a parasite ligand and its host cell receptor. *J Biol Chem* 276: 19382-19389.
154. Magdesian MH, Tonelli RR, Fessel MR, Silveira MS, Schumacher RI, Linden R, Colli W, Alves MJ, 2007. A conserved domain of the gp85/trans-sialidase family activates host cell extracellular signal-regulated kinase and facilitates *Trypanosoma cruzi* infection. *Exp Cell Res* 313: 210-218.
155. Santos MA, Garg N, Tarleton RL, 1997. The identification and molecular characterization of *Trypanosoma cruzi* amastigote surface protein-1, a member of the trans-sialidase gene super-family. *Mol Biochem Parasitol* 86: 1-11.
156. Low HP, Santos MA, Wizel B, Tarleton RL, 1998. Amastigote surface proteins of *Trypanosoma cruzi* are targets for CD8+ CTL. *J Immunol* 160: 1817-1823.
157. Alves MJ, Colli W, 1975. Glycoproteins from *trypanosoma cruzi*: partial purification by gel chromatography. *FEBS Lett* 52: 188-190.
158. Di Noia JM, Sanchez DO, Frasch AC, 1995. The protozoan *Trypanosoma cruzi* has a family of genes resembling the mucin genes of mammalian cells. *J Biol Chem* 270: 24146-24149.
159. Di Noia JM, Pollevick GD, Xavier MT, Previato JO, Mendoca-Previato L, Sanchez DO, Frasch AC, 1996. High diversity in mucin genes and mucin molecules in *Trypanosoma cruzi*. *J Biol Chem* 271: 32078-32083.

160. Di Noia JM, D'Orso I, Aslund L, Sanchez DO, Frasch AC, 1998. The *Trypanosoma cruzi* mucin family is transcribed from hundreds of genes having hypervariable regions. *J Biol Chem* 273: 10843-10850.
161. Freitas-Junior LH, Briones MR, Schenkman S, 1998. Two distinct groups of mucin-like genes are differentially expressed in the developmental stages of *Trypanosoma cruzi*. *Mol Biochem Parasitol* 93: 101-114.
162. Acosta-Serrano A, Almeida IC, Freitas-Junior LH, Yoshida N, Schenkman S, 2001. The mucin-like glycoprotein super-family of *Trypanosoma cruzi*: structure and biological roles. *Mol Biochem Parasitol* 114: 143-50.
163. Serrano AA, Schenkman S, Yoshida N, Mehlert A, Richardson JM, Ferguson MA, 1995. The lipid structure of the glycosylphosphatidylinositol-anchored mucin-like sialic acid acceptors of *Trypanosoma cruzi* changes during parasite differentiation from epimastigotes to infective metacyclic trypomastigote forms. *J Biol Chem* 270: 27244-53.
164. El-Sayed NM, Myler PJ, Bartholomeu DC, Nilsson D, Aggarwal G, Tran AN, Ghedin E, Worthey EA, Delcher AL, Blandin G, Westenberger SJ, Caler E, Cerqueira GC, Branche C, Haas B, Anupama A, Arner E, Aslund L, Attipoe P, Bontempi E, Bringaud F, Burton P, Cadag E, Campbell DA, Carrington M, Crabtree J, Darban H, da Silveira JF, de Jong P, Edwards K, Englund PT, Fazelina G, Feldblyum T, Ferella M, Frasch AC, Gull K, Horn D, Hou L, Huang Y, Kindlund E, Klingbeil M, Kluge S, Koo H, Lacerda D, Levin MJ, Lorenzi H, Louie T, Machado CR, McCulloch R, McKenna A, Mizuno Y, Mottram JC, Nelson S, Ochaya S, Osoegawa K, Pai G, Parsons M, Pentony M, Pettersson U, Pop M, Ramirez JL, Rinta J, Robertson L, Salzberg SL, Sanchez DO, Seyler A, Sharma R, Shetty J, Simpson AJ, Sisk E, Tammi MT, Tarleton R, Teixeira S, Van Aken S, Vogt C, Ward PN, Wickstead B, Wortman J, White O, Fraser CM, Stuart KD, Andersson B, 2005. The genome sequence of *Trypanosoma cruzi*, etiologic agent of Chagas disease. *Science* 309: 409-415.
165. Malaga S, Yoshida N, 2001. Targeted reduction in expression of *Trypanosoma cruzi* surface glycoprotein gp90 increases parasite infectivity. *Infect Immun* 69: 353-359.
166. Cuevas IC, Cazzulo JJ, Sanchez DO, 2003. gp63 homologues in *Trypanosoma cruzi*: surface antigens with metalloprotease activity and a possible role in host cell infection. *Infect Immun* 71: 5739-5749.
167. Ropert C, Gazzinelli RT, 2000. Signaling of immune system cells by glycosylphosphatidylinositol (GPI) anchor and related structures derived from parasitic protozoa. *Curr Opin Microbiol* 3: 395-403.
168. Camargo MM, Almeida IC, Pereira ME, Ferguson MA, Travassos LR, Gazzinelli RT, 1997. Glycosylphosphatidylinositol-anchored mucin-like glycoproteins isolated from *Trypanosoma cruzi* trypomastigotes initiate the synthesis of proinflammatory cytokines by macrophages. *J Immunol* 158: 5890-5901.
169. Mensa-Wilmot K, LeBowitz JH, Chang KP, al-Qahtani A, McGwire BS, Tucker S, Morris JC, 1994. A glycosylphosphatidylinositol (GPI)-negative phenotype produced in *Leishmania major* by GPI phospholipase C from *Trypanosoma brucei*: topography of two GPI pathways. *J Cell Biol* 124: 935-947.

170. Garg N, Postan M, Mensa-Wilmot K, Tarleton RL, 1997. Glycosylphosphatidylinositols are required for the development of *Trypanosoma cruzi* amastigotes. *Infect Immun* 65: 4055-4060.
171. Mensa-Wilmot K, Garg N, McGwire BS, Lu HG, Zhong L, Armah DA, LeBowitz JH, Chang KP, 1999. Roles of free GPIs in amastigotes of *Leishmania*. *Mol Biochem Parasitol* 99: 103-116.
172. Ilgoutz SC, Zawadzki JL, Ralton JE, McConville MJ, 1999. Evidence that free GPI glycolipids are essential for growth of *Leishmania mexicana*. *Embo J* 18: 2746-2755.
173. Hilley JD, Zawadzki JL, McConville MJ, Coombs GH, Mottram JC, 2000. *Leishmania mexicana* mutants lacking glycosylphosphatidylinositol (GPI):protein transamidase provide insights into the biosynthesis and functions of GPI-anchored proteins. *Mol Biol Cell* 11: 1183-1195.
174. Sacks DL, Modi G, Rowton E, Spath G, Epstein L, Turco SJ, Beverley SM, 2000. The role of phosphoglycans in *Leishmania*-sand fly interactions. *Proc Natl Acad Sci U S A* 97: 406-411.
175. Spath GF, Epstein L, Leader B, Singer SM, Avila HA, Turco SJ, Beverley SM, 2000. Lipophosphoglycan is a virulence factor distinct from related glycoconjugates in the protozoan parasite *Leishmania major*. *Proc Natl Acad Sci U S A* 97: 9258-9263.
176. Spath GF, Garraway LA, Turco SJ, Beverley SM, 2003. The role(s) of lipophosphoglycan (LPG) in the establishment of *Leishmania major* infections in mammalian hosts. *Proc Natl Acad Sci U S A* 100: 9536-9541.
177. Spath GF, Lye LF, Segawa H, Sacks DL, Turco SJ, Beverley SM, 2003. Persistence without pathology in phosphoglycan-deficient *Leishmania major*. *Science* 301: 1241-1243.
178. Turco SJ, Spath GF, Beverley SM, 2001. Is lipophosphoglycan a virulence factor? A surprising diversity between *Leishmania* species. *Trends Parasitol* 17: 223-6.
179. Nagamune K, Nozaki T, Maeda Y, Ohishi K, Fukuma T, Hara T, Schwarz RT, Sutterlin C, Brun R, Riezman H, Kinoshita T, 2000. Critical roles of glycosylphosphatidylinositol for *Trypanosoma brucei*. *Proc Natl Acad Sci U S A* 97: 10336-10341.
180. Lillico S, Field MC, Blundell P, Coombs GH, Mottram JC, 2003. Essential Roles for GPI-anchored Proteins in African Trypanosomes Revealed Using Mutants Deficient in GPI8. *Mol Biol Cell* 14: 1182-1194.
181. Guthrie ML, Lee S, Tetley L, Acosta-Serrano A, Ferguson MA, 2006. GPI-anchored proteins and free GPI glycolipids of procyclic form *Trypanosoma brucei* are nonessential for growth, are required for colonization of the tsetse fly, and are not the only components of the surface coat. *Mol Biol Cell* 17: 5265-5274.
182. Hirose S, Mohny RP, Mutka SC, Ravi L, Singleton DR, Perry G, Tartakoff AM, Medof ME, 1992. Derivation and characterization of glycoinositol-phospholipid anchor-defective human K562 cell clones. *J Biol Chem* 267: 5272-5278.
183. Mohny RP, Knez JJ, Ravi L, Seveler D, Rosenberry TL, Hirose S, Medof ME, 1994. Glycoinositol phospholipid anchor-defective K562 mutants with biochemical lesions distinct from those in Thy-1- murine lymphoma mutants. *J Biol Chem* 269: 6536-6542.

184. Chen R, Udenfriend S, Prince GM, Maxwell SE, Ramalingam S, Gerber LD, Knez J, Medof ME, 1996. A defect in glycosylphosphatidylinositol (GPI) transamidase activity in mutant K cells is responsible for their inability to display GPI surface proteins. *Proc Natl Acad Sci U S A* 93: 2280-2284.
185. Yu J, Nagarajan S, Knez JJ, Udenfriend S, Chen R, Medof ME, 1997. The affected gene underlying the class K glycosylphosphatidylinositol (GPI) surface protein defect codes for the GPI transamidase. *Proc Natl Acad Sci U S A* 94: 12580-12585.
186. Conzelmann A, Spiazzi A, Hyman R, Bron C, 1986. Anchoring of membrane proteins via phosphatidylinositol is deficient in two classes of Thy-1 negative mutant lymphoma cells. *Embo J* 5: 3291-3296.
187. Conzelmann A, Spiazzi A, Bron C, Hyman R, 1988. No glycolipid anchors are added to Thy-1 glycoprotein in Thy-1-negative mutant thymoma cells of four different complementation classes. *Mol Cell Biol* 8: 674-678.
188. Watanabe R, Inoue N, Westfall B, Taron CH, Orlean P, Takeda J, Kinoshita T, 1998. The first step of glycosylphosphatidylinositol biosynthesis is mediated by a complex of PIG-A, PIG-H, PIG-C and GPI1. *Embo J* 17: 877-885.
189. Watanabe R, Murakami Y, Marmor MD, Inoue N, Maeda Y, Hino J, Kangawa K, Julius M, Kinoshita T, 2000. Initial enzyme for glycosylphosphatidylinositol biosynthesis requires PIG-P and is regulated by DPM2. *Embo J* 19: 4402-4411.
190. Hong Y, Ohishi K, Watanabe R, Endo Y, Maeda Y, Kinoshita T, 1999. GPI1 stabilizes an enzyme essential in the first step of glycosylphosphatidylinositol biosynthesis. *J Biol Chem* 274: 18582-18588.
191. Watanabe R, Ohishi K, Maeda Y, Nakamura N, Kinoshita T, 1999. Mammalian PIG-L and its yeast homologue Gpi12p are N-acetylglucosaminylphosphatidylinositol de-N-acetylases essential in glycosylphosphatidylinositol biosynthesis. *Biochem J* 339 (Pt 1): 185-192.
192. Sharma DK, Smith TK, Weller CT, Crossman A, Brimacombe JS, Ferguson MA, 1999. Differences between the trypanosomal and human GlcNAc-PI de-N-acetylases of glycosylphosphatidylinositol membrane anchor biosynthesis. *Glycobiology* 9: 415-422.
193. Guthrie ML, Ferguson MA, 1995. The role of inositol acylation and inositol deacylation in GPI biosynthesis in *Trypanosoma brucei*. *Embo J* 14: 3080-3093.
194. Murakami Y, Siripanyapinyo U, Hong Y, Kang JY, Ishihara S, Nakakuma H, Maeda Y, Kinoshita T, 2003. PIG-W is critical for inositol acylation but not for flipping of glycosylphosphatidylinositol-anchor. *Mol Biol Cell* 14: 4285-4295.
195. Smith TK, Sharma DK, Crossman A, Dix A, Brimacombe JS, Ferguson MA, 1997. Parasite and mammalian GPI biosynthetic pathways can be distinguished using synthetic substrate analogues. *Embo J* 16: 6667-6675.
196. Smith TK, Sharma DK, Crossman A, Brimacombe JS, Ferguson MA, 1999. Selective inhibitors of the glycosylphosphatidylinositol biosynthetic pathway of *Trypanosoma brucei*. *Embo J* 18: 5922-5930.
197. Chen R, Walter EI, Parker G, Lapurga JP, Millan JL, Ikehara Y, Udenfriend S, Medof ME, 1998. Mammalian glycosylphosphatidylinositol anchor transfer to proteins and posttransfer deacylation. *Proc Natl Acad Sci U S A* 95: 9512-9517.

198. Maeda Y, Watanabe R, Harris CL, Hong Y, Ohishi K, Kinoshita K, Kinoshita T, 2001. PIG-M transfers the first mannose to glycosylphosphatidylinositol on the lumenal side of the ER. *Embo J* 20: 250-261.
199. Vidugiriene J, Sharma DK, Smith TK, Baumann NA, Menon AK, 1999. Segregation of glycosylphosphatidylinositol biosynthetic reactions in a subcompartment of the endoplasmic reticulum. *J Biol Chem* 274: 15203-15212.
200. Canivenc-Gansel E, Imhof I, Reggiori F, Burda P, Conzelmann A, Benachour A, 1998. GPI anchor biosynthesis in yeast: phosphoethanolamine is attached to the alpha1,4-linked mannose of the complete precursor glycosylphospholipid. *Glycobiology* 8: 761-770.
201. Gaynor EC, Mondesert G, Grimme SJ, Reed SI, Orlean P, Emr SD, 1999. MCD4 encodes a conserved endoplasmic reticulum membrane protein essential for glycosylphosphatidylinositol anchor synthesis in yeast. *Mol Biol Cell* 10: 627-648.
202. Hong Y, Maeda Y, Watanabe R, Ohishi K, Mishkind M, Riezman H, Kinoshita T, 1999. Pig-n, a mammalian homologue of yeast Mcd4p, is involved in transferring phosphoethanolamine to the first mannose of the glycosylphosphatidylinositol. *J Biol Chem* 274: 35099-35106.
203. Kang JY, Hong Y, Ashida H, Shishioh N, Murakami Y, Morita YS, Maeda Y, Kinoshita T, 2005. PIG-V involved in transferring the second mannose in glycosylphosphatidylinositol. *J Biol Chem* 280: 9489-9497.
204. Fabre AL, Orlean P, Taron CH, 2005. *Saccharomyces cerevisiae* Ybr004c and its human homologue are required for addition of the second mannose during glycosylphosphatidylinositol precursor assembly. *Febs J* 272: 1160-1168.
205. Takahashi M, Inoue N, Ohishi K, Maeda Y, Nakamura N, Endo Y, Fujita T, Takeda J, Kinoshita T, 1996. PIG-B, a membrane protein of the endoplasmic reticulum with a large lumenal domain, is involved in transferring the third mannose of the GPI anchor. *Embo J* 15: 4254-4261.
206. Sutterlin C, Escribano MV, Gerold P, Maeda Y, Mazon MJ, Kinoshita T, Schwarz RT, Riezman H, 1998. *Saccharomyces cerevisiae* GPI10, the functional homologue of human PIG-B, is required for glycosylphosphatidylinositol-anchor synthesis. *Biochem J* 332 (Pt 1): 153-159.
207. Taron CH, Wiedman JM, Grimme SJ, Orlean P, 2000. Glycosylphosphatidylinositol biosynthesis defects in Gpi11p- and Gpi13p-deficient yeast suggest a branched pathway and implicate gpi13p in phosphoethanolamine transfer to the third mannose. *Mol Biol Cell* 11: 1611-1630.
208. Hong Y, Maeda Y, Watanabe R, Inoue N, Ohishi K, Kinoshita T, 2000. Requirement of PIG-F and PIG-O for transferring phosphoethanolamine to the third mannose in glycosylphosphatidylinositol. *J Biol Chem* 275: 20911-20919.
209. Flury I, Benachour A, Conzelmann A, 2000. YLL031c belongs to a novel family of membrane proteins involved in the transfer of ethanolaminephosphate onto the core structure of glycosylphosphatidylinositol anchors in yeast. *J Biol Chem* 275: 24458-24465.
210. Benachour A, Sipos G, Flury I, Reggiori F, Canivenc-Gansel E, Vionnet C, Conzelmann A, Benghezal M, 1999. Deletion of GPI7, a yeast gene required for addition of a side chain to the glycosylphosphatidylinositol (GPI) core structure,

- affects GPI protein transport, remodeling, and cell wall integrity. *J Biol Chem* 274: 15251-15261.
211. Benghezal M, Benachour A, Rusconi S, Aebi M, Conzelmann A, 1996. Yeast Gpi8p is essential for GPI anchor attachment onto proteins. *Embo J* 15: 6575-83.
 212. Kang X, Szallies A, Rawer M, Echner H, Duszenko M, 2002. GPI anchor transamidase of *Trypanosoma brucei*: *in vitro* assay of the recombinant protein and VSG anchor exchange. *J Cell Sci* 115: 2529-2539.
 213. Kinoshita T, Inoue N, 2000. Dissecting and manipulating the pathway for glycosylphosphatidylinositol-anchor biosynthesis. *Curr Opin Chem Biol* 4: 632-638.
 214. Ralton JE, McConville MJ, 1998. Delineation of three pathways of glycosylphosphatidylinositol biosynthesis in *Leishmania mexicana*. Precursors from different pathways are assembled on distinct pools of phosphatidylinositol and undergo fatty acid remodeling. *J Biol Chem* 273: 4245-4257.
 215. Vidugiriene J, Menon AK, 1993. Early lipid intermediates in glycosylphosphatidylinositol anchor assembly are synthesized in the ER and located in the cytoplasmic leaflet of the ER membrane bilayer. *J Cell Biol* 121: 987-996.
 216. Vidugiriene J, Menon AK, 1994. The GPI anchor of cell-surface proteins is synthesized on the cytoplasmic face of the endoplasmic reticulum. *J Cell Biol* 127: 333-341.
 217. Amthauer R, Kodukula K, Gerber L, Udenfriend S, 1993. Evidence that the putative COOH-terminal signal transamidase involved in glycosylphosphatidylinositol protein synthesis is present in the endoplasmic reticulum. *Proc Natl Acad Sci U S A* 90: 3973-3977.
 218. Menon AK, Watkins WEr, Hrafnisdottir S, 2000. Specific proteins are required to translocate phosphatidylcholine bidirectionally across the endoplasmic reticulum. *Curr Biol* 10: 241-252.
 219. Baumann NA, Vidugiriene J, Machamer CE, Menon AK, 2000. Cell surface display and intracellular trafficking of free glycosylphosphatidylinositols in mammalian cells. *J Biol Chem* 275: 7378-7389.
 220. von Heijne G, 1986. A new method for predicting signal sequence cleavage sites. *Nucleic Acids Res* 14: 4683-4690.
 221. Ng DT, Brown JD, Walter P, 1996. Signal sequences specify the targeting route to the endoplasmic reticulum membrane. *J Cell Biol* 134: 269-278.
 222. Wang J, Maziarz K, Ratnam M, 1999. Recognition of the carboxyl-terminal signal for GPI modification requires translocation of its hydrophobic domain across the ER membrane. *J Mol Biol* 286: 1303-1310.
 223. Udenfriend S, Kodukula K, 1995. How glycosylphosphatidylinositol-anchored membrane proteins are made. *Annu Rev Biochem* 64: 563-591.
 224. Appel RD, Bairoch A, Hochstrasser DF, 1994. A new generation of information retrieval tools for biologists: the example of the ExPASy WWW server. *Trends Biochem Sci* 19: 258-260.
 225. Fankhauser N, Maser P, 2005. Identification of GPI anchor attachment signals by a Kohonen self-organizing map. *Bioinformatics* 21: 1846-1852.

226. Eisenhaber B, Bork P, Eisenhaber F, 2001. Post-translational GPI lipid anchor modification of proteins in kingdoms of life: analysis of protein sequence data from complete genomes. *Protein Eng* 14: 17-25.
227. Micanovic R, Kodukula K, Gerber LD, Udenfriend S, 1990. Selectivity at the cleavage/attachment site of phosphatidylinositol-glycan anchored membrane proteins is enzymatically determined. *Proc Natl Acad Sci U S A* 87: 7939-7943.
228. Micanovic R, Gerber LD, Berger J, Kodukula K, Udenfriend S, 1990. Selectivity of the cleavage/attachment site of phosphatidylinositol-glycan-anchored membrane proteins determined by site-specific mutagenesis at Asp-484 of placental alkaline phosphatase. *Proc Natl Acad Sci U S A* 87: 157-161.
229. Gerber LD, Kodukula K, Udenfriend S, 1992. Phosphatidylinositol glycan (PI-G) anchored membrane proteins. Amino acid requirements adjacent to the site of cleavage and PI-G attachment in the COOH-terminal signal peptide. *J Biol Chem* 267: 12168-12173.
230. Kodukula K, Gerber LD, Amthauer R, Brink L, Udenfriend S, 1993. Biosynthesis of glycosylphosphatidylinositol (GPI)-anchored membrane proteins in intact cells: specific amino acid requirements adjacent to the site of cleavage and GPI attachment. *J Cell Biol* 120: 657-664.
231. Moran P, Raab H, Kohr WJ, Caras IW, 1991. Glycophospholipid membrane anchor attachment. Molecular analysis of the cleavage/attachment site. *J Biol Chem* 266: 1250-1257.
232. Nuoffer C, Horvath A, Riezman H, 1993. Analysis of the sequence requirements for glycosylphosphatidylinositol anchoring of *Saccharomyces cerevisiae* Gas1 protein. *J Biol Chem* 268: 10558-10563.
233. Nuoffer C, Jeno P, Conzelmann A, Riezman H, 1991. Determinants for glycophospholipid anchoring of the *Saccharomyces cerevisiae* GAS1 protein to the plasma membrane. *Mol Cell Biol* 11: 27-37.
234. Moran P, Caras IW, 1994. Requirements for glycosylphosphatidylinositol attachment are similar but not identical in mammalian cells and parasitic protozoa. *J Cell Biol* 125: 333-343.
235. Bohme U, Cross GA, 2002. Mutational analysis of the variant surface glycoprotein GPI-anchor signal sequence in *Trypanosoma brucei*. *J Cell Sci* 115: 805-816.
236. Kodukula K, Amthauer R, Cines D, Yeh ET, Brink L, Thomas LJ, Udenfriend S, 1992. Biosynthesis of phosphatidylinositol-glycan (PI-G)-anchored membrane proteins in cell-free systems: PI-G is an obligatory cosubstrate for COOH-terminal processing of nascent proteins. *Proc Natl Acad Sci U S A* 89: 4982-4985.
237. 1998. 252. Introduction: other cysteine peptidases. Barrett AJ, Rawlings ND, JF W, eds. *The Handbook of Proteolytic Enzymes*. London: Academic Press.
238. Mayor S, Menon AK, Cross GA, 1991. Transfer of glycosyl-phosphatidylinositol membrane anchors to polypeptide acceptors in a cell-free system. *J Cell Biol* 114: 61-71.
239. Sharma DK, Vidugiriene J, Bangs JD, Menon AK, 1999. A cell-free assay for glycosylphosphatidylinositol anchoring in African trypanosomes. Demonstration of a transamidation reaction mechanism. *J Biol Chem* 274: 16479-16486.

240. Duszenko M, Kang X, Bohme U, Homke R, Lehner M, 1999. *In vitro* translation in a cell-free system from *Trypanosoma brucei* yields glycosylated and glycosylphosphatidylinositol-anchored proteins. *Eur J Biochem* 266: 789-797.
241. Kodukula K, Micanovic R, Gerber L, Tamburrini M, Brink L, Udenfriend S, 1991. Biosynthesis of phosphatidylinositol glycan-anchored membrane proteins. Design of a simple protein substrate to characterize the enzyme that cleaves the COOH-terminal signal peptide. *J Biol Chem* 266: 4464-4470.
242. Doering TL, Schekman R, 1997. Glycosyl-phosphatidylinositol anchor attachment in a yeast *in vitro* system. *Biochem J* 328 (Pt 2): 669-675.
243. Sharma DK, Hilley JD, Bangs JD, Coombs GH, Mottram JC, Menon AK, 2000. Soluble GPI8 restores glycosylphosphatidylinositol anchoring in a trypanosome cell-free system depleted of luminal endoplasmic reticulum proteins. *Biochem J* 351 Pt 3: 717-722.
244. Kodukula K, Maxwell SE, Udenfriend S, 1995. Processing of nascent proteins to glycosylphosphatidylinositol-anchored forms in cell-free systems. *Methods Enzymol* 250: 536-547.
245. Maxwell SE, Ramalingam S, Gerber LD, Brink L, Udenfriend S, 1995. An active carbonyl formed during glycosylphosphatidylinositol addition to a protein is evidence of catalysis by a transamidase. *J Biol Chem* 270: 19576-19582.
246. Vidugiriene J, Vainauskas S, Johnson AE, Menon AK, 2001. Endoplasmic reticulum proteins involved in glycosylphosphatidylinositol- anchor attachment: photocrosslinking studies in a cell-free system. *Eur J Biochem* 268: 2290-2300.
247. Spurway TD, Dalley JA, High S, Bulleid NJ, 2001. Early events in glycosylphosphatidylinositol anchor addition. substrate proteins associate with the transamidase subunit gpi8p. *J Biol Chem* 276: 15975-15982.
248. Benghezal M, Lipke PN, Conzelmann A, 1995. Identification of six complementation classes involved in the biosynthesis of glycosylphosphatidylinositol anchors in *Saccharomyces cerevisiae*. *J Cell Biol* 130: 1333-1344.
249. Leidich SD, Kostova Z, Latek RR, Costello LC, Drapp DA, Gray W, Fassler JS, Orlean P, 1995. Temperature-sensitive yeast GPI anchoring mutants gpi2 and gpi3 are defective in the synthesis of N-acetylglucosaminyl phosphatidylinositol. Cloning of the GPI2 gene. *J Biol Chem* 270: 13029-13035.
250. Schonbachler M, Horvath A, Fassler J, Riezman H, 1995. The yeast spt14 gene is homologous to the human *PIG-A* gene and is required for GPI anchor synthesis. *Embo J* 14: 1637-1645.
251. Hamburger D, Egerton M, Riezman H, 1995. Yeast Gaalp is required for attachment of a completed GPI anchor onto proteins. *J Cell Biol* 129: 629-39.
252. Vossen JH, Ram AF, Klis FM, 1995. Identification of SPT14/CWH6 as the yeast homologue of hPIG-A, a gene involved in the biosynthesis of GPI anchors. *Biochim Biophys Acta* 1243: 549-551.
253. Ellis M, Sharma DK, Hilley JD, Coombs GH, Mottram JC, 2002. Processing and trafficking of *Leishmania mexicana* GP63. Analysis using GP18 mutants deficient in glycosylphosphatidylinositol protein anchoring. *J Biol Chem* 277: 27968-27974.

254. Eisenhaber B, Maurer-Stroh S, Novatchkova M, Schneider G, Eisenhaber F, 2003. Enzymes and auxiliary factors for GPI lipid anchor biosynthesis and post-translational transfer to proteins. *Bioessays* 25: 367-385.
255. Nagamune K, Ohishi K, Ashida H, Hong Y, Hino J, Kangawa K, Inoue N, Maeda Y, Kinoshita T, 2003. GPI transamidase of *Trypanosoma brucei* has two previously uncharacterized (trypanosomatid transamidase 1 and 2) and three common subunits. *Proc Natl Acad Sci U S A* 100: 10682-10687.
256. Smith TK, Paterson MJ, Crossman A, Brimacombe JS, Ferguson MA, 2000. Parasite-specific inhibition of the glycosylphosphatidylinositol biosynthetic pathway by stereoisomeric substrate analogues. *Biochemistry* 39: 11801-11807.
257. Mann KJ, Seivlever D, 2001. 1,10-Phenanthroline inhibits glycosylphosphatidylinositol anchoring by preventing phosphoethanolamine addition to glycosylphosphatidylinositol anchor precursors. *Biochemistry* 40: 1205-1213.
258. Ohishi K, Nagamune K, Maeda Y, Kinoshita T, 2003. Two subunits of GPI transamidase GPI8 and PIG-T form a functionally important intermolecular disulfide bridge. *J Biol Chem* 278: 13959-13967.
259. *Trypanosoma cruzi* Genome Consortium, 2005. TcruziDB. Available from: <http://tcruzidb.org/>.
260. Barrett A, Morton F, Rawlings N, 2000. *MEROPS*: the peptidase database. *Nucleic Acids Res* 28: 323-325.
261. Rawlings ND, Barrett AJ, 1994. Families of cysteine peptidases. *Methods Enzymol* 244: 461-486.
262. Kembhavi AA, Buttle DJ, Knight CG, Barrett AJ, 1993. The two cysteine endopeptidases of legume seeds: purification and characterization by use of specific fluorometric assays. *Arch Biochem Biophys* 303: 208-213.
263. Alonso JM, Granell A, 1995. A putative vacuolar processing protease is regulated by ethylene and also during fruit ripening in Citrus fruit. *Plant Physiol* 109: 541-7.
264. Ishii S, 1994. Legumain: asparaginyl endopeptidase. *Methods Enzymol* 244: 604-615.
265. Chen JM, Dando PM, Rawlings ND, Brown MA, Young NE, Stevens RA, Hewitt E, Watts C, Barrett AJ, 1997. Cloning, isolation, and characterization of mammalian legumain, an asparaginyl endopeptidase. *J Biol Chem* 272: 8090-8098.
266. Chen JM, Rawlings ND, Stevens RA, Barrett AJ, 1998. Identification of the active site of legumain links it to caspases, clostripain and gingipains in a new clan of cysteine endopeptidases. *FEBS Lett* 441: 361-365.
267. Dalton JP, Hola-Jamriska L, Brindley PJ, 1995. Asparaginyl endopeptidase activity in adult *Schistosoma mansoni*. *Parasitology* 111 (Pt 5): 575-580.
268. Dalton JP, Brindley PJ, 2004. C378. Schistosome legumain. Barrett AJ, Rawlings ND, Woessner JF, eds. *The Handbook of Proteolytic Enzymes*. London: Academic Press.
269. Min W, Jones DH, 1994. *In vitro* splicing of concanavalin A is catalyzed by asparaginyl endopeptidase. *Nat Struct Biol* 1: 502-504.
270. Shimada T, Yamada K, Kataoka M, Nakaune S, Koumoto Y, Kuroyanagi M, Tabata S, Kato T, Shinozaki K, Seki M, Kobayashi M, Kondo M, Nishimura M,

- Hara-Nishimura I, 2003. Vacuolar processing enzymes are essential for proper processing of seed storage proteins in *Arabidopsis thaliana*. J Biol Chem 278: 32292-32299.
271. Takeda O, Miura Y, Mitta M, Matsushita H, Kato I, Abe Y, Yokosawa H, Ishii S, 1994. Isolation and analysis of cDNA encoding a precursor of *Canavalia ensiformis* asparaginyl endopeptidase (legumain). J Biochem (Tokyo) 116: 541-546.
 272. Hara-Nishimura I, 1998. 253. Asparaginyl endopeptidase. Barrett AJ, Rawlings ND, Woessner JF, eds. The Handbook of Proteolytic Enzymes. London: Academic Press.
 273. Manoury B, Hewitt EW, Morrice N, Dando PM, Barrett AJ, Watts C, 1998. An asparaginyl endopeptidase processes a microbial antigen for class II MHC presentation. Nature 396: 695-699.
 274. NM OB-S, Veith PD, Dashper SG, Reynolds EC, 2003. *Porphyromonas gingivalis* gingipains: the molecular teeth of a microbial vampire. Curr Protein Pept Sci 4: 409-426.
 275. Dickinson DP, 2002. Cysteine peptidases of mammals: their biological roles and potential effects in the oral cavity and other tissues in health and disease. Crit Rev Oral Biol Med 13: 238-275.
 276. Supuran CT, Scozzafava A, Clare BW, 2002. Bacterial protease inhibitors. Med Res Rev 22: 329-372.
 277. Meyer U, Benghezal M, Imhof I, Conzelmann A, 2000. Active site determination of Gpi8p, a caspase-related enzyme required for glycosylphosphatidylinositol anchor addition to proteins. Biochemistry 39: 3461-3471.
 278. Ohishi K, Inoue N, Maeda Y, Takeda J, Riezman H, Kinoshita T, 2000. Gaa1p and gpi8p are components of a glycosylphosphatidylinositol (GPI) transamidase that mediates attachment of GPI to proteins. Mol Biol Cell 11: 1523-1533.
 279. Fraering P, Imhof I, Meyer U, Strub JM, van Dorsselaer A, Vionnet C, Conzelmann A, 2001. The GPI transamidase complex of *Saccharomyces cerevisiae* contains Gaa1p, Gpi8p, and Gpi16p. Mol Biol Cell 12: 3295-3306.
 280. Ohishi K, Inoue N, Kinoshita T, 2001. PIG-S and PIG-T, essential for GPI anchor attachment to proteins, form a complex with GAA1 and GPI8. Embo J 20: 4088-4098.
 281. Hong Y, Ohishi K, Kang JY, Tanaka S, Inoue N, Nishimura J, Maeda Y, Kinoshita T, 2003. Human PIG-U and yeast Cdc91p are the fifth subunit of GPI transamidase that attaches GPI-anchors to proteins. Mol Biol Cell 14: 1780-1789.
 282. Schagger H, von Jagow G, 1991. Blue native electrophoresis for isolation of membrane protein complexes in enzymatically active form. Anal Biochem 199: 223-231.
 283. Winzeler EA, Shoemaker DD, Astromoff A, Liang H, Anderson K, Andre B, Bangham R, Benito R, Boeke JD, Bussey H, Chu AM, Connolly C, Davis K, Dietrich F, Dow SW, El Bakkoury M, Foury F, Friend SH, Gentalen E, Giaever G, Hegemann JH, Jones T, Laub M, Liao H, Davis RW, et al., 1999. Functional characterization of the *S. cerevisiae* genome by gene deletion and parallel analysis. Science 285: 901-906.

284. Hiroi Y, Komuro I, Chen R, Hosoda T, Mizuno T, Kudoh S, Georgescu SP, Medof ME, Yazaki Y, 1998. Molecular cloning of human homolog of yeast GAA1 which is required for attachment of glycosylphosphatidylinositols to proteins. *FEBS Lett* 421: 252-258.
285. Hiroi Y, Chen R, Sawa H, Hosoda T, Kudoh S, Kobayashi Y, Aburatani H, Nagashima K, Nagai R, Yazaki Y, Medof ME, Komuro I, 2000. Cloning of murine glycosyl phosphatidylinositol anchor attachment protein, GPAA1. *Am J Physiol Cell Physiol* 279: C205-212.
286. Vainauskas S, Menon AK, 2004. A conserved proline in the last transmembrane segment of Gaa1 is required for glycosylphosphatidylinositol (GPI) recognition by GPI transamidase. *J Biol Chem* 279: 6540-6545.
287. Vainauskas S, Maeda Y, Kurniawan H, Kinoshita T, Menon AK, 2002. Structural requirements for the recruitment of Gaa1 into a functional glycosylphosphatidylinositol transamidase complex. *J Biol Chem* 277: 30535-42.
288. Hong Y, Nagamune K, Ohishi K, Morita YS, Ashida H, Maeda Y, Kinoshita T, 2006. TbGPI16 is an essential component of GPI transamidase in *Trypanosoma brucei*. *FEBS Lett* 580: 603-606.
289. Zacks MA, 2007. Impairment of cell division of *Trypanosoma cruzi* epimastigotes. *Mem Inst Oswaldo Cruz* 102: 111-115.
290. Kelly JM, Ward HM, Miles MA, Kendall G, 1992. A shuttle vector which facilitates the expression of transfected genes in *Trypanosoma cruzi* and *Leishmania*. *Nucleic Acids Res* 20: 3963-3969.
291. Nozaki T, Cross GA, 1994. Functional complementation of glycoprotein 72 in a *Trypanosoma cruzi* glycoprotein 72 null mutant. *Mol Biochem Parasitol* 67: 91-102.
292. Hariharan S, Ajioka J, Swindle J, 1993. Stable transformation of *Trypanosoma cruzi*: inactivation of the PUB12.5 polyubiquitin gene by targeted gene disruption. *Mol Biochem Parasitol* 57: 15-30.
293. Nozaki T, Cross GA, 1995. Effects of 3' untranslated and intergenic regions on gene expression in *Trypanosoma cruzi*. *Mol Biochem Parasitol* 75: 55-67.
294. Liu YG, Whittier RF, 1995. Thermal asymmetric interlaced PCR: automatable amplification and sequencing of insert end fragments from P1 and YAC clones for chromosome walking. *Genomics* 25: 674-681.
295. Parker JD, Rabinovitch PS, Burner GC, 1991. Targeted gene walking polymerase chain reaction. *Nucleic Acids Res* 19: 3055-3060.
296. 2004. *Current Protocols in Molecular Biology*: John Wiley & Sons, Inc.
297. Qiagen, August 2003. *Qiagen Plasmid Purification Handbook*.
298. Novagen, May, 2001. *Perfectly Blunt Cloning Kits*.
299. Stratagene, *QuikChange Site-Directed Mutagenesis Kit Instruction Manual*.
300. Davey RA, Hamson CA, Healey JJ, Cunningham JM, 1997. *In vitro* binding of purified murine ecotropic retrovirus envelope surface protein to its receptor, MCAT-1. *J Virol* 71: 8096-8102.
301. Medina-Acosta E, Cross GA, 1993. Rapid isolation of DNA from trypanosomatid protozoa using a simple 'mini-prep' procedure. *Mol Biochem Parasitol* 59: 327-329.

302. Nielsen H, Engelbrecht J, Brunak S, von Heijne G, 1997. Identification of prokaryotic and eukaryotic signal peptides and prediction of their cleavage sites. *Protein Eng* 10: 1-6.
303. Jackson MR, Nilsson T, Peterson PA, 1990. Identification of a consensus motif for retention of transmembrane proteins in the endoplasmic reticulum. *Embo J* 9: 3153-3162.
304. Gaynor EC, te Heesen S, Graham TR, Aebi M, Emr SD, 1994. Signal-mediated retrieval of a membrane protein from the Golgi to the ER in yeast. *J Cell Biol* 127: 653-665.
305. Hernandez-Munain C, De Diego JL, Bonay P, Girones N, Fresno M, 1993. GP 50/55, a membrane antigen of *Trypanosoma cruzi* involved in autoimmunity and immunosuppression. *Biol Res* 26: 209-218.
306. Kendall G, Wilderspin AF, Ashall F, Miles MA, Kelly JM, 1990. *Trypanosoma cruzi* glycosomal glyceraldehyde-3-phosphate dehydrogenase does not conform to the 'hotspot' topogenic signal model. *Embo J* 9: 2751-2758.
307. Todd AE, Orengo CA, Thornton JM, 2002. Plasticity of enzyme active sites. *Trends Biochem Sci* 27: 419-426.
308. Goldberg AL, 2003. Protein degradation and protection against misfolded or damaged proteins. *Nature* 426: 895-899.
309. Bartholomeu DC, Batista JA, Vainstein MH, Lima BD, de Sa MC, 2001. Molecular cloning and characterization of a gene encoding the 29-kDa proteasome subunit from *Trypanosoma cruzi*. *Mol Genet Genomics* 265: 986-992.
310. de Diego JL, Katz JM, Marshall P, Gutierrez B, Manning JE, Nussenzweig V, Gonzalez J, 2001. The ubiquitin-proteasome pathway plays an essential role in proteolysis during *Trypanosoma cruzi* remodeling. *Biochemistry* 40: 1053-1062.
311. Bouzat JL, McNeil LK, Robertson HM, Solter LF, Nixon JE, Beever JE, Gaskins HR, Olsen G, Subramaniam S, Sogin ML, Lewin HA, 2000. Phylogenomic analysis of the alpha proteasome gene family from early-diverging eukaryotes. *J Mol Evol* 51: 532-543.
312. Zou CB, Nakajima-Shimada J, Nara T, Aoki T, 2000. Cloning and functional expression of Rpn1, a regulatory-particle non-ATPase subunit 1, of proteasome from *Trypanosoma cruzi*. *Mol Biochem Parasitol* 110: 323-31.
313. Gonzalez J, Ramalho-Pinto FJ, Frevert U, Ghiso J, Tomlinson S, Scharfstein J, Corey EJ, Nussenzweig V, 1996. Proteasome activity is required for the stage-specific transformation of a protozoan parasite. *J Exp Med* 184: 1909-1918.
314. McConville MJ, Menon AK, 2000. Recent developments in the cell biology and biochemistry of glycosylphosphatidylinositol lipids (review). *Mol Membr Biol* 17: 1-16.
315. Wilkinson SR, Meyer DJ, Taylor MC, Bromley EV, Miles MA, Kelly JM, 2002. The *Trypanosoma cruzi* enzyme TcGPXI is a glycosomal peroxidase and can be linked to trypanothione reduction by glutathione or tryparedoxin. *J Biol Chem* 277: 17062-17071.
316. Thomas MC, Gonzalez A, 1997. A transformation vector for stage-specific expression of heterologous genes in *Trypanosoma cruzi* epimastigotes. *Parasitol Res* 83: 151-156.

Vita

Michele Anne Zacks was born in Detroit, Michigan in 1967 to Howard Ronald and Claudia Jeanette Zacks. She attended grade school and high school in Flint, Michigan (Walker, Valley and Flint Northern Schools) and in Birmingham, Michigan (Cranbrook-Kingswood Academy). During and after her undergraduate and master's level studies, Michele obtained professional experience in biomedical research in the Longwood Medical Area in Boston, Massachusetts. During college, she worked as a Diener in the Department of Pathology at the Brigham and Women's Hospital in her sophomore year and as a laboratory intern in the Histocompatibility Laboratory at Michigan State University in her junior year. After graduating from college, Michele moved to Boston, Massachusetts and worked as a technical research assistant at the Brigham and Women's Hospital where she contributed to a clinical trial evaluating the efficacy of adoptive immunotherapy for cancer. Next, she worked as the administrative coordinator of scientific research grants for the Allergy-Immunology Fellowship Program at the Children's Hospital. After Michele received her M.S. in International Health (Infectious Disease Epidemiology), she worked as the coordinator and data manager for an International Center for Infectious Disease Research Grant, a collaborative grant between U.S. and Brazilian investigators studying schistosomiasis, malaria, and leishmaniasis. In August of 1998, she entered the Ph.D. program in Experimental Pathology at the Graduate School of Biomedical Sciences in Galveston, Texas where she eventually pursued her dissertation research on GPI-anchored proteins in *Trypanosoma cruzi*. Within the past year, in addition to her dissertation work, she has contributed as a freelance editor and writer to the following manuscripts on arboviruses: Paessler et al. J. Virol. 2006, 80(6); 2784-96 and Paessler S, Pfeffer M. *Togaviruses causing encephalitis*

(*Togaviridae*), Encyclopedia of Virology, 3rd Edition (Elsevier Press, 2008). She was instrumental in devising and overseeing the implementation of a centralized data management system for establishment of GLP-compliant studies of viral pathogenesis in animal models, for writing standard operating procedures for molecular virology studies, and for training other investigators in design and completion of molecular biology experiments.

Education

B.A., 1989, Kalamazoo College, Kalamazoo, Michigan
M.S., 1995, Harvard School of Public Health (HSPH), Boston, Massachusetts

Publications

Peer-reviewed articles (accepted)

1. Zacks MA. 2007. *Impairment of cell division of Trypanosoma cruzi epimastigotes*. Mem Inst Oswaldo Cruz 102(1):111-5.
2. Ni H, Yun N, Zacks MA, Weaver SC, Tesh RB, Travassos da Rosa AP, Powers AM, Frolov I, Paessler S. 2007. *Recombinant alphaviruses are safe and useful serological diagnostic tools*. Am. J. Trop. Med. Hyg. 76: 774-781.
3. Paessler S., Yun NE, Judy BM, Dziuba N, Zacks MA, Grund H, Frolov I, Campbell GA, Weaver SC and Estes DM. 2007. *Alpha-beta T cells provide protection against lethal encephalitis in the murine model of VEEV infection*. Virol. (in press).

Peer-reviewed articles (submitted)

1. Yun NE, Linde NS, Zacks MA, Barr IG, Hurt AC, Smith JS, Dziuba N, Holbrook MR, Zhang L, Kilpatrick JM, Arnold CS, and Paessler S. (Feb. 2007, PLoS Med.) *Injectable peramivir mitigates disease and promotes survival in ferrets and mice infected with the highly virulent H5N1 influenza virus isolate A/Vietnam/1203/04*.

Review articles

1. Zacks MA and Garg N. 2006 *Recent developments in the molecular, biochemical and functional characterization of GPI8 and the GPI-anchoring mechanism*. Mol. Membr. Biol. 23(3): 209-225.
2. Zacks MA, Wen JJ, Vyatkina G, Bhatia V, Garg N. 2005. *An overview of chagasic cardiomyopathy: pathogenic importance of oxidative stress*. An. Acad. Bras. Cienc. 77(4):695-715.

Book chapters

1. Bhatia V, Wen J-J, Zacks MA, Garg N. (in press, 2007) *American trypanosomiasis and perspectives on vaccine development*, in Vaccines Against Biothreats and Emerging Infections, A. Barrett and L. Stanberry, Editors. Elsevier Academic Press: St. Louis.
2. Ling C, Zacks M, Geha RS. *Evaluation of allergic-type reactions*, in: The Clinical Evaluation of a Food Additive: Assessment of Aspartame. Tschanz C, Butchko HH, Stargel WW, Kotsonis F (eds.) CRC Press: New York. pp. 267-274, 1996.

Meeting abstracts

1. Kendirgi F, Yun NE, Linde NS, Zacks MA, Smith J, Smith J, McMicken H, Chen Y, Paessler S. *A Novel DNA-based vaccine protects mice against lethal infection with H5N1 influenza virus isolate A/Vietnam/1203/04*. Options for the Control of Influenza VI. 2007. Toronto, Ontario, Canada.
2. Yun N, Linde NS, Zacks MA, Barr IG, Hurt AC, Smith JN, Dziuba N, Holbrook MR, Zhang L, Kilpatrick JM, Arnold CS, Paessler S. *Injectable peramivir mitigates disease and promotes survival in ferrets and mice infected with the highly virulent H5N1 influenza virus isolate A/Vietnam/1203/04*. Options for the Control of Influenza VI. 2007. Toronto, Ontario, Canada.
3. Paessler S, Gorchakov R, Yun NE, Linde NS, Zacks MA, and Frolov I. *Alphavirus-based vaccines against Rift Valley fever virus*. International Meeting on Emerging Diseases and Surveillance. February 23-25, 2007. Vienna, Austria.
4. Paessler S, Yun NE, Ni H, Judy BM, Dziuba N, Zacks MA, Frolov I, Campbell GA, Weaver SC and Estes DM. *Development of a live-attenuated, chimeric alphavirus-based vaccine against Venezuelan equine encephalitis virus*. International Meeting on Emerging Diseases and Surveillance. February 23-25, 2007. Vienna, Austria.

5. Zacks MA, Dziuba N, Ni H, Frolov I, Campbell G, Yun NE, Weaver SC, Estes DM, and Paessler S. *Persistence of attenuated variants of Venezuelan equine encephalitis virus (VEEV) in the murine brain*. Am. J. of Trop. Med. Hyg., 75 (5 Suppl.); 2006.
6. Ni H, Yun N, Zacks MA, Weaver SC, Tesh RB, Travassos da Rosa AP, Powers AM, Frolov I, Paessler S. *Recombinant alphaviruses are safe and useful serological diagnostic tools*. Am. J. of Trop. Med. Hyg., 75 (5 Suppl.); 2006.
7. Paessler S, Yun NE, Ni H, Judy BM, Dziuba N, Zacks MA, Frolov I, Campbell GA, Weaver SC and Estes DM. *Impact of selective lymphoid deficiencies on encephalitis and virus persistence in the murine brain (VEEV)*. Am. J. of Trop. Med. Hyg., 75 (5 Suppl.); 2006.
8. Paessler S, Yun NE, Ni H, Judy BM, Dziuba N, Zacks MA, Frolov I, Campbell GA, Weaver SC and Estes DM. *Role of CD4⁺ and CD8⁺ T cells in protection against lethal encephalitis mediated by a Sinbis-VEEV chimeric vaccine*. 55th Annual Meeting of the American Society of Tropical Medicine and Hygiene. Nov. 12-16, 2006, Atlanta, GA.
9. Yun NE, Linde N, Zacks MA, Dziuba N, Smith J, Grund H, Paessler S. *Peramivir mitigates disease and promotes survival in ferrets and mice infected with H5N1 influenza virus isolate A/Vietnam/1203/04*. 55th Annual Meeting of the American Society of Tropical Medicine and Hygiene. Nov. 12-16, 2006, Atlanta, GA.
10. Paessler, S, Gorchakov R, Yun NE, Linde NS, Zacks MA, and Frolov I. *Alphavirus-based vaccines against Rift Valley Hemorrhagic Fever Virus*. The Changing Landscape of Vaccine Development: Vaccines for Global Health. November 8-10, 2006. Galveston, Texas.
11. Slobodan, P, Yun NE, Ni H, Judy BM, Dziuba N, Zacks MA, Frolov I, Campbell GA, Weaver SC and Estes DM. *Impact of selective lymphoid deficiencies on encephalitis and virus persistence in the murine brain (VEEV)*. The Changing Landscape of Vaccine Development: Vaccines for Global Health. November 8-10, 2006. Galveston, Texas.
12. Arnold CS, Zacks MA, Dziuba N, Yun N, Linde N, Smith J, Babu YS, Paessler S. *Injectable peramivir is effective in the treatment of highly pathogenic avian influenza A/Vietnam/1203/04 (H5N1) infections in mouse and ferret models*. 46th Annual Interscience Conference on Antimicrobial Agents and Chemotherapy. September 27-30, 2006. San Francisco, California.
13. Zacks MA, Suzuki E, Garg N. *Characterization of GPI anchoring mechanism in Trypanosoma cruzi by over-expression of GPI8p active site mutants*. Third McLaughlin Symposium. Infectious Diseases from Nature: Mechanisms of Viral Emergence and Persistence. March 18-21, 2004. Galveston, Texas.

14. Zacks MA, Suzuki E, Garg N. *Evaluation of the biological significance of GPI-anchored proteins in Trypanosoma cruzi by over-expression of GPI8p active site mutants*. Molecular Parasitology Meeting XIII. September 22-26, 2002. Marine Biological Laboratory, Woods Hole, Massachusetts.
15. Zacks MA, Suzuki E, Garg N. *Biological Studies of GPI-anchoring in Trypanosoma cruzi*. Gulf Coast Tropical Medicine Association Meeting. April 26-27, 2002. Galveston, Texas.
16. Zacks MA, Suzuki E, Garg N. *Characterization of GPI anchoring mechanism in Trypanosoma cruzi by over-expression of GPI8p active site mutants*. 2nd Biennial Cell Biology Poster Session & Forum. October 2, 2001. University of Texas Medical Branch, Galveston, Texas.
17. Zacks MA, Suzuki E, Garg N. *Characterization of GPI anchoring mechanism in Trypanosoma cruzi by over-expression of GPI8p active site mutants*. American Journal of Tropical Medicine and Hygiene, 65 (3); 2001.
18. Zacks MA, Soong L. *T cell receptor-restricted usage in cutaneous leishmaniasis: expansion of CD4+ T cells of a limited repertoire following L. amazonensis infection*. National Student Research Forum. April 6-8, 2000, Galveston, Texas.

Permanent address: 2108 56th Street, UP, Galveston, Texas 77551

This dissertation was typed by Michele A. Zacks.